UNIVERSITÀ
DEGLI STUDI
DI BRESCIA

DOTTORATO DI RICERCA IN TECHNOLOGY FOR HEALTH

ING-INF/06

XXXIII Ciclo

INTEGRATED APPROACHES SUPPORTED BY NOVEL TECHNOLOGIES IN FUNCTIONAL ASSESSMENT AND REHABILITATION

DOTTORANDO:
Paolo Mosna

RELATORE:
Prof. Nicola Francesco Lopomo

SOMMARIO

Questo lavoro di tesi si inserisce all'interno dell'attuale e sempre più emergente bisogno di introdurre soluzioni per la riabilitazione e la valutazione funzionale che possano supportare il clinico all'interno del processo diagnostico-terapeutico con informazioni quantitative e ripetibili, e che possano essere utilizzate in modo facile ed affidabile in ambito ambulatoriale e/o domiciliare. Le attività di ricerca qui descritte sono state in particolar modo focalizzate su due diversi contesti applicativi legati a problematiche cliniche ben definite ed associate entrambe all'arto superiore: (1) la riabilitazione motoria in soggetti post-ictus e (2) la valutazione funzionale della spalla, con particolare attenzione all'articolazione scapolo-omerale; in ambedue i casi, è stato introdotto l'utilizzo di soluzioni tecnologiche integrate all'interno di approcci innovativi rivolti alla specifica problematica clinica.

Relativamente al primo contesto applicativo, le attività di tesi hanno portato allo sviluppo di una soluzione originale, basata su tecnologie facilmente reperibili sul mercato consumer ed indirizzata a coadiuvare ed estendere le procedure normalmente utilizzate per la riabilitazione degli arti superiori in soggetti post-ictus; in particolar modo, questo approccio si è basato sull'introduzione dell'Action Observation Therapy (AOT) integrata con soluzioni di realtà virtuale e mista (VR e MR). L'AOT è un approccio identificato all'interno delle problematiche di riabilitazione neuromotoria di tipo "top-down" e sfrutta il paradigma proprio del mirror neuron system; l'AOT include quindi prima l'osservazione dell'azione che il paziente dovrà poi eseguire all'interno del percorso riabilitativo, favorendo la plasticità del sistema motorio. In questo specifico contesto, l'AOT, realizzata attraverso stimoli visivi 3D somministrati attraverso visori VR, ha complementato la realizzazione del training motorio sviluppato attraverso i principi del "exergaming" in un contesto di MR, dove oggetti virtuali – con cui il paziente poteva interagire - sono stati collocati all'interno dell'ambiente reale. La soluzione realizzata oltre a supportare la riabilitazione post-ictus seguendo il paradigma dell'AOT e il training in MR, ha proposto metriche originali (i.e., primary key indicator - PKI) basate su misure cinematiche atte a quantificare e monitorare le performance dei pazienti durante il programma riabilitativo, così da adattare attivamente l'esercizio e fornire informazioni utili al clinco sul percorso terapeutico. Nello specifico, queste misure sono state realizzate mediante l'utilizzo di diversi dispositivi magneto-inerziali (IMD) che, attraverso opportune procedure di setup e calibrazione, hanno permesso di acquisire i dati di cinematica articolare degli arti superiori (spalla, gomito e polso); al fine di render il sistema adattivo, ulteriori informazioni sono poi state raccolte attraverso un

sistema di tracking markerless del movimento della mano, integrato ad un framework appositamente progettato e sviluppato ed in grado di gestire diversi eventi di interazione tra la mano del paziente e gli oggetti virtuali, così da identificare le specifiche strategie di esecuzione dei task durante il training. Dal punto di vista del design software, la soluzione proposta ha presentato una separazione tra la consolle di gestione (utilizzabile dal clinico) e l'ambiente di realtà aumentata e mista, permettendo l'implementazione di un approccio altamente flessibile dove un canale di comunicazione basato su web-socket garantisce la capacità di espansione del sistema sia verticalmente – includendo quindi sia tecnologie desktop che più flessibili soluzioni mobile – sia orizzontalmente – aggiungendo nuove componenti e servizi (e.g., utilizzo di IMD integrati attraverso dispositivi mobile come soluzioni a basso costo per l'acquisizione della cinematica articolare). La configurabilità della soluzione implementata è stata progettata per permettere un facile ed attivo adattamento dell'esercizio (e del livello di difficoltà associato) alle specifiche caratteristiche del paziente all'interno del percorso terapeutico, e al clinico quindi di definire e verificare protocolli personalizzati. La soluzione proposta è stata valutata in termini di usabilità generale attraverso uno studio preliminare di tipo "proof of concept" realizzato presso l'IRCCS Fondazione Don Carlo Gnocchi ONLUS di Rovato (BS). Vale la pena sottolineare come il personale clinico dell'istituto abbia preso parte già nella fase di design della soluzione e di definizione dei casi d'uso e degli esercizi implementati, attraverso un approccio di co-design che ha portato in poco tempo all'identificazione del sistema ottimale. Il lavoro realizzato ha dimostrato come l'utilizzo di tecnologie comuni mutuate dal mercato consumer, quando vengono integrate in modo ottimizzato rispetto al contesto e sono supportate da un corretto design dell'applicazione risultano efficaci nel supportate gli operatori clinici durante il loro lavoro quotidiano, estendendo quindi le possibilità dei protocolli e delle procedure di riabilitazione standard. Questo studio ha evidenziato inoltre l'efficacia della MR come elemento chiave a supporto della fase di esecuzione nel contesto dell'AOT. Le attività sviluppate all'interno di questo primo specifico contesto applicativo hanno presentato diversi tratti innovativi legati in particolar modo all'integrazione dell'AOT - realizzata attraverso stimoli 3D fruiti dal paziente mediante sistemi di VR – con approcci di exergaming implementati tramite MR, e all'identificazione di diverse metriche di performance che possono portare alla definizione di sistemi adattivi in grado di supportare percorsi di riabilitazione motoria altamente personalizzati, anche in ambito domiciliare.

Il secondo contesto applicativo ha spostato il focus sul bisogno di approcci user-friendly da poter utilizzare in ambito ambulatoriale per la realizzazione di specifiche

valutazioni funzionali; la seconda parte di questo lavoro di tesi presenta e analizza quindi lo sviluppo e i risultati preliminari relativi alla soluzione per la valutazione dello stato funzionale della spalla (SSA). La fase di design del sistema SSA ha portato allo sviluppo di una soluzione innovativa progettata per essere eseguita su dispositivi mobili (come smartphone e tablets) ed integrante l'uso di IMD, così valutare in tempo reale la funzionalità della spalla con la possibilità di identificare la presenza di possibili patologie. Il sistema proposto ha esplorato in particolar modo la possibilità di utilizzare un set ridotto di IMD (2-3 sensori, considerando la possibilità di interfacciamento con tecnologie realizzate da produttori diversi) e un protocollo applicativo rapido, in grado di acquisire in maniera specifica la cinematica dell'articolazione scapolo-omerale. La fase di progettazione ha portato inoltre a definire la possibilità di salvataggio dei dati sia localmente, sia su database condivisi sul cloud, permettendo così di tracciare e monitorare nel tempo l'evoluzione della condizione all'interno di un percorso riabilitativo. L'approccio proposto è stato testato in via preliminare all'interno di prove sperimentali realizzate su soggetti volontari. Un'analisi dettagliata dei dati di movimento acquisiti nella prima fase di abduzione sul piano scapolare dell'arto superiore ha permesso la definizione di un insieme di indicatori primari originali (i.e., shoulder primary key indicators - SPKI) che si sono dimostrati efficaci nella classificazione della funzionalità articolare. Anche per questa seconda applicazione è stato adottato un approccio agile nel design della soluzione, puntando a caratteristiche di estrema usabilità che tengano conto dei vincoli specifici del contesto di utilizzo. Inoltre, la raccolta preliminare dei dati ha permesso la predisposizione di un'analisi propedeutica indirizzata all'applicazione di soluzioni di intelligenza artificiale (i.e. multilayer artificial neural networks) al fine di realizzare una sistema di "clinical support" in grado di suggerire possibili classificazione dello stato patologico della spalla.

Per entrambe i contesti clinici individuati, l'attività di ricerca – oltre alla progettazione ed alla realizzazione delle soluzioni proposte – si è concentrata principalmente su tre aspetti: (1) possibilità di implementazione di sistemi integrati che potessero utilizzare dispositivi provenienti dal mercato consumer, (2) co-design degli approcci generali realizzato con il coinvolgimento diretto degli end user (i.e., clinici), (3) valutazione delle soluzioni dal punto di vista dell'usabilità hardware-software. In entrambe le aree di applicazione, la ricerca realizzata - partendo da un'estesa analisi della letteratura scientifica – ha portato all'introduzione di diversi elementi innovativi che hanno caratterizzato sia l'approccio riabilitativo – AOT con stimoli 3D, exergaming in MR e metriche di performance per un percorso terapeutico personalizzato – sia la valutazione funzionale della

spalla – introduzione di un insieme di indicatori specifici e discriminanti nuovi per l'analisi della funzionalità dell'articolazione scapolo-omerale. Anche se con diverse limitazioni dovute all'emergenza sanitaria legata al diffondersi della patologia COVID-19, i risultati ottenuti in termini di usabilità e di affidabilità generale – ed in considerazione anche di diverse indicazioni preliminari di efficacia - possono reputarsi estremamente positivi e di stimolo per procedere con lo sviluppo ulteriore degli approcci proposti, che necessariamente richiederà ulteriori fasi sperimentali e di validazione.

ABSTRACT

This thesis work is part of the current and increasingly emerging need to introduce solutions for rehabilitation and functional evaluation that can support the clinician within the diagnostic-therapeutic process with quantitative and repeatable information, and that can be used easily and reliably in outpatient and/or home settings. The research activities described here have been particularly focused on two different application contexts linked to well-defined clinical problems and both associated with the upper limb: **(1)** motor rehabilitation in post-stroke subjects and **(2)** functional evaluation of the shoulder, with particular attention to the scapulohumeral joint; in both cases, the use of integrated technological solutions was introduced within innovative approaches aimed at specific clinical problems.

Regarding the first application context, the thesis activities led to the development of an original solution, based on technologies – easily available on the consumer market – aimed at assisting and extending the procedures normally used for the rehabilitation of the upper limbs in post-stroke subjects; in particular, this approach was based on the introduction of Action Observation Therapy (AOT) integrated with virtual and mixed reality solutions (VR and MR). AOT is an approach identified within the "top-down" type of neuromotor rehabilitation problems and exploits the paradigm of the mirror neuron system; actually, the AOT includes first the observation of the action that the patient will have to perform within the rehabilitation process, favoring the plasticity of the motor system. In this specific context, AOT - achieved through 3D visual stimuli administered through VR headset – complemented the implementation of motor training developed through the principles of "exergaming" in a MR context, where virtual objects – with which the patient could interact – were placed within the real environment. The implemented solution, besides supporting post-stroke rehabilitation by means of the AOT paradigm and the training in MR, proposed also original metrics (i.e., primary key indicator - PKI) based on kinematic measures aimed at quantifying and monitoring patients' performance during the rehabilitation program, to actively adapt the exercise and provide useful information to the clinician on the therapeutic path. Specifically, these measurements were carried out through the use of different magneto-inertial devices (IMDs) which, through appropriate setup and calibration procedures, made it possible to acquire the joint kinematics data of the upper limbs (shoulder, elbow and wrist); in order to make the system adaptive, further information was then collected through a markerless tracking system of the hand movement, integrated with a specially designed and developed framework capable of managing various interaction events

between the patient's hand and the virtual objects, so as to identify the specific task execution strategies realized during the training. From the point of view of software design, the proposed solution presented a separation between the management console (used by the clinician) and the augmented and mixed reality environment, allowing the implementation of a highly flexible approach where a communication channel based on web-socket guarantees the system's expansion capacity both “vertically” – thus including both desktop technologies and more flexible mobile solutions – and “horizontally” – by adding new components and services (e.g., use of integrated IMDs through mobile devices as low-cost solutions for the acquisition of joint kinematics). The configurability of the implemented solution was designed to allow an easy and active adaptation of the exercise (and the associated level of difficulty) to the specific characteristics of the patient within the therapeutic path, and therefore the clinician to define and verify personalized protocols. The proposed solution was evaluated in terms of general usability through a preliminary "proof of concept" study carried out at the IRCCS Don Carlo Gnocchi ONLUS Foundation in Rovato (BS). It is worth underlining how the clinical staff of the institute took part already in the design phase and in the definition of the use cases and implemented exercises, through a co-design approach that led in a short time to the identification of the optimal system. The work carried out has shown how the use of common technologies borrowed from the consumer market, when they are integrated in an optimized way with respect to the context and are supported by a correct design of the application, are effective in supporting clinical operators during their daily work, extending hence the possibilities of standard rehabilitation protocols and procedures. This study also highlighted the effectiveness of MR as a key element in support of the execution phase in the context of the AOT. The activities developed within this first specific application context have presented several innovative features linked in particular to the integration of AOT – achieved through 3D stimuli used by the patient through VR systems – with exergaming approaches implemented through MR, and the identification of different performance metrics that can lead to the definition of adaptive systems capable of supporting highly personalized motor rehabilitation paths, even in the home environment.

The second application context shifted the focus on the need for user friendly approaches that can be used in the outpatient setting for carrying out specific functional assessments; the second part of this thesis then presents and analyzes the development and preliminary results related to the solution for the evaluation of the functional status of the shoulder (SSA). The design phase of the SSA system led to the development of an innovative

solution designed to be performed on mobile devices (such as smartphones and tablets) and integrating the use of IMDs, thus evaluating the functionality of the shoulder in real time with the possibility of identifying the presence of possible pathologies. The proposed system has explored the possibility of using a reduced set of IMDs (2-3 sensors, considering the possibility of interfacing also with technologies made by different manufacturers) and a rapid application protocol, capable of specifically acquiring the kinematics of the scapulohumeral joint. Further, the design phase led to define the possibility of saving data both locally and on databases shared on the cloud, thus allowing the evolution of the condition to be tracked and monitored over time within the rehabilitation process. The proposed approach was preliminarily tested within experimental tests carried out on voluntary subjects. A detailed analysis of the movement data acquired in the first abduction phase on the scapular plane of the upper limb allowed the definition of a set of original primary indicators (i.e., shoulder primary key indicators - SPKI) that have proved effective in classifying the joint function. Furthermore, also in the development of this second application an agile approach has been adopted in the design of the solution, aiming at obtaining high level of usability, considering the specific constraints of the context of use. In addition, the acquired preliminary data allowed the definition of a preparatory analysis aimed at applying specific artificial intelligence solutions (i.e., multilayer artificial neural networks) to create a "clinical support" system capable of suggesting possible classification of the pathological state of the shoulder.

For both clinical contexts identified, the research activities - in addition to the design and implementation of the proposed solutions - was mainly focused on three aspects: (1) possibility of implementing integrated systems that could use devices from the consumer market, (2) co-design of the general approaches realized with the direct involvement of end users (i.e., clinicians), (3) evaluation of the solutions from the point of view of hardware-software usability. In both areas of application, the research carried out - starting from an extensive analysis of the scientific literature – has led to the introduction of several innovative elements that have characterized both the rehabilitation approach – AOT with 3D stimuli, exergaming in MR and metrics of performance for a personalized therapeutic path – and the functional evaluation of the shoulder – introduction of a set of new specific and discriminating indicators for the analysis of the functionality of the scapulohumeral joint. Although with various limitations due to the health emergency linked to the spread of the COVID-19 pathology, the results obtained in terms of usability and general reliability – and also in consideration of various preliminary indications of efficacy – can be considered extremely positive and stimulating for proceed with the further development of the proposed

approaches, which will necessarily require future experimental and clinical validation phases.

ACRONYMS

9DOF: Nine Degrees Of Freedom

ADL: Activity of Daily living

ANN: Artificial Neural Network

AOT: Action Observation Theory

AR: Augmented Reality

ARPL: Android Room Persistence Library

BBT: Box & Block Test

BLE: Bluetooth Low Energy

CIMT: Constrained Induced Movement Therapy

CR: Central Repository

DBMS: DataBase Management Systems

DMD: Dynamic Motion Data

DPS: Data Provisioning Service

DPS: Degrees per second

DTV: Discriminant Threshold Value

EEG: Elecroencephalography

EG: Exergaming

ERD: Exercise Related Data

FANT: FANN Tool

FIM: Functional Independence Measure

FOV: Field Of View

HNN: Hidden Neural Network

HWS5: Degrees of humerus abduction when scapula reaches 5 degrees of upward rotation

HWSS: Degrees of humerus abduction when scapula starts

ICC: Intraclass Correlation Coefficients

IMD: Inertial and Magnetic Device

IR: Infra Read

ISG: International Shoulder Group

IVR: Immersive Virtual Reality

JSON: JavaScript Object Notation

LAN: Local Area Network

LM: Leap Motion

LMD: Leap Motion Device

LULA: Loaded ULA

MAXH: Maximum abduction of the humerus

MAXS: Maximum upward rotation of the scapula

MEMS: Micro-Electro-Mechanical-Systems

MI: Moto Imagery

MIT: Mean Interaction Time

MK: Microsoft Kinect

MN: Mirror Neurons

MNS: Mirror Neuron System

MNT: Mirror Neuron Theory

MR: Mixed Reality

MRPR: Mean Reach Path Ratio

MRT: Mean Resolution Time

MT: Mirror Therapy

NIVR: Non-Immersive Virtual Reality

NN: Neural Network

NPFSG: Non-Pathological Female Subjects Group

NPMSG: Non-Pathological Male Subjects Group

PAR: Partial Area Ratio

PFSG: Pathological Female Subjects Group

PHOENICS: Physiotherapy and action-Observation thErapy: aN Integrated approaCh supported by novel technologieS

PMSG: Pathological Male Subjects Group

PULA: Passive ULA

RCT: Randomized Clinical Trial

SAL: Spectral Arch Length

SDF: Skeleton Description File

SDS: Scapula Delta Start

SP: Stroke Patients

SPKI: Shoulder Primary Key Indicator(s)

SSA: Shoulder Stability Assessment

SUS: System Usability Test

TMD: Tip Max Distance

TMS: Transcranial Magnetic stimulation

TRL: Technology Readiness Level

UI: User Interface

UL: Upper Limb

ULA: Upper Limb Abduction

VAS: Visual Analogue Scale

WAN: Worldwide Area Network

WDS: Workout Description File

WID: Wireless Inertial Device

CONTENTS

INTRODUCTION

1.1 PERSONAL MOTIVATIONS

As an engineer, I always have had a deep interest in new technologies (both hardware and software) to acquire and analyze human motion data with the aim to implement tools to be employed by clinicians and healthcare personnel to easily identify pathologies, which affect our movements. I started working with inertial and magnetic sensors since the late 2010 when I was committed with the design and development of a novel 9DoF inertial device. Since then, I have been always involved in this field of research developing systems for the functional assessment and providing solutions for exergaming able to support patients during the rehabilitation phase.

Given my specific expertise and skills developed in technology for health and information technology, I decided to get involved in designing of innovative and integrated solutions addressing both post-stroke rehabilitation – whose outcomes are of great interest and have positive impact on functional, motor, and cognitive recovery –, and the functional assessment, above all, in an outpatient setting. During this research journey, I was specifically in contact with the mirror neurons theory (that will be detailed later in this thesis), which led my attention towards the action observation therapy and is still maintaining opened the doors to a whole plethora of possible innovations in the field of motor rehabilitation.

This thesis represented the occasion to apply my background and knowledge to better understand and investigate different clinical contexts with the possibility to finally implement integrated approaches, on a strong multidisciplinary basis, which embedded latest hardware and software technologies, thus to realize a self-consistent solution to support and to extends standard clinical protocols and procedures in the field of rehabilitation.

1.2 GENERAL BACKGROUND

In the latest years, new technologies and innovative advances in Extended Reality (XR) – including Virtual Reality (VR), Augmented Reality (AR) and Mixed Reality (MR) – , Artificial Intelligence (AI), robotics, wearable devices – with the recognition of inertial and magnetic sensors – and “big data”, are feeding the technology transfer from the research context to the clinical environment, thus supporting and enhancing the overall diagnostic and therapeutic process and greatly impacting on healthcare management. These new enabling

technologies can be considered a real game changer for the clinical applications, since they are shifting the standard paradigms addressing how patients can be treated, monitored, and examined both in hospital and at home. To make these approaches reliable and effective, it is mandatory to consider large-scale, sustainable, and effective strategies; in fact, implementing innovations is a complex task and there is a need to better understand the key factors that support the successfully introduction of novel solutions, from adopting to sustaining, spreading, and scaling specific approaches. These tasks are particularly important when focusing on healthcare.

In this context, the research activities described in this thesis were focused on a twofold perspective: 1) to exploit an integration of several technologies, even coming from the consumer market, to identify the most effective rehabilitation intervention, which can be considered indeed a recognized priority in stroke research and provides an opportunity to achieve a more reliable and effective impacts [1]; 2) to introduce easy-to-use systems – even integrating mobile technologies – that can be used during the functional assessment and also in outpatient settings. The importance of these topics is also underlined by the increase of the prevalence of muscle-skeletal and neurological pathologies and disfunctions – acute or sub-acute – which are leading to a wide increment of subjects with severe functional limitations [2].

Considering the necessity to evaluate, understand and extend the actual knowledge about mirror neurons theory, action observation therapy and mixed reality, and evaluate the effectiveness of a mobile-based solutions, this thesis also addresses the importance to bring specific technologies and their integration out of the research field into real clinical environments; this requires that the proposed solutions shall be easy to use, fast to setup, have few functional constraints and provide effective and reliable results and data. Moreover, of paramount importance it is the need to break the entry barriers due to clinicians warries about the fact that these technologies – most of the time – are too much time-consuming due to their intrinsic complexity and often cumbersome, due to issues and blocks emerging during normal use.

1.3 MAIN OBJECTIVES

The work of this thesis concerns the research and implementation of innovative integrated solutions supported by novel technologies specifically addressing 1) motor rehabilitation and 2) functional assessment.

In the context of post-stroke rehabilitation, the research on mirror neurons theory recently led to the definition of the Action Observation Therapy (AOT), which represents indeed an effective approach for several neurological pathologies [3], [4]. Starting from the latest scientific literature about this topic, the first aim of this thesis was to realize a full-featured hardware&software solution, which makes use of multi low-cost technologies and consumer devices (i.e., Leap Motion, 3D passthrough ZED mini camera, HTC Vive 3D viewer, and inertial sensors) to provide a reliable and effective approach and to integrate AOT and exergaming through mixed reality. Despite the possible intrinsic complexity of the solution, my work aimed to keep it as simple as possible to use and works without substantial issues. Moreover, during the development phase, particular attention has been dedicated to the user's needs in terms of system requirements and usability; finally, a strong commitment has been dedicated to system-test and system-validation in the most clinical context.

Following the very same approach, a "smart" solution to assess shoulder stability using a mobile phone and a set of two inexpensive inertial and magnetic devices has been developed and deployed on clinical field. The idea behind this work was to provide a rapid and easy-to-use application for shoulder stability assessment based on a set of newly introduced SPKI (i.e., Shoulder Primary Key Indicator) and verify whether such a solution would have been accepted and used by clinicians in their daily work activity.

It is well known that for any solution to have a widespread on the clinical field and find a huge plethora of users, a key aspect is the ratio in between the effectiveness of the solution with respect the overall costs of the solution. For both the main objectives of this thesis, we considered the possibility to adopt inexpensive devices – in general off-the-shelf devices which can be acquired easily on the market – to realize a solution able to provide effective results when directly employed on field. One of the inherent objectives of the work was so to verify if an inexpensive solution would provide effective data and being accepted by clinicians as support in their daily activity. In the overall system designs – as previously underlined – attention has been also dedicated to usability and portability of the solution as key aspects for a more friendly adoption of the solution, and, moreover, as fundamental aspects for the employment of the proposed solution in the context of tele-rehabilitation.

Moving to clinical context, it is worth highlight that the applied research is nothing if not supported by a correspondent basic research aimed to identify the scientific bases and theories on which the provided solution would be lately implemented. In this thesis we also present the scientific research realized to support the design and development of the proposed solutions. The first activity involved research on mirror neurons as key aspect for AOT to

boost solutions based on MR and VR to support and improve post-stroke rehabilitation. On the functional perspective, the shoulder stability assessment system involved research on shoulder biomechanics and pathologies to find out a model able to describe pathological shoulder behavior by means of specific SPKIs.

The research activities related to the application to post-stroke patients was conducted with the great support of domain experts working at the IRCCS Fondazione Don Carlo Gnocchi ONLUS, Rovato (BS), whereas the preliminary validation concerning the assessment of the shoulder stability was realized with the support of Genetica Amica Association, Riva del Garda (TN).

1.4 OUTLINE

This thesis presents the activities realized and the results obtained addressing two specific topics: 1) the research on AOT and MR to support post-stroke rehabilitation, and 2) the research on SSA. Although, for sake of clearness, these topics are reported separately, the main umbrella covering them is based on the need for effective and reliable technological solutions. The thesis starts with the description of the AOT solution, followed by the presentation of the SSA application. Concerning this narrative approach, in order to give more room to the final findings, for each specific context and application, the developed solutions are initially presented as a whole and then the main obtained results are reported, whereas only at the end of the chapter several specific details describing the used hardware devices and their characteristics and the software realization process are highlighted. Finally, at the end of each specific chapter, a discussion on the solutions is presented to close and summarize the topic.

2 ACTION OBSERVATION THERAPY AND EXERGAMING IN MIXED REALITY

This chapter presents the research and development activities exploited in the context of the investigation on AOT, exergaming and MR to adjuvate and extend standard treatments for rehabilitation in post-stroke patients. The section "Background and Main Objectives" presents an overview of the motivations, the objectives, and the expected results of the research. The section "From Mirror Neuron Theory to Action Observation Therapy" details the overall theory behind the work presenting the "mirror neuron system" and the "action observation therapy"; video optimization for AOT and motion analysis for patient's performance evaluation are also presented. The section "Technologies description" presents the software and hardware technologies adopted in the final solution. Technology evaluation discusses advantages and disadvantages about currently available off-the-shelf technologies and their integration, motivating the reasons concerning the choice of the final technological approach. "System Architecture and Integration" presents the overall architecture of the provided solution describing the work done to define the architecture design, the problems faced and the final implementation; this section also presents the issues related to data collection analysis thus to explains which information are acquired and how these are assessed. "Main Results" presents and discusses the experimental phase and the results obtained by on-field application of the implemented solution, which specifically included the definition of a proper clinical trial. Finally, the section "Discussion" presents consideration on the overall work from a general perspective and more specific for the final solution and future works.

3.1 BACKGROUND AND MAIN OBJECTIVES

In the latest year – due also to a global population aging – stroke has been identified as a medical emerging problem that requires immediate attention having a direct socio-economic impact world-wide. It is estimated that there are 4.5 million deaths a year from stroke in the world and over 9 million stroke survivors. Almost one in four men and nearly one in five women aged 45 years can expect to have a stroke if they live to their 85th year. The overall incidence rate of stroke is around 2-2.5 per thousand population. The risk of recurrence over 5 years is 15-40%. It is estimated that by 2023 there will be an absolute

increase in the number of patients experiencing a first ever stroke of about 30% compared with 1983. There is a total prevalence rate of around 5 per thousand population. One year after a stroke, 65% of survivors are functionally independent, stroke comprising the major cause of adult disability [5].

Moreover, with increasing opportunities to reduce this impact, it is important that there are reliable baseline figures on the needs of stroke patients and robust tools for monitoring improvements in outcome [5]. It is in the context of tool to support and extends clinicians in their standard procedure and protocols and in the context of tool to monitor patient's improvement during rehabilitation cycle, that this thesis finds its motivation.

Insufficient motor control compromises the ability of Stroke Patients (SP) to perform activities of daily living and will likely have a negative impact on the quality of life. In this context, stroke impacts – above all – the upper limb functions. As reported in [6] and summarized in [7], upper limb and lower limb motor deficit are the most common disabilities after a stroke event, with an incidence of about 77.4% and 72.4%. More than 50% of stroke survivors suffer from impaired motor function in the upper extremity [8]; starting with a solution targeting upper limb would anyway cover a mayor part of the cases. The UL motion functionality recovery is most of the time difficult, only around 50% of the subjects undergoing UL rehabilitation presents positive and significative results roughly after six months since the beginning of the treatments [9]. Moreover, the possibility to implement occupational and cognitive tasks could even support and provide rehabilitation therapies for cognitive impairments.

Improving Upper Limb (UL) function is an important part of post-stroke rehabilitation in order to reduce disability [10]. UL rehabilitation in post-stroke patients is an undergoing research domain since years ago which aims to identify treatments and methodologies to reduce negative impact of UL post-stroke symptoms, improving everyday activities concerning the arm, wrist, hand, and fingers [11].

Standard and conventional physiotherapy approaches for post-stroke rehabilitation and recovery are traditionally focused on the treatment of the peripheric body parts by means of the repeated execution of the movement to recover. These approaches are a "learning" process where lost motion abilities trying to get recovered by practice. New technologies to improve post-stroke rehabilitation outcomes are of great interest and have a positive impact on functional, motor, and cognitive recovery. The identification of the most effective rehabilitation intervention is a recognized priority for stroke research and provides an opportunity to achieve a more desirable effect [1].

Survey on currently available approaches to improve UL functionality after stroke for daily-live activities, highlighted a relative deficiency of the various proposed solutions [12]. It is important to keep sustaining the research to identify effective and adequate treatments to support UL rehabilitation with particular attention to daily living motor function recovery. Moderate quality evidence showed beneficial effects of constrained induced movement therapy (CIMT), mental practice, mirror therapy, intervention for sensory impairment, virtual reality and a relatively high dose of repetitive task training; evidences also indicated that unilateral arm training may be more effective than bilateral arm training [12].

Following the "mirror neuron theory" (MNT), recently has been widely introduced a new rehabilitation strategy known as "action observation therapy" (AOT), which is centered on the observation of the motor action(s) (which can be a single motor action or multiple sequence of elementary motor actions) executed by other subjects and followed by the repetition of the same motor action(s) by the patient. This new approach has demonstrated to be effective to recover and to maintain motor functionalities and to treat various neurologic pathologies such as Parkinson, stroke, and autism. The same approach has demonstrated to be also effective with non-neurological pathologies such as knee or hip arthro-prothesis due to coxarthrosis or broken femur [13]. Mirror therapy combined with a conventional stroke rehabilitation program enhances lower and upper-extremity motor recovery and motor functioning in subacute stroke patients [14].

Considering this necessity, the MNT and the associated AOT was envisaged as an optimal approach to support and extends standard treatments, protocols, and procedures for post-stroke rehabilitation. Within this context, the activities here presented relied on the PHOENICS project ("Physiotherapy and action-Observation thErapy: aN Integrated approaCh supported by novel technologieS"), which was funded within University of Brescia "Health&Wealth 2015" call and aimed at basic research and industrial transfer by involving public organizations and private companies with two main general objectives:

1. To validate a new methodology to integrates conventional physiotherapy and AOT by means of a "computer assisted" approach.
2. To realize a prototypal implementation usable in clinical environment and for "telecare" solutions [51].

This first section of the thesis specifically addresses the possibility to support AOT-based rehabilitation of post-stroke patients, by introducing novel technologies to provide an immersive MR environment where exergaming is supported by a self-consistent hardware and software solution.

Therefore, the main efforts of this study – beside the basic research involved in the specific context – was accordingly addressed to design and implement a solution, which employs novel technologies – such as leap-motion, 3D passthrough ZED mini camera, HTC Vive 3D headset, and inertial and magnetic sensors, as hereinafter described – all supported by a common software framework developed by exploiting Unity™ (a cross-platform game engine). In this way, we aimed to provide a practical, reliable, and usable solution supporting clinicians in daily therapeutic activities on post-stroke patients, approaching two main objectives:

1. To acquire additional information behind the overall rehabilitation process to analyze patient performance, to develop motion pattern analysis and to support data persistence thus, to have the possibility to assess data over time.
2. To extend standard and well-known rehabilitation procedures by considering the possibility to implement a patient-specific approach.

The advantages of the proposed solution, based on AOT and MR to support post-stroke rehabilitation, are related with the possibility to keep under control the full virtual environment providing various levels and types of rehabilitation ranging from basic rehabilitation games, passing through exergaming up to more complex occupational tasks with the possibility to tailoring the system to the specific patient's needs.

Therefore, this thesis aims to realize a fully integrated solution based on set of novel off-the-shelf inexpensive technologies to support UL motor function recovery using AOT as basic approach. The solution does not want to replace conventional port-stroke rehabilitation practices and protocols, but it wants to extend and to support them, providing an innovative playground into clinicians and doctors hands. The proposed solution would allow to investigate still opened questions or gain insight already known practices. Other than investigate how to improve the overall AOT protocols, there is still the needs for further research related to the amount of dose of the therapy to apply to the patient in various training sessions and in the overall training period in order to have an effective recovery and or to maximize the therapy efficacy [12]. Among possibly relevant parameters which effect the

solution, one of the less investigated in humans, is the perspective from which the actions of the AOT are observed [15]. Ultimately, the proposed solution would allow to investigate how to measure and how to track the patient performance from a static and dynamic point of view. In this context, we present an innovative approach based on inertial devices and Leap Motion™ joined interaction data to correlated static and dynamic arm position with respect time and functional actions such as overall time execution, hand position in object interaction and pick-and-place position. Various basic exercises get proposed and implemented such as target-reaching, reach-to-grasp, pick-and-place, goalkeeper, and occupational task as reported in [12].

The expected results from this work are to realize a self-consistent solution which can be easily adopted in real clinical environment with a positive acceptance by the clinicians and patients and able to provides effective improvement in the overall post-stoke rehabilitation process as extension to the standard rehabilitation procedures and protocols based on AOT. Part of the overall effort has been also dedicated to support user's requests and to fix issues emerging during all – and still now – experimentation phase. The care to the user's requests and to the implementation details – such as easily software configuration and personalization – are fundamental to the realization of solution which would be employed in real clinical environment. Moreover, as a long-term objective and expected results, there is also the envisage of an engineered version of the solution which would be marketable, paving the basis to found of a start-up on the field of rehabilitation technologies. Indeed, the research's objective is to understand if the adoption of MNT and AOT in the final solution would really provide an effective improvement in the patient's rehabilitation process.

The development and validation of the proposed work was possible by embracing domain experts in the field of post-stroke rehabilitation, here represented by the physicians and physiotherapists of IRCCS Fondazione Don Carlo Gnocchi ONLUS (Rovato - BS), who were heavily involved in system design and specification, and during the realization of the preliminary clinical test. Unfortunately, the COVID-19 pandemic heavily impacted on the possibility to fully conclude the clinical validation; however, promising results in terms of usability and system reliability were underlined.

3.2 From Mirror Neuron Theory to Action Observation Therapy

In between 80's and 90's a group of researchers of the University of Parma (coordinated by the Prof. Giacomo Rizzolatti) initiated a set of studies on pre-motor cortex

to study specialized neurons involved in the main control of movements: such as picking of handling objects. During their normal duty on a primate (connected to the devices for register neural activities), the researchers found by chance, that the same neurons that were activated when executing the movement were activated also when the primate was observing the scene where a man was picking-up a banana from a fruit basket [16]. This discovery opens streets to the research on *Mirror Neuron Theory*. Mirror Neurons are a particular class of neurons which get activated when a subject executes an action and also when the subject observes the same action executed by a second subject [17].

This type of neurons (Mirror Neurons) has been found in primates, in some birds and in human being. In human beings these neurons are mainly located in motor and premotor areas of the brain (the premotor cortex is a region of the motor cortex located in the frontal lobe before the primary motor cortex) [18]. Other studies, performed with magnetic resonance, find out that the same neural activity is also present in subjects with amputations or plegias of the upper or lower limbs [19]. On the wave of the research on MNT two different treatments have been discovered to provide effective results to restore motion functions: Mirror Therapy (MT) and Action Observation Therapy (AOT). Rehabilitation therapies based on the mirror neuron theory – mirror therapy and action observation therapy – can activate the mirror neuron system. Activation is critical for the recovery of limb function in patients with strokes [20].

The first use of MT was to treat patient who suffered from a phantom limb pain after amputation [21]. The principles of MT are the use of visual feedback created using a mirror to reproduce a “virtual” illusion of an effective limb to trick the brain into thinking movements has occurred without any pain or to create positive visual feedback of a limb movement. Many studies indicate that mirror therapy and AOT are mainly effective for upper limb treatment, but it has potential as alternative treatment for pain that is difficult to control [22]. AOT has been derived as a novel approach to the rehabilitation process to support and extends conventional therapy, which is centered on repeated execution of the same movement, defining a learning process based on practices. At the contrary, the AOT is based on the observation. In this case the patient observes the action performed by external subjects; and then he/she tries to repeat the same action. AOT has been demonstrated effective for neurological and non-neurological pathologies such as: (neurological) Parkinson, Ictus, Autism, (non-neurological) knee or hip prothesis, gonarthrosis, coxarthrosis and various bone fractures. Researches have indeed shown that the distance of the visible stimulus is an important variable for activating many neurons [23]; underlining

the fact that the characteristic of visible stimulus presented to the patient results to be important to maximize the effectiveness of the overall therapeutic approach. AOT, MT and Motor Imagery (MI, the mental execution of action without an overt motor output), might enhance the efficacy of motor training and/or motor recovery by stimulating the activity of the sensorimotor system. The existence of a shared neural representation would support the hypothesis that Action Observation (AO) and MI may promote neural plastic changes and behavioral improvements in a way similar to movement execution [24]. Other than plasticity, has been demonstrated that AOT can recover broken neuronal circuits [25] and strongly support the overall motor action re-learning [26]. Further research underlines the fact that the AOT, to be effective, does not need to have a real person to reproduce the action nor even the final effector (the hand) has to be seen [27].

AOT efficacy has been demonstrated using Transcranial Magnetic stimulation (TMS) and Elecroencephalography (EEG) comparing patients undergoing traditional rehabilitation protocols with respect patients undergoing AOT rehabilitation protocols [3], [28]. For upper limb hemiparetic rehabilitation an increase of motion capability has been demonstrated using Fugl Meyer scale, on Frenchay Arm Test, on Box & Block Test (BBT), on the Modified Ashworth Scale and on the Functional Independence Measure (FIM) for the Activity of Daily Living (ADL) exercise type. The same approach has demonstrated to be effective even on chronical post-stroke patients, underlining improvements on Wolf Motor Function Test and on the Frenchay Arm Test. Moreover, another study shown how an experimental group which was observing a video reproducing normal walking has remarkably improved walking balancing with respect a reference group which was watching a landscaping video [29]–[32]. Nowadays, literature is still not able to provide a clear answer on the efficacy of AOT in hemiparetic and hemiplegic pathologies, mainly due to a lack of parametric outcomes able to standardize obtained results, underlining the needs to deeper investigate such arguments with more randomized studies [33]. In the next section we present exergaming and mixed reality as key elements to support innovative rehabilitation solutions based on AOT approach.

3.3 Exergaming and Mixed Reality

Virtual Reality can be divided in immersive virtual reality (IVR) and non-immersive virtual reality (NIVR). IVR are all those solutions based on full immersive 3D headsets such as HTC Vive, Oculus Quest 2, and Sony PlayStation VR, just to cite some. All these devices provide a full immersive experience inside a virtual world where the subject itself can be

fully visible or not or even, only some parts of it can be visible (such as hands, arms or legs and foots). The main idea is to virtually reproduce daily living situation in which the subjects get engaged to operate as naturally as possible. In the NIVR the subject is in front of a flat screen (very similar to a computer monitor) where the scene is projected. The user can interact with such systems using mouse, joystick, or other input devices. These solutions are less immersive but are easier to handle and less expensive with respect previous solutions. In the context of IVR the entire world – where the user is set to interact – is purely virtual and artificially recreated. To realize an effective replication of a real world is very difficult, time consuming and expensive. Without considering that each single patient has its own daily living environment which would have to be recreated for each single subject. To overcome this drawback, augmented reality (AR), and mixed reality (MR) provide good alternative approaches. Behind the idea of AR there is the possibility to merge and mix real user's environment with part of the virtual environment or virtual objects. MR, also known as hybrid reality (HR), is a combination of aspects from both the physical and virtual world, generating a hybrid environment where virtual objects can be mapped to the physical environment. There is a light difference in between AR and MR. MR describes virtual objects that are integrated in the physical view, meanwhile AR is more like plain overlay of the virtual objects with respect the real world; furthermore, MR can be realized only using full immersive 3D headsets, whereas AR can be reproduced also on mobile phones. MR allows for the 3D perception without isolating the user from the outside real world [34]. This aspect is very important in clinical environments because it allows the patient to see and easily interact with clinicians without undressing the headset. Additionally, MR better improve the sensation for the patient to be in its normal world avoiding classical problems related with full immersive pure virtual environment such as disorientation, symptoms of motion sickness, disturbance of balance and eye-hand coordination, drowsiness, and even instances of memory "flashback" [35]. Other than physical problems, pure virtual environment open concerns, especially in areas where the sensory stimulation requires high accuracy. Imperfections in the rendering models, limitation of the visual display are all source of artifacts for this type of research [36].

All the previous consideration and the state of the art in literature are key element supporting our work in realizing a solution based on virtual environment where MR is used to extend the possibility for the subject to interact with virtual objects. There are four key elements which are altogether impacting on this thesis and which have been consider when deciding to move research in this direction: the improvement on marker-less motion

detection devices (Leap Motion™, inertial and magnetic devices), an emerging interest and improved technologies for Virtual Reality (VR) and MR, the MNT and AOT, and the socio-economic impact of stroke world-wide. All these ingredients perfectly fit in this phase of the activities, where one of the final objectives is to realize a self-consistent, inexpensive, and easy-to-uses solution to extends and support standard protocols and procedures to treat upper limb post-stroke patients during rehabilitation phase with particular attention to daily live activities. Next section presents and details the methodologies used to integrate AOT protocol in the proposed solution.

3.4 METHODOLOGIES

In the first part of this section, we approach the problem of the visual stimulus for the AOT presenting the motivation to support first person view as the optimal solution. In the second part we present the set of rehabilitation exercises and the overall rehabilitation protocol. In the final part of the section, the kinematic outcomes and usability score are presented and discussed. Furthermore, the establishment of specific approaches is – when required – justified from a neurological, functional, and technological point of view.

3.4.1 VISUAL STIMULUS FOR AOT

AOT is mainly driven by the visible stimuli presented during the AO phase of the overall application protocol. To optimize AOT efficacy, it is mandatory to enhance the response of the mirror neuron system to specific visual stimuli. In this section we justify the first-person perspective in video realization and then we present the video realization process for the proposed rehabilitation exercises.

3.4.1.1 Video Optimization

AOT is composed by two main phases: the action observation phase and the action execution phase. In the action observation (AO) phase the subject is asked to watch an immersive video where the action requested in the execution phase is performed by a third person. In the execution phase the subject is asked to repeat the very same exercise within a mixed reality virtual environment. It is evident that the AO phase plays a very important role in the overall AOT process. During OA phase, several visual features of observed action can impact the level of sensorimotor reactivity in the onlooker [15]. The initial research on MNS was concentrated on the match in between the visual and motor response only. New research on MNS found out that visual perspective is impacting on mirror neurons (MN), as reported

in [37]. Recently, a set of new mirror neurons have been identified which are strictly related with visual properties such as space-position, right or left hand, and for specific directions. For what concerns space-sensitive MN, has been demonstrated that the visual response is influenced by the location in space of the observer motor acts with respect the reachable space (i.e., peripersonal space) and the non-reachable space (i.e., extrapersonal space). This finding suggests that a possible functional role of space-sensitive mirror neurons is that they may set which is the most appropriate behavioral reaction according to the location of the observed action in space [37]. Other recent study highlighted the fact that a particular class of MNs can also provide information concerning the perspective from which the action is observed [38]. Furthermore, a related research, compared effect of real action observation with respect video-clip based action observation. Even though the video-clip based observation is typically weaker respect to live action observation, nevertheless they were consistent and strong enough to be studied. Because of the research is that view dependent MNs play a role in the perception of the visual perspective of the observed action. The latest finding about MNs is related with different MNs activation with respect the *value* the object represent for the observing subject. In this case the "value of the object" means what is the subject's interest for that object, not the object's shape itself. In case of monkey the difference was in between food and devoid of value objects. In conclusion has been found that with the use of "valued object" a larger majority of these neurons were strongly activated [37]. In conclusion, the key results of the latest research on MNs types can be summarized in the following list:

- The distance between the subject and the position where the observed action is preformed impact the effectiveness of the observed action itself.
- The perspective used to watch the executed action effect how the MNs system deals with the observed action.
- Video-clip based representation of the observed action despite the less effectiveness are anyway accepted to be studied.
- The subject's value of the object used in the interaction play a role to improve MNs stimuli.

Among the aforementioned consideration, the less investigated in humans is the visual perspective from which the action is observed [15]. The study reported in [15] assessed the reactivity of alpha and beta mu rhythm subcomponent to various visual perspective defined by the position of the observer relative to the moving subject, these are:

first-person, third-person and later-viewpoint. In conclusion, the strongest sensorimotor responsiveness emerged from **first person** perspective. The next section reports the characteristic of the AO videos used in the proposed solution and the work involved in their realization.

3.4.1.2 Video acquisition

All the research and findings reported in the previous section, have been considered during the exercise definition phase and when realizing video used during the AO phase of the overall rehabilitation treatment. In particular, all the exercises were recorded using a stereoscopic high-resolution wide-angle camera (LucidVR by Lucid Creative with 180 degrees of stereoscopic view); the video get acquired in the same environment used for the execution phase of the AOT process; the video were all recorded in first-person view; the videos were divide by male-female and left/right hand; the video get recorded with undressed arms in order to avoid to impact of possible different clothes; and finally, all the videos get recorded using as much as possible the same objects used for the execution phase, as reported in Figure 1 showing the video realization for exercise "move objects to target" (a) and for the exercise "goalkeeper" (b).

(a) (b)

Figure 1: Examples of video realization. Move objects to target (a) and Goalkeeper (b)

All the videos have been recorded positioning the camera to an height which has been empirically identified to be the hypothetical position of the eyes of the reference subject. During the AOT, the subject is seated on a regulable chair or stool. During the initial setup phase, the chair/stool height is set to have the subject's eyes positioned as much as possible to the same heigh used for the camera when recording the videos, as shown in Figure 2.

Empirical test demonstrated that this configuration reproduces the most realistic effect when watching the video.

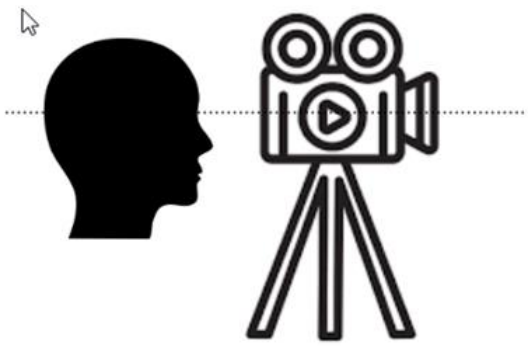

Figure 2: Camera and subject's height position while recoirding video and when executing AOT.

The proposed solution support four different exercises: reaching, goalkeeper, pick-and-trash, and move-objects-to-target. The last one exercise simulates a daily living activity which could be of major interest for the subject. Each exercise has been designed considering both what would be realized in the exercise proposed during execution phase of the AOT and what available to realize the video in a more corresponded way as possible. So, colors and objects have been chosen accordingly when realizing the final video. In the next sections we present and discuss the exercises included in the proposed solution.

3.4.2 UPPER LIMB REHABILITATION EXERCISES

This section presents and review the set of upper limb rehabilitation exercises implemented in the first stage of proposed solution:

- reaching (RE),
- pick-and-trash (PNT),
- goalkeeper (GE),
- move-objects-to-target (MOTT).

Additional exercises could be included in the system if required. As better described later in the document, the adopted architectural approach in Unity allows for an easy and rapidly development of other rehabilitation exercise. In the following of the section, all the four exercise are presented and discussed. Each exercise has a set of configurable parameters which effect the overall difficulty of the exercise, so the final part of the section describes

the level-based approach used to customize the exercise's characteristics. In general – but this can be configured by the clinician which supervise the overall rehabilitation process – the exercise elapsed time and the overall exercise score is shown to the patient inside the virtual environment. There has been a long discussion if such an information should or should not be proposed to the patients during the rehabilitation exercise. From one point of view this information could reduce patient's attention impacting the efficacy of the rehabilitation process, from the other point of view, this information provides an idea of the overall exercise duration and provide information to the patient about the exercise score improving patient's engagement. A specific investigation on this aspect has not been yet performed, but from the result of the usability survey – better discussed in later sections – none of the involved subject complin anything about this topic. The set of rehabilitation exercise have been designed and implemented following the study reported in [39]. In all the exercise, once the patient completes the movement, his/her hand must return to the starting position. To note that all the element in the virtual environment are "physics" enabled objects so they can interact among them and all the virtual objects are subject to "virtual gravity" so they can fall off the table, can naturally interact with the patient's hands and can interact one each other's in a normal natural way.

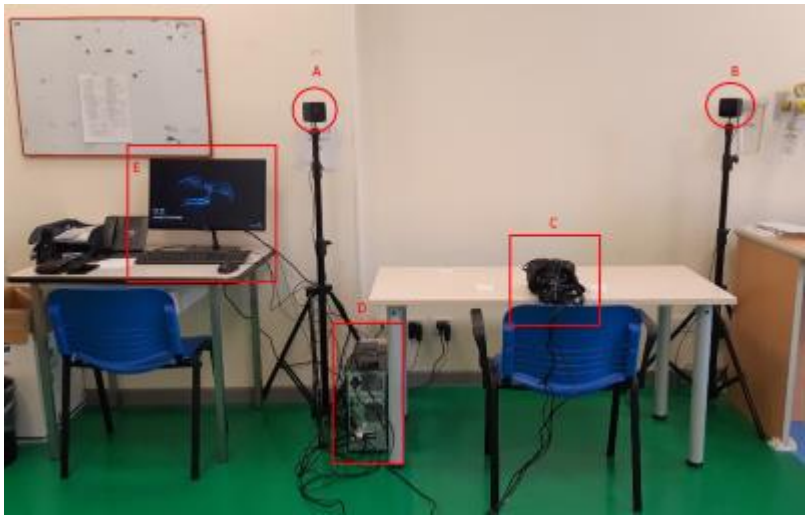

Figure 3: The used setting at IRCCS Fondazione Don Carlo Gnocchi in Rovato (BS).

Figure 3 shows the test area use during on-field test conducted at Don Gnocchi Institute in Rovato (BS). A and B are the HTC Vive headset base-stations, C is the HTC headset with Leap Motion and ZED camera mounted on top of it, D is the PC and finally E

is the monitor where the clinician can control the rehabilitation process using the provided application management console. The same area has been also used to record training video.

The study was approved by the ethical committee of IRCCS Fondazione Don Carlo Gnocchi (Regione Lombardia) on 13th February 2019 (protocol number 09_13/02/19).

3.4.2.1 Reaching exercise

The reaching exercise requires the patient to reach an object in the space ant touch it with any finger. When the virtual object gets touched the object explodes. If the object is not reached within a given amount of time the object gets destroyed and a new object is shown to the user in a different position. Figure 4 shows the reaching exercise from the patient's perspective. This exercise is the easiest exercise among the proposed set due to the following two facts: the task only requires reaching an object and the object is not moving.

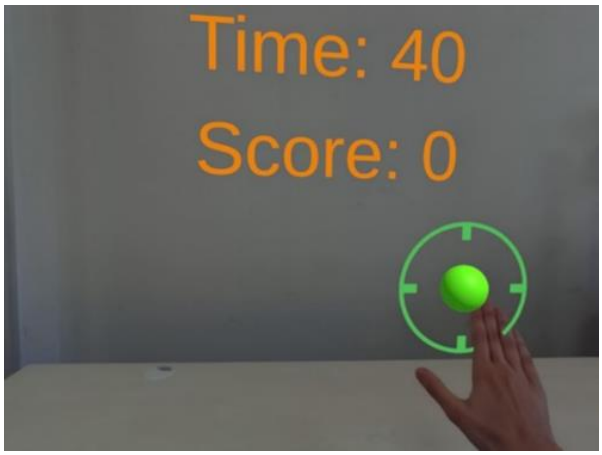

Figure 4: Reaching exercise from the patient's perspective.

Despite the simplicity of the task, reaching is a functional multi-joint task requiring inter-joint coordination in addition to feedback and feedforward control to position the hand optimally at a desired location so that it may interact with the environment. From the literature, biomechanical measures of reaching such as movement time, movement distance and inter-joint coordination have been shown to discriminate changes to hand path quality following brain injury [40].

Various exercise parameters can be configured to change exercise difficulty based on a level scale. Configuration parameters concern the target object lifetime, the delay in between the destruction and creation of a new target object, the size of the target object and finally the size of the volume where the object can be displayed. Figure 5 shows the detailed geometry configuration for the reaching exercise. In the geometry, the 3D zero position is the center of the 3D reference frame (X, Y, Z). The Y zero position in the virtual environment is the floor. Whereas the X, Z zero position is the position of the patient. The volume where to place target objects can be changed in size and position for each supported exercise's level. In general, higher is the level higher is the volume where objects can be shown. The figure shows the volume for the right-hand subjects, the situation is completed symmetric when exercises are planned for left-hand subjects.

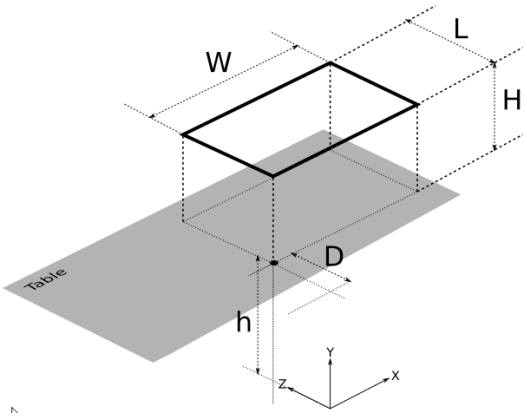

Figure 5: Reaching exercise geometry configuration.

During the exercise execution various time-based event are collected. Such events are *patient start moving the hand* and *patient reaches the target object*. These two events are used to separate the whole motion path in two sub-paths (1) the forward paths from the initial hand position up to the position when the hand reaches the target, and (2) the backward path from when the target get reached up to the final hand position. This approach allows to study motion dynamics for both parts of the whole movement: the forward and the backward paths.

3.4.2.2 Goalkeeper exercise

In the goalkeeper exercise a ball of various sizes is thrown toward the patient from the other side of the table. The patient must wait the ball reaches the very end of the table before trying to block the ball with his/her hand, as shown in Figure 6.

Figure 6: The goalkeeper exercise from patient's perspective.

When touched, the ball explodes. A unity score is gained for each stopped ball. The ball can be thrown starting from the same level of the table, to increase exercise difficulty the ball can be thrown from a higher position, allowing the ball bouncing while approaching the patient. In this exercise, the difficulty gets controlled varying the following parameters: ball size, ball speed and the volume where the ball get thrown.

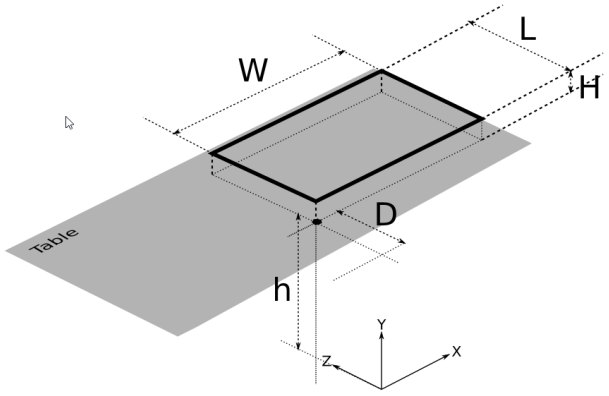

Figure 7: The parametrization for Goalkeeper exercise.

Figure 7 shows the exercise parametrization for the position and size of the volume where ball can be thrown. The parameter H can be zero for the ball not to bounce while rolling toward the patient.

This exercise, with respect the reaching exercise, introduces a one-dimensional dynamic of the target object which is moving toward the patient and patient must coordinate wrist prono-supination to block the rolling balls. Event for this exercise, the time-based collected events are *patient start moving the hand* and *patient reaches the target object*. The two events are used to break down the whole motion path in two separate paths the forward

movement to stop the ball and the backward movement to return the hand to the initial position.

3.4.2.3 Pick and trash exercise

In the pick and trash exercise the patient is asked to pick-up an object from the table and to put the object into a bowl positioned above the table in a specific position, as shown in Figure 8 from the patient's perspective.

Figure 8: Pick and trash exercise seen from the perspective of the patient.

Figure 9 shows the geometric configuration for the pick and trash exercise. In the exercise the target object (represented by a cubic brick) is positioned on the table. In this case there is not a volume but an area where the object can be placed. The target bowl can be positioned anywhere in the playground volume.

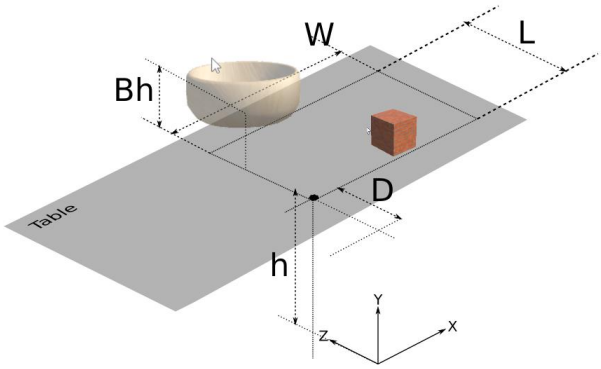

Figure 9: Pick and trash exercise configuration.

The exercise level can be changed changing the sized of the bowl and the size of the target object, changing the position of the bowl – mainly changing the heigh of the bowl with respect the table – and changing the position of the target object.

During the exercise, various time-based events are collected, such events are hand start moving, object picked and, object released. These events can be used to breck down the whole movement in three sub paths, as shown in Figure 10.

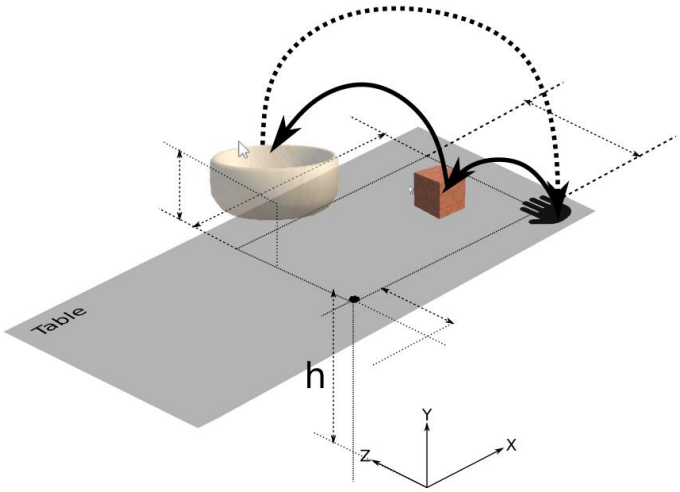

Figure 10: Hand path subdivision for pick and trash exercise.

First path is from the initial hand movement up to the pick-up of the target object. The second path is from the pick-up event up to the release of the target object (eventually in the bowl) and finally the third path is the return path from the release event to the final hand position. This exercise introduces a new level of complexity which is the capability of picking up an object and to move the object to a given target. A unit point is scored if the target object gets correctly released in the bowl.

During the on-field test the clinicians noticed some difficulties for the patient to pick-up the virtual cube. The difficulty in pinching the object arises from the fact that there is no

feedback when the user executes the pinch of the cube, so it results in a not realistic action, and moreover, sometimes, the cube was falling from the hand of the patients. To solve this problem the clinician asked to change the cube with alternative objects such as an octahedron or dodecahedron. Currently, the pick and trash exercise allows the clinicians to choose among a cube, an octahedron, or a dodecahedron, as shown in Figure 11. The octahedron and the dodecahedron both, when lying on the table with one of the flat surfaces, offer an easy to grab vertex, which result must easier to pinch for the patient with a more realistic feedback. The on-field tests shown that the best result get obtained using the octahedron which provides a more prominent vertex to get pinched with respect the dodecahedron.

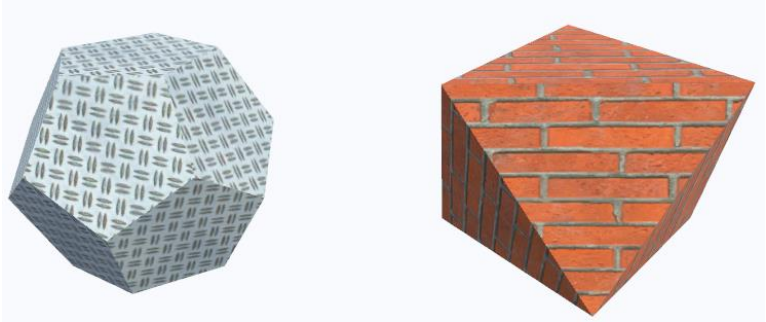

Figure 11: Alternative virtual objects available in pick and trash exercise.

3.4.2.4 Move objects to target exercise

Tha last supported exercise is the exercise called move objects to target. This exercise requires the patient to pinch a virtual object from one side (left or right) and place the object on one of the available targets on the table. In general, in this exercise, the virtual objects are real living everyday objects such as glasses, cola cans or others.

Figure 12: Move objects to target exercise from the patient's perspective.

Figure 12 shows the move objects to target exercise from the perspective of the patient. A unit score is gained each time all the cola cans get placed on the visible targets on the table. The patient has a limited time to complete the exercise, if time ends, the exercise gets reset back to the initial status.

As for the other exercises, also for this exercise a set of interaction events get collected, these are: hand start moving, objects picked-up, object positioned correctly. These interaction events allow to break down the whole path in sub paths which can be analyzed separately. Figure 13 shows the sub path for the current exercise.

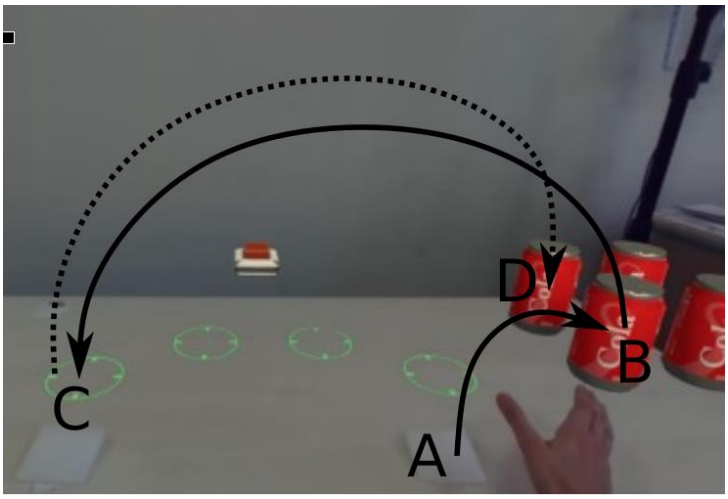

Figure 13: Sub paths for the move objects to target exercise.

The hand of the patient starts from point A to reach the first can on the right, reaching point B where the cola-can get picked-up. The second path goes from point B to the point where the patient decides to deposit the can, let us say point C on the left of the image.

Finally, the hand moves back to the second can on the right, reaching point D and so on, up to when all the cans get placed on the targets. This exercise allows to study the strategies employed by the patient to complete the exercise, for example which cola-can get moved first and which position get filled-in first other than the full path followed to complete each single sub-task.

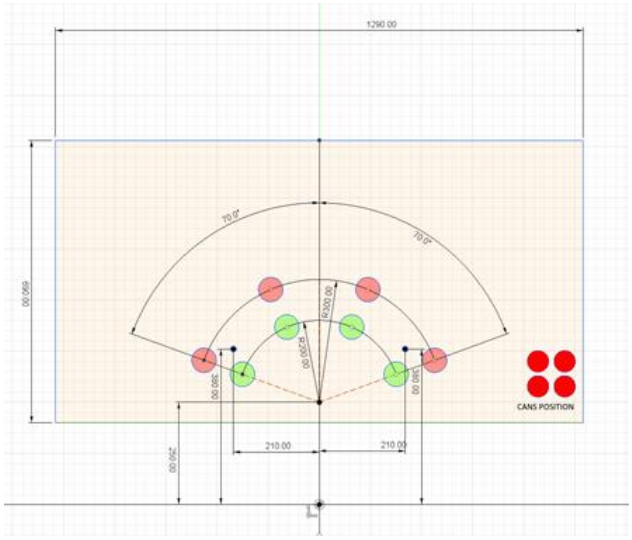

Figure 14: Parametrization of the targets for the move object to target exercise.

As well, in this exercise various parameter allows to configure the difficulty level of the exercise. The configuration parameters are, the size of the cola cans, the distance of the cola cans (from themselves and from the patient) and the distance (relative and from the patient) and the size of the targets. The targets are positioned considering a parametrized arch, as shown in Figure 14. The clinician, for each level, can configure the center of the arch, the amplitude of the arch and the radius of the arch where the targets get placed.

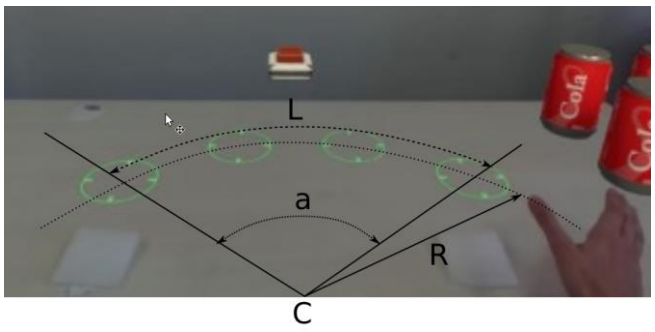

Figure 15: Arch parametrization

Figure 15 details the arch parametrization used to set the position of the targets. The arch amplitude is **a**, the arch radius is **R**, and the arch position is **C**. The targets are then uniformly distributed on the arch length (**L**).

During the AO phase of the rehabilitation exercises the patient must keep the hand steady on the table in the starting position. Moreover, each time an exercise has completed, the patient must return the hand to the starting position before starting over with a new exercise execution. The hand starting position is draws on the table, for example in Figure 15, the left- and right-hand starting positions are identified with two white post-its placed on the table. In all the exercises, the clinician requested a mechanism to monitor the movement of the patient's hand while watching the training video (AO phase). The solution has been implemented with a configurable mechanism able to alerts the clinician when the patient moves the hand outside of a given configurable range with respect the initial hand position. The reference hand position must remain in the view of the leap motion while the patient watch the 3D video. The hand movement are tracked with the Leap Motion and a repeated cycle of measurement is performed to monitor the hand's movement. If the movement of the hand goes outside the hand's region an alarm is shown on the application management console. In this case the clinician can decide autonomously if keep going-on with the exercise or start over repeating the AO phase.

3.4.3 REHABILITATION PROTOCOL

The on-field test conducted at IRCCS Fondazione Don Carlo Gnocchi in Rovato (BS) has been conducted and designed as a between-subjects Randomized Clinical Trial (RCT). A clinical trial is defined as an experiment that involves human subjects in whom treatment is initiated for a therapeutic intervention. In RCT, each patient is assigned to receive a specific treatment intervention by a chance of mechanism [41].

The objective of our clinical trial was to demonstrate the effectiveness of AOT to improve motor function recovery in post-stroke patients. Two randomized group of patients has been identified by a group of domain expertise to have similar characteristic, the Control Group (CG) and the Intervention Group (IG). All the patients undergo to a precise medical evaluation to identify possible characteristic which would impact on the result. Inclusion and exclusion criteria for the two groups has been defined as follows:

Inclusion criteria:

1. Ischemic and hemorrhagic ictus acute patients (3-6 months).
2. Fugl-Meyer scale score between 20-60.
3. Age > 18 years old.
4. Include both genders.
5. Acceptance of the informed consent.

Exclusion criteria:

1. Conjunction of other neurologic diseases.
2. Presence of visual deficit (hemianopia or ipovisus).
3. Neuropsychological deficits that could affect the comprehension of instructions or the treatment execution (aphasia, apraxia or neglect).
4. Mini-Mental State Examination (MMSE) < 24.
5. Orthopedic or musculoskeletal limitations.
6. Clinical instability.
7. Epileptic patients.
8. Subjects with implanted electronic medical devices (pacemakers).

The numerosity of the two groups was identified as reported in a previous study [30] where the upper extremity part of the Fugl-Meyer Assessment scale was used. The IG group were asked to watch the training video scene, in the knowledge they would then attempt to reproduce the same movement task. At the contrary, for the CG, a generic relaxing vide was showed during AO phase. The full AO video administered to the IG group, is the repetition of a single video where the task is reproduced once. The clinician – in the exercise configuration phase – can decide how many repetitions of the training video to show to the patients before entering the execution phase. In other studies the video time duration is used as parameter instead of the number of video repetitions.

The whole AOT rehabilitation session complains a single execution of each of the provided rehabilitation exercises: reaching, pick and trash, Goalkeeper and move objects to targets. Figure 16 shows the overall rehabilitation protocol for both CG and IG groups. In the protocol, various timestamp (T0, T1, …, T4) have been identified. At the time-intervals various evaluations are executed. The protocol starts with the subject preparation and the explanation of the overall rehabilitation protocol, this phase would take about 20 min the first time the patient undergoes to the protocol. The following preparation phases get completed in a shorter time. T0 identify the moment before starting the rehabilitation

process. T4 is the moment the patient completes the rehabilitation process. The whole process takes around 16 minutes to get completed. Longer process has been considered but given the overall preparation time it was not acceptable from a clinician perspective considering also the other daily activities. Moreover, at Don Gnocchi Institute, they must unset the entire room at the end of the daily training session and to setup again the entire room at the following daily training session; this because they cannot leave unsupervised tools around during the night. After each daily room set-up they also have to re-calibrate the HTC Vive headset.

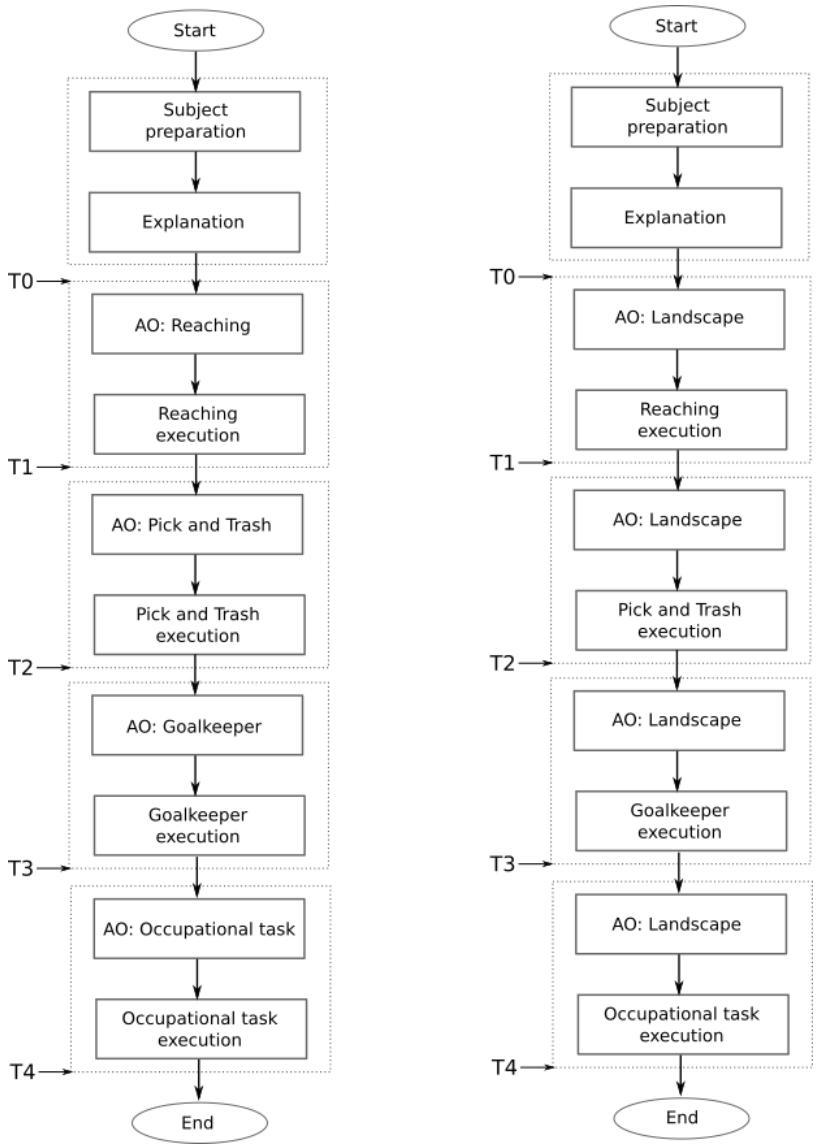

Figure 16: AOT overall rehabilitation protocol for IG (left) and CG (right) groups.

After each exercise (T1, T2, T3 and T4) the following metrics get evaluated (all metrics get explained later in "Metrics for Patient's Performance Assessment"):

1. Reaction Time.
2. Correct task normalized on the overall number of attempts.
3. Mean time of exercise execution.
4. Difficulty level reached.
5. Hand Max Reaching Velocity.
6. %Cycle Hand Max Velocity.
7. Mean SPARC.
8. Mean Reach Path Ratio.
9. Tip Max Distance.
10. Tip Max Velocity.
11. Mean Interaction Time.
12. Mean Resolution Time.

At T0 the following metrics get also evaluated:

1. Upper-extremity portion of the Fugl-Meyer Scale (UE-FM).
2. Autonomy using Barthel Index.
3. Quality of Life (EuroQoL).

In the protocol the exercise phase and the observation phase have the same duration of 2 minutes. At time T4, hand kinematics and Box and Block are also evaluated. At the very end of the rehabilitation protocol (after T4 to be clear) a Likert scale will be submitted to the patients and a usability survey is requested to be filled-out to both the patients and the clinician. Further details about only the quantitative metrics and the overall usability assessment of the system are hereinafter reported.

3.4.4 Metrics for Patient's Performance Assessment

In this section we present and discuss the data acquired, the performed motion analysis and the patient's performance evaluation based on acquired motion data.

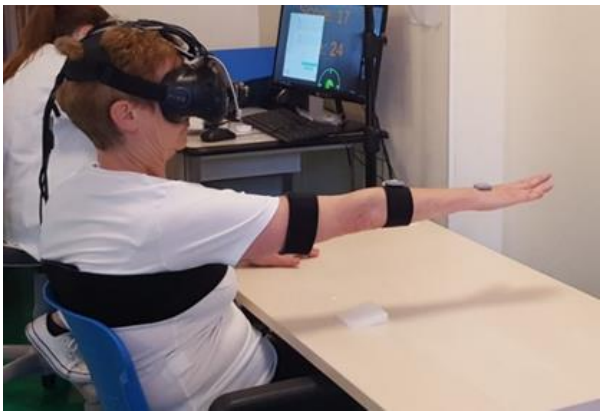

Figure 17: Patient with inertial sensors on the right arm

During AOT various data are collected. Data are collected from within the software engine, using the Leap Motion and using the IMD devices positioned on the patient upper limbs. The collected data can be divided in Exercise Related Data (ERD) and Dynamic Motion Data (DMD) which are both used to assess patient's performance. ERD data are measured during the exercise execution, these are the reaction time, the total number of successful trials with respect the number of repetitions, the time-based events such as object-reached, object-picked, object-released, object-destroyed, the maximum exercise level reached, the overall execution-time for each single exercise repetition, and the overall mean time of exercise execution. DMD data are indeed used to compute dynamic parameters such as Hand Max Reaching Velocity, %Cycle Hand Max Velocity, Mean SPARC, Mean Reach Path Ratio, Tip Max Distance and Tip Max Velocity. ERD data are directly extrapolated by the software during the AOT process, meanwhile DMD data are computed from dynamic data acquired by Leap Motion and by a set of four inertial devices mounted on the patient. Three of the IMDs are positioned respectively on the upper side of the palm, on the forearm and on the upper arm. An extra IMD device is positioned on the patient's chest. Figure 17 shows the patient while training and the three IMUs on the upper right arm are well visible. The following section presents and discusses the kinematic outcomes computed during the exercise execution using the DMD dataset.

3.4.4.1 Kinematic outcomes

The kinematic analysis has been used to extrapolate a series of outcomes used to assess the patient's performances. In order characterize the dynamics of the upper limb movements during the exercise execution we introduced a set of kinematics outcomes some of them are present in literature and wide used to assess such type of dynamics, other

outcomes are less diffuse but of interest in our work. The dynamic parameters are computed following what has been presented in [42] and [43]. Thanks to the time-based events, dynamic parameter can be computed on the whole movement and even for all the sub-movements identified using time-based events.

Hand Max Reaching Velocity (HMRV)

HMRV is the maximal tangential speed of the hand during the reaching phase of the whole movement. This parameter is computed directly from the data acquired by the Leap Motion device mounted on the patient's headset. The HMRV is computed with the following equation Eq 1.

$$v_{max}^{hand} = \max\left(\frac{ds_{hand-palm}}{dt}\right) \quad \textit{Eq 1}$$

Where **ds** is the palm motion space covered in the interval dt and **dt** is the interval sampling time. In the initial reaching movement only the maximum value is considered. This outcome provides a good indication of subject dynamics and motion speed during the exercise execution.

% Cycle Hand Max Velocity (CHMV%)

The CHMV% [44] is the normalized target reach time given as a percentage of the total reach cycle in which the hand reaches its maximum velocity, as described by the following equation:

$$CHMV\% = \frac{tr}{Tvmax}\ 100 \quad \textit{Eq 2}$$

Where *tr* is the target reaching time and *Tvmax* is the total time of the execution (start, reaching and return to initial hand position) where the hand velocity reaches its maximum value.

The data used to estimate this parameter are those acquired with the Leap Motion device; to compute this parameter, the patient's palm speed is used. This parameter provides indication about the target-reaching performance of the subjects providing information about

where in the overall cycle the upper limb reaches maximum velocity, providing information where maximum velocity is located (proximal or distal) with respect the subject.

Mean Spectral Arch Length (SPARC)

The SPARC is a modified version of the SAL (Spectral arch length measure) [45]. SAL estimate movement smoothness computing the arch length of the Fourier magnitude spectrum within the frequency range 0-20 Hz of a given velocity profile.

$$SAL = -\int_0^{\omega_c}\left[\left(\frac{1}{\omega_c}\right)^2 + \left(\frac{d\hat{V}(\omega)}{d\omega}\right)^2\right]^{\frac{1}{2}} d\omega\,;\ \hat{V}(\omega) = \frac{V(\omega)}{V(0)} \qquad \textit{Eq 3}$$

Where $V(\omega)$ is the Fourier magnitude spectrum, $\hat{V}(\omega)$ is the normalized magnitude spectrum respect to the DC magnitude $V(0)$, and ω_c is fixed to be 40π (corresponding to 20 Hz). In SPARC ω_c is adaptively selected based on a threshold $\bar{V}$ and is upper bound by ${\omega_c}^{max}$.

$$\omega_c = \min\left\{{\omega_c}^{max}, \min\left\{\omega, \hat{V}(r) < \bar{V}\ \forall\, r > \omega\right\}\right\} \qquad \textit{Eq 4}$$

SPARC is independent of temporal movement scaling and retains the good sensitivity and reliability of SAL.

Mean Reach Path Ratio (MRPR)

MRPR in general is defined [46] as the ratio in between the length of the arch followed by the center of the palm from the starting point to the target object with respect the length of the direct line in between the two points (optimal path). This index gives an information on how much the patient can optimize the movements.

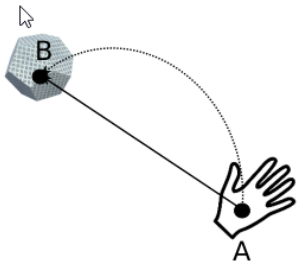

Figure 18: Mean Reach Path Ratio example.

Figure 18 shows an exemplification of the MRPR index. The straight line between A and B is the shortest path and considered the optimal solution for the patient to reach the target object. The arch in between A and B is the real path followed by the patient's palm to reach the target object. The same parameter is also estimated for the subsequent movement required by the patient to move the target object from its original position to the final position, where applicable.

Tip Max Distance (TMD)

The TMD is an estimation of the maximum distance in between the distal index and the thumb phalange which provides the information about the hand aperture capabilities of the patient. This parameter is estimated using the data provided by the Leap Motion device.

Mean Interaction Time (MIT)

MIT is an estimation of the time the patient holds the target object while moving through the target position [47].

Mean Resolution Time (MRT)

MRT is the mean time the patient requires to complete a single exercise repetition; in case of pick and trash exercise this is the time from the hand first movement to the moment where the patient release the target object and the object falls within the bowl.

Both MRT and MIT can be estimate thanks to the time-based events collected by the system. Not all the indexes are estimated for all the provided exercise, the set of indexes depends by the exercise at hand.

The upper limb joint angle are estimated using data provided by IMDs devices mounted on the arm and chest of the patient using what explained in [48], [49]. The procedure requires a good positioning of the device on the right points on the patient's body. The positioning is performed by patient's palpation and driven by the experience of the clinician that has been previously trained in executing this operation.

We consider the devices matching exactly the patient's bone reference system so each MIDs rotation quaternion directly corresponds to the associated bone rotation in the same global reference frame. This approach is the most effective in case of patient with partial impairment [48]. During the initial phase 5 second of data are acquired to determine the initial position of the patient. The following angles are estimated: chest vs. upper arm, upper arm vs. forearm and forearm vs. hand palm (wrist angle).

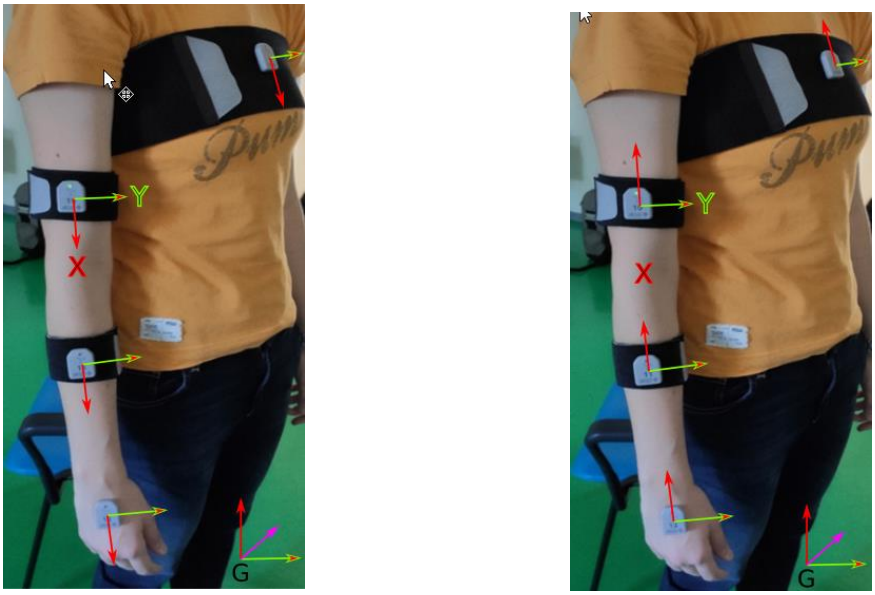

Figure 19: IMD s positioning on the patient's body and device reference frame.

Figure 19 shows the IMDs positioning on the patient's body. The figure on the left shows the device's reference frame, where the green arrows represent the Y axis, and the red arrows represent the X axis. The device reference frames after device frame correction are shown in the figure on the right. After correction, the device reference frame matches the global reference frame G, so devices rotation directly matches the bones rotation in the global reference frame.

To note that after the initial period of on-field tests, we changed the position of the IMD device on the forearm – as shown in Figure 19 and Figure 17 – in order to more reliably acquire pronation-supination movements; the IMD position was specifically moved towards the wrist, as shown in Figure 20.

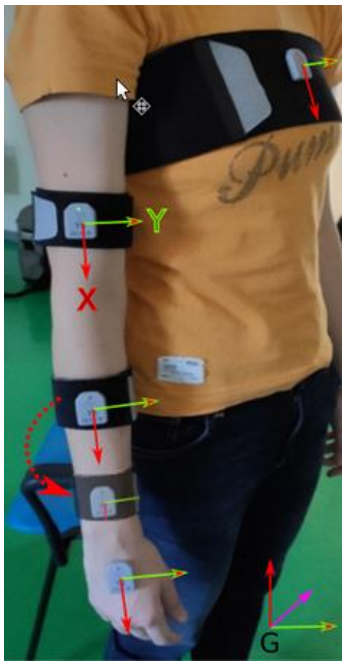

Figure 20: Correct IMD positioning on subject's forearm.

3.4.5 INTER INTRA-OPERATOR CONSIDERATIONS

In the previous section we presented the overall protocol and how the IMDs devices get placed on the patient's upper limb and chest. The IMDs positioning phase is conducted by the same – previously trained – clinicians using palpation and "experience". As we have already reported concerning the mispositioning of the forearm IMD device, is evident that IMDs position on the body would change from time to time for the same clinician and among different clinicians that would execute the same IMDs positioning task. Different IMDs positioning changes the overall motion data acquired for the upper limb, directly changing the estimated kinematics outcomes. Intraclass correlation coefficient (ICC) measures how much the acquired data would change among different application by the same subject or among the application by different subjects.

Intraclass correlation coefficient (ICC) is a widely used reliability index in test-retest, intra-rater, and inter-rater reliability analyses [50]. In particular, Correlation Coefficients are

measures of agreement between paired variables (xi, yi), where there is one independent pair of observations for each subject [51]. In a simple form the ICC is an index that express the fact that results are independent by the subject that prepared the environment and the patient for data acquisition.

Despite we consider this analysis an important aspect of the overall investigation – also because it would somehow impact the proposed protocol – in this initial phase of the work, we did not take in consideration the analysis of this problematic. As already explained, the initial phase mainly concentrates to evaluate the usability of the system – for clinicians and patients – and to initially estimate the patients' performances using an exercise-based metrics. As an extension we added other kinematic outcomes based on upper limb kinematic data acquired with IMDs devices. Such data would be better investigating and improved once the system would have been completed and fully accepted by clinicians and patients. Moreover, inter and intra-operation data have not been possible to be investigated do to the COVID-19 pandemic event which stopped the on-field test. We hope to proceed soon to a new on-field test phase where more data could be acquired, and inter- and intra-operator effect could be correctly approached and investigated.

3.4.6 USABILITY SCORE FOR SYSTEM ASSESSMENT

In the recent years lot of regulation at European level has been introduced to improve medical device security for the user and for the patients, with reference to risk management and usability. ISO standard defines many classes to identify the risk of the device or solution at hand. These changes began in 2016 when major changes took place in European's medical device regulatory regime to face the concern that the market is becoming full of too many products being rushed to consumers without enough proof for their suitability for release.

In this work we concentrated to evaluate the usability of the proposed solution without for the moment to proceed to a risk assessment for the solution itself. The work has been conducted following the guide lines reported in [52]. The mayor aspects we concentrated on with this usability evaluation is the collection of the system failure, the acceptance of the solution by the clinician and the acceptance of the solution by the patients. The acceptance by the clinicians concerns mainly about stability and adherence to the planned use-cases, meanwhile for the patient the acceptance concerns the usability of the adopted devices for what concerns wearing and using during a training session. Usability can only be defined in the context where the technology is used so the measure of the usability must necessarily be defined in that context [53] as requested by ISO-9241-11 and

the European Community ESPRIT project MUSiC. In our case the System Usability Test (SUS) has been evaluated on the bases of a 10 questions survey. Each question has five optional answers. The subject is asked to rate each question with a range from 1 (strongly disagree) to 5 (strongly agree). The final score gets computed using following equations:

$$X = (\sum \text{odd} - \text{numbered questions}) - 5 \qquad \textit{Eq 5}$$

$$Y = 25 - (\sum \text{even} - \text{numbered questions}) \qquad \textit{Eq 6}$$

$$\text{SUS Score} = (X + Y) \text{ x } 2.5 \qquad \textit{Eq 7}$$

The highest score is 100 where each question has a weight of 10. The average score is 68. The general scheme used is reported in Table 1.

Table 1: SUS score

SUS Score	Grade	Adjective Rating
> 80.3	A	Excellent
68 – 80.3	B	Good
68	C	Okay
51 – 68	D	Poor
< 51	F	Awful

Other outcome used to evaluate the SUS score, are the Completion Rate (CR), Error-Free rate (EFR), Time on Task, and subjective patient's and clinicians' opinions about the system.

Completion Rate (CR)

The CR is measured as the percentage computed on the number of successfully completed trials with respect the total number of trials. A failure is considered the impossibility to complete the exercise or the impossibility to obtain a valid score. Moreover, if a patient needs assistance to achieve a correct output, the task gets classified as failed.

Error-Free Rate (EFR)

EFR is the percentage of patients who completed the task without any errors.

Time on Task Rate (TOTR)

TOTR is the time requested to a patient to complete the task.

3.5 TECHNOLOGIES DESCRIPTION

The final implemented solution in term of architecture, software adopted, devices used, and the overall integration has not been immediately available, but has been the result of a continuous process of implementation and evaluation of various alternatives for what concerns software and hardware up to the identification of the final optimal solution. In this section we briefly present the various steps we have been going through to reach the final proposed solution.

3.5.1 TECHNOLOGY ASSESSMENT

At the very beginning, the solution was implemented with the use of 3D headset and the Microsoft Kinect (MK) as a device to acquire patient's upper-limb motion data and to replicate such movement in the virtual environment. Many studies reported good results of the use of MK in rehabilitation and for motion captures [54]–[57]. Supported by these and many other studies, we started to investigate the possibility to use MK to acquire motion data and to replicate movements in the 3D virtual environment applying such movement on a patient's avatar. The use of MK allows to avoid the use of wearable inertial devices to acquire motion data; meanwhile for fully detailed hand and finger motion tracking the Leap Motion was still needed.

The initial idea was to use a fully 3D virtual environment where the patient's get included in term of a pure virtual avatar where patients' characteristics and ethnicity were replicated with maximum fidelity.

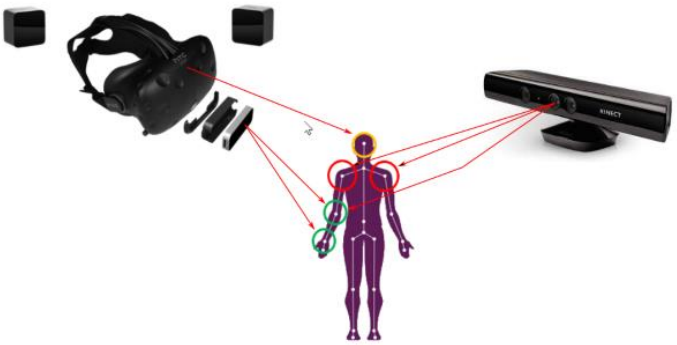

Figure 21: Controlled part of the body when MK was used as motion tracking solution.

In the initial approach, the HTC Vive headset was used to acquire the patient's head motion; meanwhile, MK was used to acquire the neck, the shoulder, and the upper arm kinematic and finally LM (Leap Motion) was used to acquired lower arm and hand kinematic, as shown in Figure 21.

Figure 22: 3D Virtual environment seen by the patient's perspective.

Figure 22 shows the initial results and experimentation with the proposed approach. For the patient's hands we found very realistic 3D models as for example those reported in Figure 23. Thanks to the LM SDK it has been possible to apply the acquired motion data for each single bone of the hand to the 3D hand model, providing a very realistic effect.

Figure 23: Realistic 3D hand model.

Despite the promising initial results, we immediately faced numerous problems related with the proposed approach. Here is the list of problems emerged during the initial experimentation phase:

- The need to merge the hand 3D realistic model with the 3D patient's model.
- The need to replicate real environment in 3D virtual environment with realistic similarity.
- The need to join MK motion data of upper arm with LM motion data of lower arm.
- The need to replicate patient's ethnicity features on the patient's avatar.
- The need to have realistic hand motion in any possibile conditions.

All these major problems and many smaller problems were not impossible to resolve, but the required effort was not acceptable; consider for example the effort require to replicate patient's ethnicity in a realistic manner or even the effort required to reproduce realistic environment whereas a minimum error would have unknown impact on the final validation of the proposed solution. Moreover, other technical problems emerged during the initial development. Moreover, the main technical problems can be summarized in the following list:

- Microsoft Kinect performance with different light condition.
- IR interferences in between Leap Motion and Kinect.
- Loss of Kinect bones when bones get hidden behind other part of the body.
- Loss of Leap Motion hand rendering in particular hand's position.

Even moving from Kinect v1 to Kinect v2 the reported problems remined. Moreover, the IR interferences problems in between MK and LM get worst moving from Kinect v1 to Kinect v2 since Kinect engineers augmented IR intensity to improve Kinect precision and at the same time to reduce external light interferences.

Moreover, if the LM performances were acceptable to replicate human interaction with virtual objects, the seme was not true for the hand's motion rendering. In conclusion, the results were not acceptable in term of realistic hand motion feedback. Too many details were emerging which would have produced uncertainty on the result of the experimentation. After a deep work to try to mitigate and eventually remove all the side-effect and discussion with domain expertise, we decided to move for a totally different approach. Instead to try to reproduce a full 3D virtual environment, we moved for a more realistic approach based on MR where a passthrough camera is used. The new approach has many advantages with respect initial approach; in particular, we do not need to replicate patient's body nor replicate virtual environment dedicating effort only to provide a realistic interaction feedback of the patient's hands with the virtual objects. In conclusion the MK device was abandoned deciding to use IMDs wearable device to acquire patient's motion data. LM get used to provide patient's interaction with virtual objects and to acquire hands kinematic, and Zed Mini has been adopted to support passthrough camera to support MR.

In the following of the document, we present the technical details of the devices used to realize the final solution: HTC Vive Headset, Leap Motion, Zed camera, and the Cometa WaveTrack Inertial System.

3.5.2 Devices Characteristics

This section presents and details the technical characteristics of the hardware devices adopted to realize the proposed solution.

3.5.2.1 HTC Vive Headset

The HTC Vive Headset, shown in Figure 24, is a 3D head mounted display able to provide immersive experiences in 3D virtual environment. The screen is realized with a dual AMOLED 3.5'' diagonal, with a resolution of 1440x1600 pixels per eye which in turn provides a combined resolution of 2880x1600 pixels. It has a refresh rate of 90Hz with a field of view of 110 degrees. The device is a powerful solution to provide immersive 3D game experiences. These solutions are continuously improving augmenting resolution,

refresh rate and reducing weight. Latest solution supports a wireless communication channel avoiding wearing problematic cables.

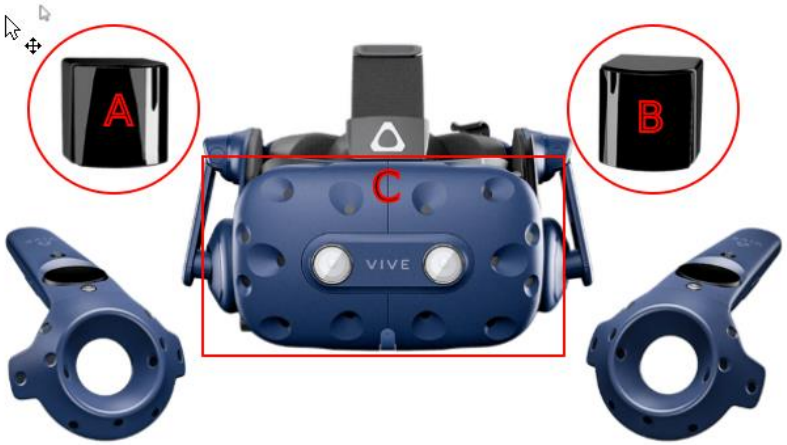

Figure 24: HTC Vive headset.

The full headset is composed of two base stations (A and B in Figure 24) and head mounted device (C in Figure 24) of a weight of around 563g. Two controllers are also available, but not used in our work. The two base stations are infrared devices which recognize the position of the headset in the virtual environment with a covered area of about 3x3 meters providing a good precision on head position and video resolution. This equipment can be bought on the marked to an affordable price for around 500 to 800 euros depending by the acquired set. Despite to be designed for gaming, this device has been early adopted in field of immersive VR motor rehabilitation also for patients with neurological deficits [58]–[60]. Freely available SDK (for Unity and Unreal game engines) allows for an easy integration with our development platform. Borrego [61] proposed a comparison in between the Oculus Rift (a market-available valid alternative to HTC as 3D headset mounted display) with HTC Vive in term of the working range of head tracking, the working area, the accuracy and the jitter in a room size environment in order to evaluate the feasibility to employ such devices for exergaming, rehabilitation and health-related applications. As a result, the study highlighted the fact that HTC Vive provided a working area larger twice the area covered by Oculus Rift (the HTC Vive presented a working range of 7 m, meanwhile Oculus Rift presented a working range of 4.25 m). Both devices showed excellent and comparable performance at sitting height (accuracy up to 1 cm and jitter <0.35 mm), and the HTC Vive presented worse but still excellent accuracy and jitter at standing height (accuracy up to 1.5 cm and jitter <0.5 mm). Note that these consideration could have changed in the latest

months due to a continuous improving of such technologies. In Table 2 is reported a comparison between the technical specification of the two systems.

Table 2: Technical features of the devices selected to be integrated into the system.

Technical Feature	**Oculus Rift**	**HTC Vive**
Display	OLED	OLED
Display size (mm x ppi)	90 x 2456	91.9 x 2446
Resolution (pixels)	2160 x 1200	2160 x 1200
Refresh Rate (Hz)	90	90
Field of view – horizontal (°)	94	Big (Ø = 120 mm)
Field of view – Vertical (°)	93	113
Lens Type	Fresnel	Fresnel
Sensors	Accelerometer, gyroscope, magnetometer	Accelerometer, gyroscope
Integrated camera	No	Yes
Wireless Technology	Bluetooth	Bluetooth
Weight (g)	470	563

3.5.2.2 Leap Motion Controller

The Leap Motion Controller (LMC) is an optical hand tracking hardware module that captures the movements of hands in real time with a good accuracy. The device is a low cost off the shelf device which can be easily found on the market. From the technical data the manufacturer reports an accuracy in fingertip position estimation of approximately 0.01 mm. The device is capable of tracking hands with 3D interactive zone which extends up to 60 cm or more, extending from the device in a 140x120 degrees almost as the typical field of view. The device firmware and software can discern up to 27 distinct hand elements include bones and joints and track them even when they are obscured by other parts of the hand.

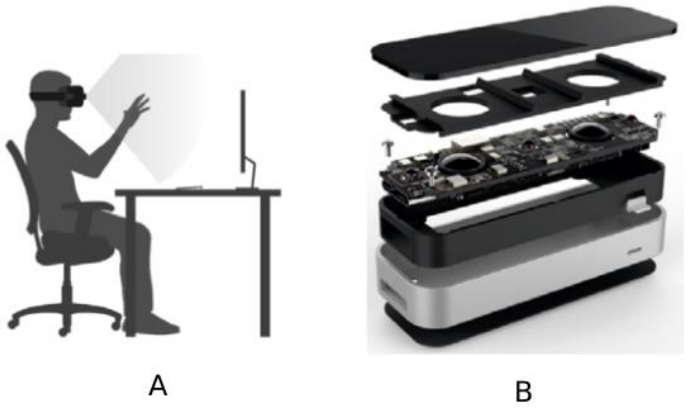

Figure 25: Leap Motion Hardware.

The LMC device can be mounted on the headset or let it lay down horizontally on the table. The better results are obtained with device mounted on the headset because the subject would watch to the hands when interacting with objects in the virtual environment.

The manufacturer also provides plugins for Unity and Unreal game engines to support application development. The software is compatible with Windows and Mac OS X. The device is connected to the workstation with a USB 2.0 standard port. The device is composed of Two 640x240-pixel near-infrared cameras; spaced 40 millimeters apart; with infrared-transparent window, operate in the 850 nanometer +/-25 spectral range; typically operates at 120Hz; capable of image capture within 1/2000th of a second. Figure 26 shows the measures of the LM device.

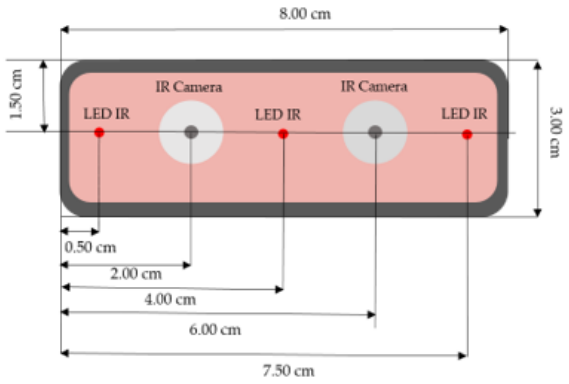

Figure 26: Leap Motion Controller measures.

As for Kinect, also for LM there are many studies which evaluate such device in field of rehabilitation [62]–[64]. In particular, Weichert in his study [65], presented the evaluation of the Leap Motion Controller in term of accuracy and repeatability for both static and dynamic conditions. In static test an axis-independent deviation between a desired 3D

position and the measured positions less than 0.2 mm has been obtained. In case of dynamic test an accuracy of less than 2.5 mm could be obtained (average of 1.2 mm) and good repeatability (less than 0.17 mm). A second interesting study has been completed by Smeragliuolo [66]. In the study, wrist flexion/extension and radial/ulnar deviation showed good overall agreement (r=0.95; RMSE=11.6°, and r=0.92; RMSE=12.4°, respectively). However, when tracking forearm pronation/supination, there were serious inconsistencies in reported joint angles. Hand posture significantly influenced the quality of wrist deviation and forearm supination/pronation, but not wrist flexion/extension. The study concludes that the LM can provide data that are clinically meaningful for wrist flexion/extension, and perhaps wrist deviation. It cannot yet return clinically meaningful data for measuring forearm pronation/supination. In our solution the LM device is used only to acquire time-based events and to allows the user to interact with virtual objects, so the forearm motion data are acquired using IMDs devices instead. The reported result support our approach where the positioning errors for what concerns static and dynamic measures are enough to provide a realistic feedback for what concerns the interaction with virtual objects.

3.5.2.3 Zed Mini Passthrough Camera

The Zed Min passthrough camera (https://www.stereolabs.com/zed-mini/), shown in Figure 27, is a low-cost device able to captures high-resolution stereo video to experience mixed-reality applications in 3D. The ZED is the ideal solution to implement MR applications.

Figure 27: ZED mini passthrough camera.

Its light weight of about 62.9g and the compact size (124.5 x 30.5 x 26.5 mm) allows the ZED to be easily mounted on the HTC Vive headset. The ZED requires a type 3 USB Type-C connector which require relatively new hardware to support a data transmission rate of up to 3 Gb/s. The video output ranges from 100 fps for a WVGA resolution to 15 fps for

a full 2.2K resolution which corresponds to a 4416x1242 pixels. The depth range of from 0.1 to 15 m with a FOV (Field Of View). A motion sensor with accelerometer and gyroscope allows for a position update frequency of up to 100Hz with a very small position drift of 1% for translation and 0.013 deg/m for rotation. The lens provides a FOV of 90 (H) x 60 (V) x 100 (D) degrees. This is not a particularly wide ranges, but we have experimentally seen it is quite adequate for the proposed solution. As for the LM and HTC Vive, the ZED provides freely available Unity SDK to support ZED camera into Unity based solutions.

This device can determine distances between objects through the analysis of the displacement of pixels in the images recorded by the two lenses. This depth perception of the camera is utilized by the device to correctly estimates where to put virtual elements in the scene and recreate depth perception also in the MR environment. Furthermore, the device can estimate its position relative to the real world (positional tracking). Movement of the subject in the 3-dimensional space is tracked with the use of information sent by motion tracking sensors with six degrees of freedom. Another interesting feature is the ability to internally store a spatial representation of the environment that is updated while moving and discovering the surrounding space. Heuristic maps are created, through artificial intelligence algorithms, and those are used to give users a more reliable perception of realness in the scene. It is also used to remove errors introduced by sensors, like positional drift that accumulates over time, comparing the map previously recorded with the new one and optimizing results (loop-closure technique).

3.5.2.4 Leap Motion and Zed Camera Calibration

Figure 28 shows the Zed Mini passthrough camera and the Leap Motion device mounted on the HTC Vive headset.

Figure 28: Zed Mini camera and LeapMotion position on the HTC Vive headset.

Leap Motion performs hand tracking and allows to interact with virtual objects providing grabbing and poking as much as in real life. Zed Mini provides the MR/AR passthrough capabilities to bring AR/MR to a new experience.

Clearly the Zed and the Leap are not perfectly aligned so a difference in between the real physical hand position and the virtual hand position my occur. During our initial experimentation and during the on-field test this misalignment produces a very frustrating effect to the subject which is no more able to interact naturally with the virtual environment.

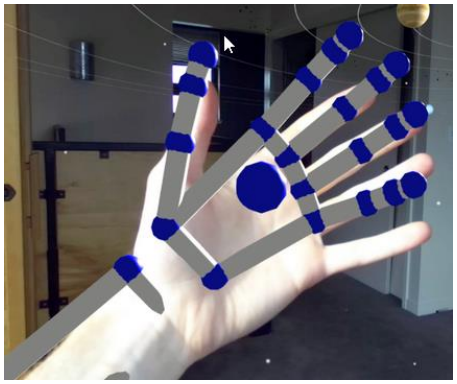

Figure 29: Physical hand and virtual hand misalignment example.

Figure 29 shows the example of misalignment in between the physical hand and the virtual hand due to Zed and Leap different positioning. As much as these two devices are misaligned, as much as far is the virtual hand with respect the physical hand. In this section we present how is possible to correct this error using an offset transform in Unity.

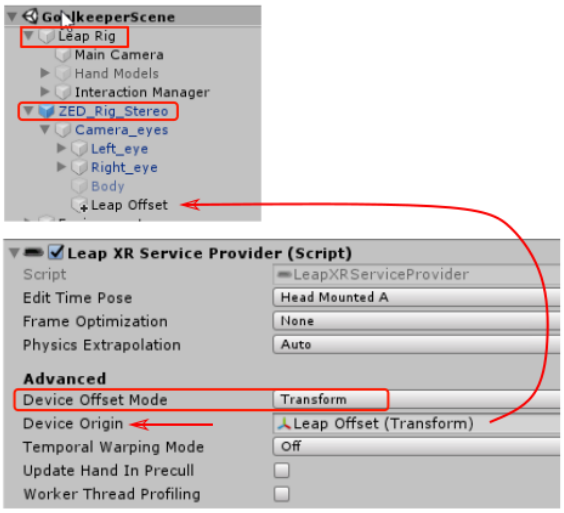

Figure 30: Goalkeeper scene in Unity: Leap Motion and Zed integration.

As shown in Figure 30, each scene must have the Leap_Rig object and the Zed_Rig_Stereo object. The Leap_Rig controls LeapMotion and Zed_Rig_Stereo controls the ZED camera. In the Leap XR service sets Device Offset Mode to “Transform” and set Device Origin to point to Laep Offset object in the Zed_Rig_Stereo object. The Leap Offset is a Transformation object where values on X, Y and Z represent the rotation on the three axes to align the ZED camera frame with the Leap Motion frame.

At this time, the Leap Offset is estimated empirically following the given procedure:

- Open a scene (e.g., Goalkeeper scene).
- Enable the option to set visible the Leap Motion virtual hand.
- Change the Leap Offset Transform.
- Verify the hand vs. virtual hand alignment moving the hand around in the space.
- Repeat until the hand and the virtual hand alignment result acceptable.

By experimentation we have seen that the most important calibration is the Y axis, but also the other axes are important. After calibration, the result would be as the one shown in Figure 31.

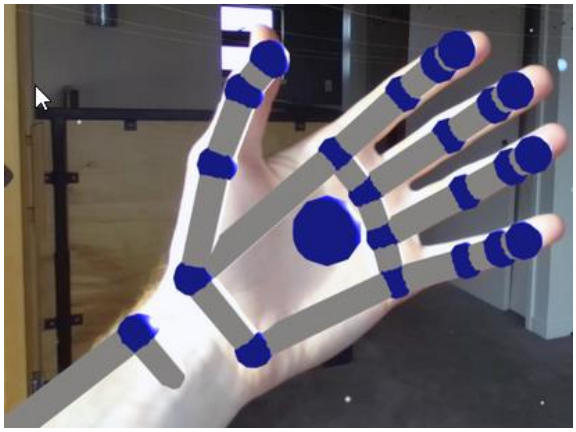

Figure 31: Physical hand and virtual hand after calibration.

The ZED camera vs. Leap Motion calibration process is not easy nor fast to be completed, it requires some time to find out empirically the optimal Transformation also since you must put on and off the headset each time you change the Leap Offset transformation. Fortunately, this calibration process must be performed once the first time the ZED camera and the Leap Motion get mounted on the headset. Recalibration is required each time the ZED and the LM change position one each other. Future improvement task – also in the plan to realize a marketable solution – would review this calibration process to

provide an automatic procedure and algorithms to better estimate the Leap Offset roto-translation matrix.

3.5.2.5 Inertial Measurement Units

For the tracking of the complete upper limb kinematics, three different inertial measurement solution were integrated, and a dedicated interface was implemented. Among various available solution on the market, we chose the following:

- Cometa Wavetrack, by Cometa Systems (Figure 32, A).
- Notch Pioneer Kit, by Notch Interfaces (Figure 32, B).
- DOT by Xsens (Figure 32, C).

(A) (B) (C)

Figure 32: Cometa Wavetrack (A), Wearnotch (B) and DOT by XSens inertial sensor system used for upper limb movement tracking.

Of the adopted technologies for UL motion tracking, the Cometa Wavetrack is the professional one, meanwhile the other two represent the off-the-shelf inexpensive solutions.

Cometa Wavetrack Inertial System (CWIS)

The CWIS is the professional choice. The technical characteristics are reported below:

- 10 grams of weight, as much as two regular A4 sheet of paper (smallest in the market).
- 70 or 140 Hz of fused data (quaternions) with 9 Dof.
- 140 or 280 Hz of fused data (quaternions) with 6 Dof (highest in the market).

- 280 Hz of raw data (accelerometers, gyroscope, magnetometer), highest in the market.
- Same sampling frequency for any number of channels involved (from 4 to 32).
- 8 hours battery life (one full day of operation).
- Basic software for acquisition for research.
- Compatible with Wave Plus receiver.
- Memory on board for remote synchronous recording.
- Inductive recharge (compatible with all Wave chargers).
- Possible to have it waterproofed for underwater acquisitions.
- Full SDK for total control of the hardware and the acquisition via USB.
- Up to 50 meters indoor transmission range.

The CWIS provides an easy to integrate C# library which allows full control on the system. By our on-field experience, using this solution we could identifies pro and cons, as reported in Table 3.

Table 3: Pro and Cons of Cometa WaveTrack Inertial System.

PRO	**CONS**
Small devices	Quite expensive
Good system stability	Incompatibility with USB device when integrating with Unity.
Easy to use API	Needs of external received
Up to 8 devices	

One of the more significative cons of the CWIS is the incompatibility of the USB device with other USB devices connected to the same PC when integrating with Unity. To fix this problem, we had to move the code implementation for the UL motion acquisition from the Unity to the external console application. Another drawback of this solution is the fact that to use four device you must move around a full set of 16 devices (8 inertial devices plus 8 ECG devices) all fit in a carry-on baggage, with an extra receiver to be connected to the PC. The carry-on baggage works also as recharger for the wireless devices.

To reduce complexity and costs, other two wireless inertial devices kits have been considered: **Notch Pioneer Kit** by Wearnotch and the **DOT** by Xsens. The two kits are inexpensive alternative to Cometa Wavetrack providing a more portable and easier solution to use. The only drawback of these kits is the fact that both kits support only Bluetooth communication channel, and the SDK is available only for Android or iOS. To integrate these two kits, an Android gateway application has been realized providing a wireless communication channel with a dedicated JSON command/response protocol to communicate with the implemented console application, as better explained in section "Improvements" in Chapter 3.

Notch Pioneer Kit by Wearnotch

Notch Pioneer Kit is a practical solution sold in a compact package of 6 devices where the container itself exploit the function of battery recharger, as shown in Figure 32 (B). Each device is equipped with 3 high-accuracy MEMS sensors, including an accelerometer, a gyroscope, and a compass with a total weight of only 10 grams. On board memory allows to motion capture without a constant smartphone connection. Bluetooth Low Energy allows to reduce battery consumption. Technical specifications are reported in Table 4:

Table 4: Notch Pioneer Kit technical specifications.

Gyroscope	±250, ±500, ±1000, ±2000, **±4000 dps**
Accelerometer	±2, ±4, ±8, ±16, **±32 g**
Magnetometer	±4/ ±8/ ±12/ ±16 gauss
Sampling frequency	5Hz, 10Hz, 20Hz, 40Hz, 50Hz, 100Hz, 125Hz, 200Hz, 333Hz, 500Hz
Sample rate	100Hz in real-time and 500Hz in non-real time

Moreover, properly calibrated Notch devices static accuracy is about 1-2° yaw/pitch/roll. The devices are waterproof and mount a multi color RGB led which results very useful when identify device to bone association. The charging time is around one hour and the battery charge last for about 6 hours.

The provided SDK is very completed, stable, and easy to use and to integrate. Various high-level services are available such as a 3D avatar to show the body movement in real-time and a default calibration procedure.

The on-field use of this kit demonstrated to be very practical and easy to use, the only drawback was the need to recalibrate the device daily the first time they get used. The gyroscope tends too often to lose calibration and a fastidious rotation drift is sometime present. Nevertheless, the calibration solves the problem. To mention the fact that we used a quite old version of the Pioneer Kit, considering the speed of technology improvement for MEMS devices we expect recent kits would provide better stability.

DOT by XSens

XSens is one of the world industry leaders in motion tracking technologies based on MEMS devices. DOT kit (shown in Figure 32 (C)) is a quite new solution and the first inexpensive solution proposed by Xsens which provides high-accuracy wearable inertial sensors. As for Pioneer Kit, DOT supports Bluetooth communication channel and Android or iOS SDKs. The DOT devices are sold as 5 devices kits, but it is possible to buy a single unit. Each unit provides a MicroUSB connector which can be used to recharge the unit and to turn-on the device. A monochrome led is used to notify various device's statuses and a button can be used to turn-off device (if pressed for more than 3 seconds) or it can be used to notify the controller application. The DOT technical characteristics are reported in Table 5.

Table 5: DOT by XSens technical specifications.

Latency	30 ms
Weight	10.8g
Dimensions	36.30 x 30.35 x 10.80 mm
Waterproof rating	IP 68
Precision	Static: 0.5 deg or 1.0 deg RMS Dynamic: 1.0 deg or 2.0 deg RMS
Full scale	±2000deg/s, ±16g, ±8 Gauss

One of the drawbacks of the DOT solution is represented by the fact that it is a quite recent solution, with an SDK still under development. This means that we had to update the SDK few times during the development phase to take advantages of the newly implemented features. The documentation was not completely clear and the demo software and the SDK where not easy to understand. The on-field use of the DOT solution demonstrated to be the solution with the more stable devices and the one with the more precise acquired data.

3.6 System Architecture and Integration

The main objective of this work is to provide a hardware & software solution to assists both physicians and patients during the rehabilitation phase. From the physician side, the system aims to provide support to plan the rehabilitation process and to track the rehabilitation scores for each single patient over time. The system also provides tools to analyze results and scores during the full rehabilitation process. From the patient's side, the system aims to provide a controlled MR and virtual environment where patients can execute exercises otherwise not possible in real life.

During exercise execution, the patient's movements are fully monitored using inertial sensors for the upper body links and Leap Motion for the left and right hand. All the acquired data are stored and offline analyzed. The system high level model can be represented as in Figure 33.

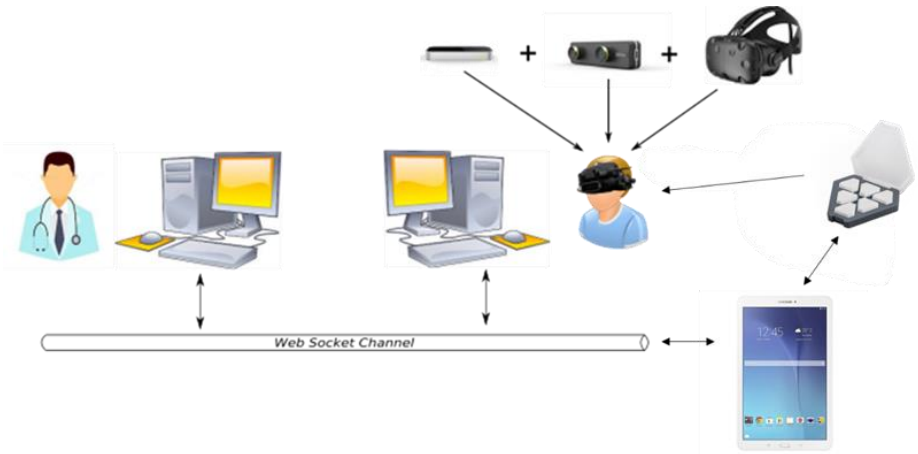

Figure 33: The system high level model. On the left side the doctor plans the patient's activities; on the right side the patient executes activities using Leap Motion, Zed camera, inertial sensors, and 3D HTC Vive headset.

The doctor or the physician interact with a console application, planning the details of the patient's activity session. When ready, the rehabilitation session's start and the patient perform the activities projected inside a mixed virtual environment. During patient's activity the score and other parameters are collected (such as execution mean time, overall score – for both success and failed execution).

When patient's activity has been completed, the physician receive notification to proceed with further training. Data and partial result can be analyzed by the doctor eventually archived or saved for further assessment. In the following of the thesis, we present the project architecture and describe how the final solution get realized.

3.6.1 SOFTWARE ARCHITECTURE

In this section we present the software architecture adopted for the realization of the final solution. The main idea behind the realization of the software is to keep the main controller separated from the exergame engine, as shown in Figure 34.

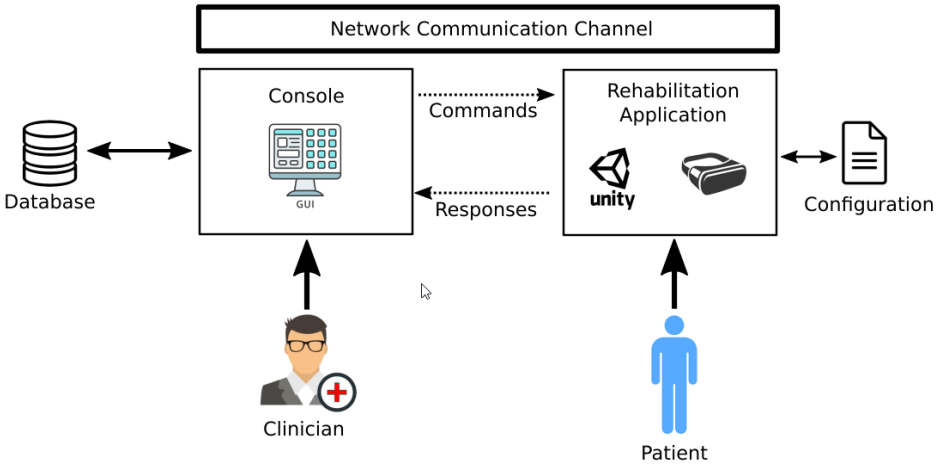

Figure 34: Software architecture.

The console allows the clinician to control the whole application, configuring the exercises for the patients and monitoring exercise execution. On the other side, the rehabilitation application provides the playground for the patient. The two components are separated processes running on the same workstation or running on separate workstations. The two processes communicate one each other with a network connection. The communication channel is realized with a full duplex web socket protocol on which a JSON messaging is used to exchange commands and responses. The separation between console and rehabilitation application using web-socket channel allows to realize flexible solutions where for example the console could be implemented as an Android application running on mobile phone or tablets providing a more flexible and portable solution.

3.6.2 CONSOLE APPLICATION

The console application is realized with C# and provides the main controller of the whole solution. The console GUI is shown in Figure 35.

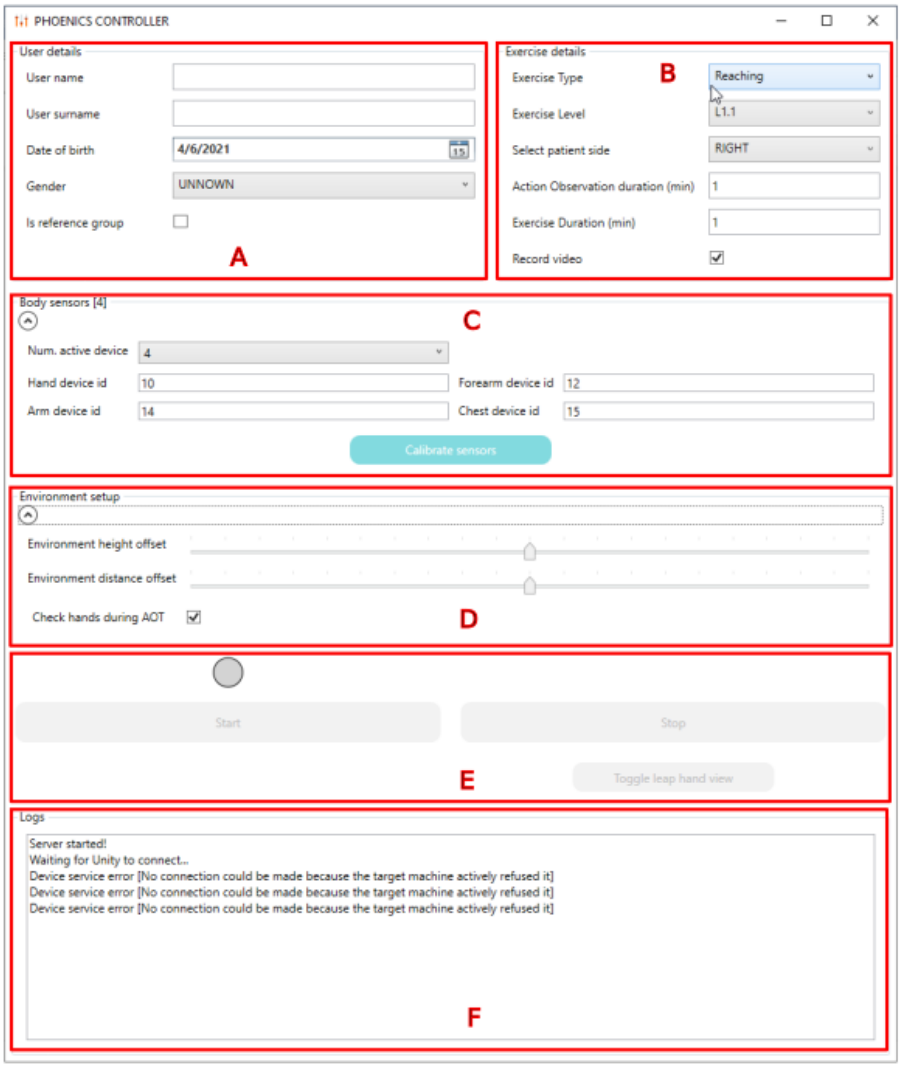

Figure 35: Consolle GUI.

The console has six major panels (from A to F) which can be used to control the current rehabilitation session. Panel A holds the patient's information: name, surname date of birth and gender. A check box allows to identify if the patient belong to the reference group or not.

Panel B holds the rehabilitation exercise details. The panel allows to select the exercise type (reaching, goalkeeper, pick and trash and move objects to target), set the exercise level (1.1, 1.2, 2.1, 2.2, 3.1 or 3.2), select the laterality to train, the duration in minutes of the AO phase, the full exercise duration in minutes and finally if the patient's view must be recorded or not.

Panel C provides the IMDs device configuration. The "Num. active device" single selection list-box allows to select the number of IMDs device to be used for the patient,

allowing to select a value from 1 to 4. The device's association sequence is hand, forearm, arm, and chest. The other four textblocks are used to associate the device with the specific part of the body. In the Cometa Wavetrack System, each IMD device is identified with a unique ID. To place the device on the patient's body, the clinician can follow the reported sequence, or he/she can place device randomly and then correct the IDs. This can be useful when some devices must be changed due to exhausted battery.

Panel D concerns the virtual environment setup. In this version of the software, the clinician can set the height offset and the distance offset for the patient's respect the virtual table. These two values allow to change the zero-position used as reference in the virtual environment, as shown in Figure 5, Figure 7 and Figure 10. The checkbox "Check hands during AOT" allows the clinician to enable or disable the patient's hand movement control during the AO phase, as already explained in previous sections. If enabled, this function monitors the movements of the patient's hand during the AO phase. If the patient moves the hand more than the configured range, the system alerts the clinician with a notification message. The clinician can decide to stop the AO phase and start over again, or the clinician can ignore the event proceeding normally to the execution phse.

Panel E allows the clinician to start and stop the AOT rehabilitation exercise. These two buttons get enabled when the console connects to the rehabilitation application. The button "Toggle leap hand view" allows to enable or disable the visualization of the virtual Leap Motion hands, so the clinician can control if the real vs. virtual hand alignment is correct. The led above the start button notify the clinician when an external IMDs acquisition service is connected to the console.

Finally, panel F provides an event logger to keep the clinician updated with the current phase and status of the overall AOT process, such as start, end, AO phase started, and AO phase completed. Other various events are notified inside this scrolling panel.

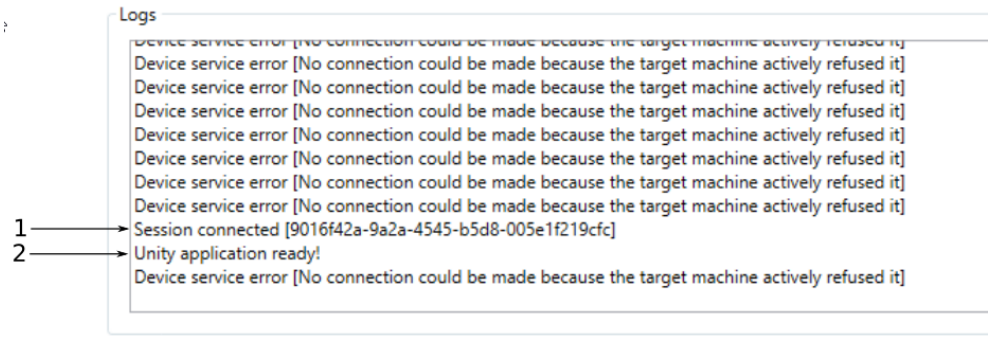

Figure 36: Log for Unity connection.

Figure 36 shows the log when Unity rehabilitation application get connected to the console. The consolle start looking for the Cometa Wavetrack IMDs connection. If not available, the console tries to connect to the web-socked device service using the web socket url set in the configuration file. Only when one of the two implementations is available, it is possible to proceed with the AOT.

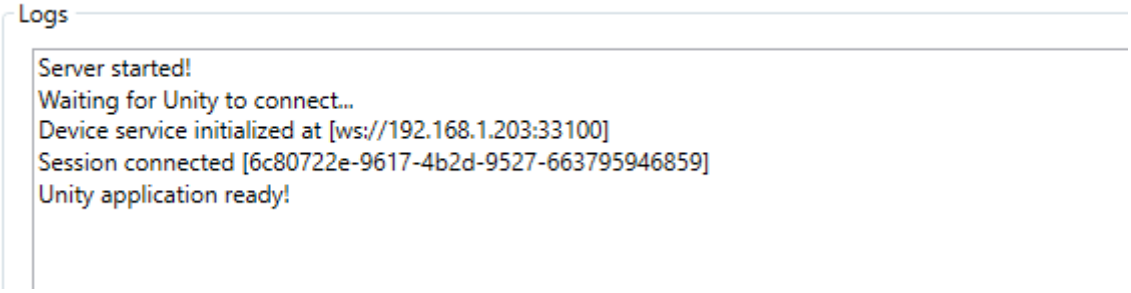

Figure 37: Console log when connected to IMDs service and to rehabilitation application.

Figure 37 shows the console log when connected to the IMDs device service and when connected to the Unity rehabilitation application. Only in this condition it is possibile to proceed with AOT execution. The console application supervises the whole AOT session controlling the rehabilitation application. All the hand's motion data are acquired by the rehabilitation application – presented in the next session – and sent to the console application to be saved on the persistent storage.

3.6.3 Rehabilitation Application

The rehabilitation application (RA) is responsible to create the MR virtual environment for the patient and to acquire all the data meanwhile the patient undergoes to

the AOT session. The RA application has been realized using Unity and compiled as a stand-alone application. The operations of the RA are fully controlled by the console application using JSON commands. For each command received, the RA application replays with a correspondent JSON response.

The Message framework has been realized as independent C# library which can be shared among the console application and the RA, as shown in Figure 38.

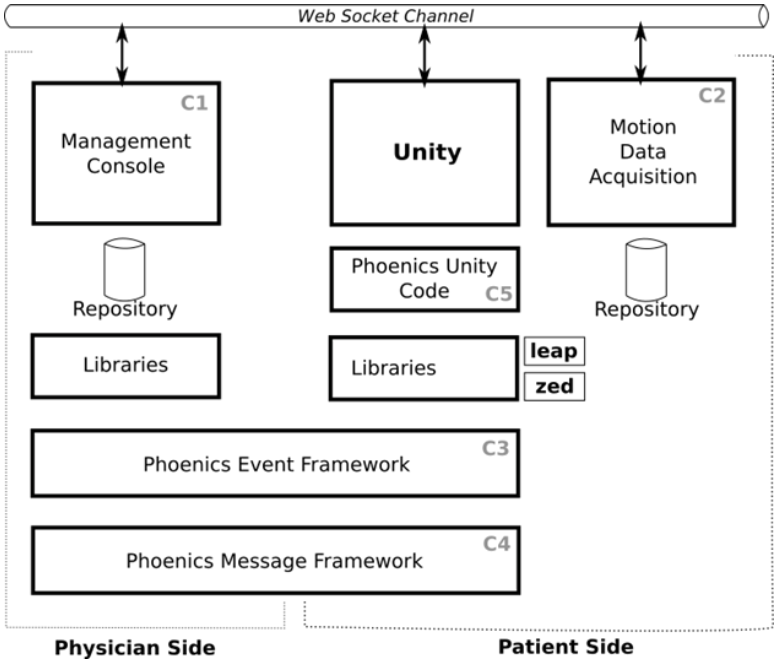

Figure 38: Library architecture.

The message framework supports the following commands:

- EnvDistanceOffsetChanged.
- EnvHeightOffsetChanged.
- StartExerciseMessage.
- StopExerciseMessage.
- ToggleLeapHandViewMessage.

The RA application notify back the console application with the following list of responses:

- ApplicationReadyMessage.
- ErrorMessage.
- ExerciseSessionStarted.

- ExerciseSessionTerminated.
- ExerciseStartedMessage.
- ExerciseTerminatedMessage.
- HandMovedMessage.
- VideoTrainingStartedMessage.
- VideoTrainingTerminatedMessage.

The AppServerLibrary provides the web-socket connection and communication manager to be used in Unity for the realization of RA. To provide maximum flexibility and extendibility in the development of RA, the AppServer uses an event dispatcher mechanism to notify all the registered listeners when a communication message gets received, as shown in Figure 39. The event dispatcher mechanism has been used not only for the communication channel but extended to any possible event of interest for the whole application.

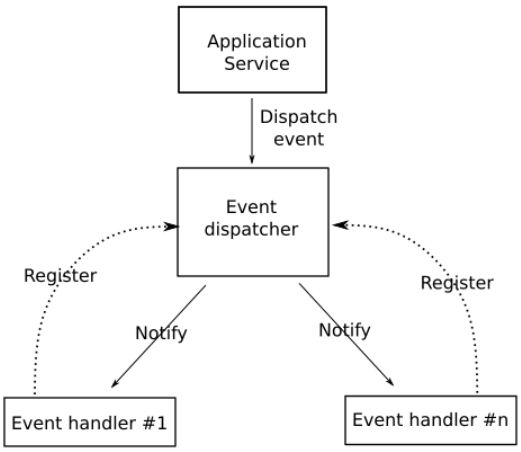

Figure 39: Event dispatcher architecture.

Using event dispatcher allows the single rehabilitation exercise implementation to be notified of any kind of event with a standard generalized mechanism. Each scene controller register itself as an event handler for a specific type of event, so each time such an event gets dispatched the associated even handler gets invoked.

Inside Unity particular attention has been dedicated to the architecture used to design and to implement the rehabilitation exercise. Each rehabilitation exercise is defined as a Unity scene with a given name. The scene name must follow a simple rule: the scene's name

must be composed by the name of the exercise, without spaces, ended with the suffix "Scene", so we would have the GoalkeeprScene, the PickAndTreshScene and so on.

Each scene can be created from a basic template called TemplateScene, show in Figure 40. The figure shows the template scene with the basic objects instantiated in the scene. The template scene contains the Leap Motion controller "Leap Rig", the ZED mini controller "ZED_Rig_Stereo" and two generic objects used as containers: Environment and Controllers. Environments is used to hold all the environment objects such as Table, Floor, Messages and ScorePanel. Controller's object is used to hold all the custom developed controllers for the scene. A controller is a custom C# classe used in Unity to coordinate various scene activities. Each scene is coordinated by a main controller which name is <NameOfTheExercise>SceneController. Where NameOfTheExerecise is the name of the implemented rehabilitation exercise.

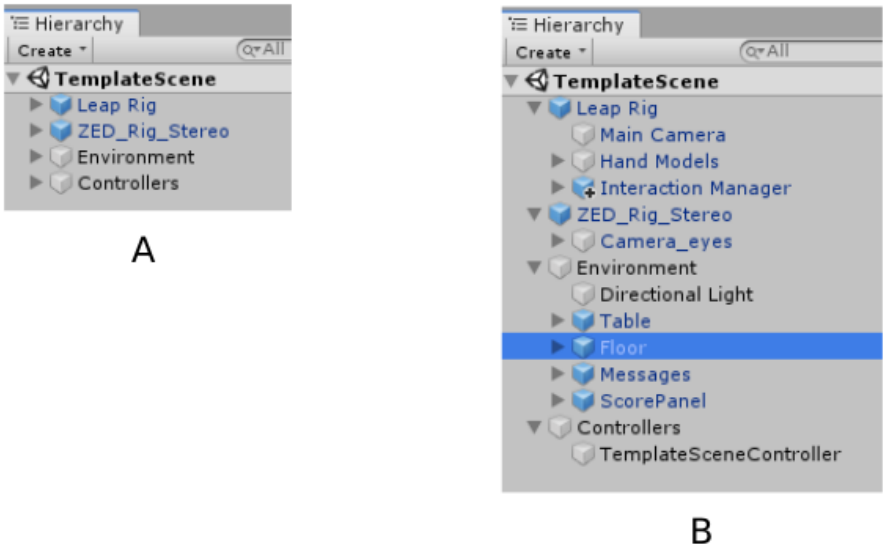

Figure 40: Template scene for Unity.

Each scene controller extends the basic controller **APhoneicsScene** which provides basic behavior and services for the new scene under development, as shown in Figure 41. The basic scene's controller provides a constructor which requires two parameters: the name of the exercise and the name of the next scene to be activated when the current exercise gets completed (which by default is the initial scene). For each exercise, the next scene's name is stored in the configuration file, so the clinician can easily decide the scene sequence workflow. In the on-field experimentation, after each scene the next scene has been configured to be the initial scene.

Whenever a new scene is created the RA configuration file must also be updated adding the configuration session for the newly created scene. The RA configuration is named **PhenicsUnityConfig.ini** and is a standard INI file containing all the configuration about each supported scene/exercise.

```
using log4net;
using System;
using UnityEngine;

public class TemplateSceneController : APhoenicsScene {
  #region Logger
  /// <summary>
  /// Logger
  /// </summary>
  static readonly ILog _Logger = LogManager.GetLogger(typeof(GoalkeeperSceneController));
  #endregion

  /// <summary>
  ///
  /// </summary>
  public TemplateSceneController() : base("TemplateScene", INITIAL_SCENE_NAME) {
    _Logger.Debug(">>> ENTER: PickAndTrashSceneController");

    try {

      // IMplement code herein

    } catch (Exception ex) {
      _Logger.Error(ex);
      Debug.Log(ex);
    }

    _Logger.Debug("<<< EXIT: PickAndTrashSceneController");
  }

  public override string GetSceneName() {
    return "TempletScene";
  }

  // Start is called before the first frame update
  override protected void Start() {

  }

  // Update is called once per frame
  override protected void Update() {

  }
}
```

Figure 41: Template scene controller.

3.6.4 CALIBRATION

In the previous section we presented the solution from the user perspective and from an architectural point of view. In this section we discuss the system calibration required for both: head-set and inertial sensors. For inertial sensors, the calibration process is described for Cometa Wavetrack system, but the same process can be easily extended to the other two inertial solutions supported: DOT by Xsens and Pioneer Notch Kit.

3.6.4.1 Headset calibration

HTC Vive headset is the device the system adopts to identifies the position and motion of the camera inside the Unity game's scene. Two base stations which emits infrared can identify the headset position in the environment, as shown in Figure 42. The headset calibration process is the process required to permit the headset system to compute the position of the headset with respect to a reference position. The integration of headset with Unity is fully handed by the HTC Vive SDK libraries loaded in the Unity game engine. So, even the calibration process is fully handled by the Steam VR library. The headset calibration process is very smooth and fast and requires only two calibration steps: (1) headset central position calibration and (2) headset high position calibration. The headset high position calibration is the process that identifies the position of the floor in the virtual environment.

The headset calibration is very stable. The only reasons that require to perform calibration – beside the first initial setup – is when the base stations get moved or when there is huge modification in the volume of the environment. If the environment does not change and the base stations are kept in the same position, no calibration is required for the headset even after days of use.

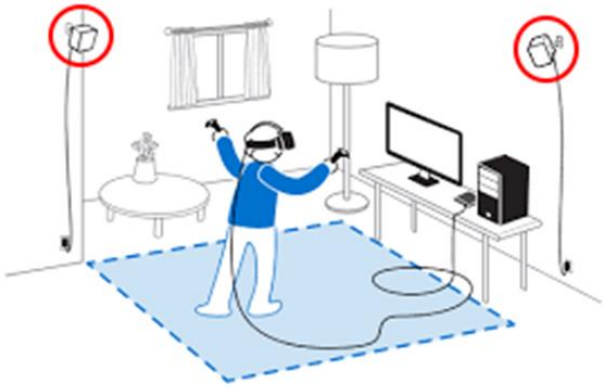

Figure 42: An example of Vide head-set environment setup. On the upper left and right corner is possible to see the Vive base stations (inside the red circle) used to track the head-set position in the 3D environment.

The calibration of the headset center position is just a matter of remaining in the working position for few seconds, meanwhile the calibration of the vertical position just requires placing the headset on the table, measure the distance in between the floor and the headset table position and enter that value in input field as required. The whole headset calibration process does no take more than 1/2 minutes.

3.6.4.2 Inertial sensors calibration

In the previous section we presented the headset calibration process. In this section we present the Cometa Wavetrack inertial system calibration process.

Inertial sensors are positioned on the patient's body and are used to acquire the quaternion rotation of each single body link. Inertial sensors use a 9DOF algorithm to estimate the 3D orientation of the device. The 9DOF uses signals from inertial and magnetic sensors (accelerometers and gyroscope) which are known to be quite sensitive to environmental changes. Magnetometers are sensitive to ferromagnetic objects which are moving in the environment meanwhile gyroscope is sensible to varying of the environment's temperature. To mitigate those environment negative effects, a device calibration is required before the starting of each patient's exercise session. The inertial device calibration process aims to record 3 seconds of data from each active sensor. The calibration data must be recorded positioning the inertial devices in a pre-defined position using an ad-hoc-created plastic stamp shown in Figure 43.

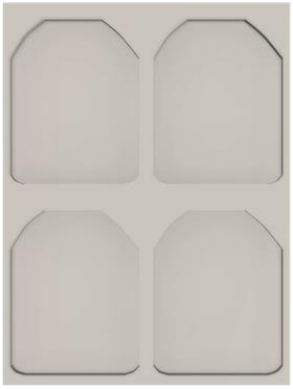

Figure 43: The plastic container used to place the inertial devices during device calibration phase. Calibration requires 3 seconds, after that devices can be removed from the plastic container and positioned on the body of the patient.

The calibration data are saved on a local file (in the shared folder). Inertial sensors calibration data are used to compute the correct motion of the upper limb of the patient during exercise. Regarding the reported calibration procedure, at current stage, no accuracy evaluation of any joint kinematic variables was performed. In this initial phase of the project – where may other critical aspects are under investigation – this topic was left outside the scope of the current phase. Data acquired during the first and second on-field test would be evaluated to infer if the calibration procedure would be acceptable, if not more investigation

would be performed to improve calibration procedure even eventually comparing it with a gold standard such as stereophotogrammetric systems to improve the quality of the upper limb cinematic data analysis.

3.6.5 DATA FILE DESCRIPTION

This section presents the files used by the solution to store acquired data. The data acquired during the exercise execution are reported in the following list:

- Full hand motion data (Leap Motion).
- Arm cinematic data (Cometa WaveTrack).
- Inertial sensor calibration data (Cometa WaveTrack).
- Runtime exercise events (Unity).
- Exercise info (Management Consolle).

All the data are stored in four different files with following naming convention:

(1) Full hand motion data and runtime exercise events:

`<name>_<surname>__<exercise>_<level>_<class>_<side>_<datetime>`

(2) Arm cinematic data:

`<name>_<surname>_M_<exercise>_<level>_<class>_<side>_<datetime>`

(3) Inertial sensor calibration data:

`SensorCalibrationData_<datetime>`

(4) Exercise information:

`<name>_<surname>_E_<exercise>_<level>_<class>_<side>_<datetime>`

The exercise information file contains some information about the executed exercise. These information are the patient's name, surname and born date, the exercise type, the exercise level, the number of exercise repetitions, the exercise side, the overall score, and the mean reaction time, as shown in Table 6.

```
<phoenics-data>
      <user>
            <name>XXXXX</name>
            <surname>XXXXX</surname>
            <dateofbirth>XXXXX</dateofbirth>
      </user>
      <exercisetype>
            <description>Goalkeeper</description>
            <code>4</code>
      </exercisetype>
      <exerciselevel>
            <name>L1.1</name>
            <code>0</code>
      </exerciselevel>
      <repetitions>3</repetitions>
      <exerciseside>
            <description>RIGHT</description>
            <side>RIGHT</side>
      </exerciseside>
      <score>
            <value>31</value>
      </score>
      <mean-reaction-time>
            <value>782</value>
      </mean-reaction-time>
</phoenics-data>
```

Table 6: Example of exercise information file.

The inertial sensor calibration file contains the quaternions data from the inertial devices acquired with patient in steady position. The calibration is usually required once a daily session. But more calibration can be executed over time. The file also contains the time stamp at which the calibration gets started, as shown in Table 7.

```
<phoenics-data>
      <start-time>2019-09-24 10:07:20.242</start-time>
      <motion-data>
            <sample id="15" type="quaternion" timestamp="292" x="0,087"
y="0,216" z="-0,056" w="0,971" />
            <sample id="12" type="quaternion" timestamp="292" x="0,005"
y="0,001" z="-0,082" w="0,997" />
            <sample id="14" type="quaternion" timestamp="292" x="0,001"
y="0,002" z="-0,073" w="0,997" />
            <sample id="10" type="quaternion" timestamp="292" x="0,040"
y="0,060" z="-0,070" w="0,995" />
            <sample id="15" type="quaternion" timestamp="393" x="0,087"
y="0,217" z="-0,056" w="0,971" />
            <sample id="12" type="quaternion" timestamp="393" x="0,005"
y="0,001" z="-0,082" w="0,997" />
            <sample id="14" type="quaternion" timestamp="393" x="0,001"
…
<phoenics-data>
```

Table 7: Example of calibration data file.

The upper arm cinematic file contains all the inertial devices' orientation quaternions for each device and with the associated timestamp. For each device, the file contains the ID and the correspondent device position on the patient's body. A timestamp is used to identify the acquisition start-time and is lately used to synchronize upper arm cinematic data with Leap Motion data. An example of such file is shown in Table 8.

```
</exerciselevel>
      <repetitions>3</repetitions>
      <exerciseside>
            <description>RIGHT</description>
            <side>RIGHT</side>
      </exerciseside>
      <sensors>
            <sensor>
                  <id>12</id>
                  <position>HAND</position>
            </sensor>
            <sensor>
                  <id>9</id>
                  <position>FOREARM</position>
            </sensor>
            <sensor>
                  <id>13</id>
                  <position>ARM</position>
            </sensor>
            <sensor>
                  <id>16</id>
                  <position>CEST</position>
            </sensor>
      </sensors>
      <start-time>2019-09-24 11:12:53.072</start-time>
      <motion-data>
            <sample id="12" type="quaternion" timestamp="362" x="-
0,140" y="0,146" z="0,210" w="-0,957" />
            <sample id="9" type="quaternion" timestamp="362" x="-0,284"
y="0,021" z="0,352" w="-0,892" />
            <sample id="13" type="quaternion" timestamp="362" x="-
0,373" y="-0,113" z="0,584" w="-0,712" />
            <sample id="16" type="quaternion" timestamp="362" x="-
0,300" y="-0,720" z="0,387" w="-0,491" />
            <sample id="12" type="quaternion" timestamp="463" x="-
0,140" y="0,146" z="0,210" w="-0,957" />
            <sample id="9" type="quaternion" timestamp="463" x="-0,284"
y="0,021" z="0,352" w="-0,892" />
```

Table 8: Example of upper arm cinematic data file.

Finally, the full hand motion data file records the hand motion in 3D space as acquired by the Leap Motion for each single part of the hand. Each hand position's data has its own timestamp and contains position, rotation, direction, and length of each single hand's bone. At the end of the file is stored the full set of the runtime exercise events.

```
<?xml version="1.0" encoding="utf-8"?>
<XmlData xmlns:xsd="http://www.w3.org/2001/XMLSchema"
xmlns:xsi="http://www.w3.org/2001/XMLSchema-instance">
  <StartTime>2019-09-24 11:12:52.982</StartTime>
  <HandPositionList>
    <HandPosition>
      <TimeStamp>107</TimeStamp>
      <IsLeft>true</IsLeft>
      <Palm>
        <PalmBone>
          <Name>palm</Name>
          <Position>
            <x>-0.275679946</x>
            <y>-0.224710658</y>
            <z>0.456273854</z>
          </Position>
          <Rotation>
            <x>0.5863821</x>
            <y>-0.0292949211</y>
            <z>0.4175705</z>
            <w>-0.693493068</w>
          </Rotation>
        </PalmBone>
```

Table 9: The initial part of the file with the full hand motion data.

Table 9 shows the initial part of the file with the full hand motion data as provided by the Leap Motion device. Meanwhile, in Table 10 is shown the final part of the file where runtime exercise events are saved.

```
<InteractionEventList>
    <InteractionEvent>
      <Id>object-created</Id>
      <TimeStamp>3051</TimeStamp>
    </InteractionEvent>
    <InteractionEvent>
      <Id>contact</Id>
      <TimeStamp>4301</TimeStamp>
    </InteractionEvent>
    <InteractionEvent>
      <Id>object-created</Id>
      <TimeStamp>7315</TimeStamp>
    </InteractionEvent>
    <InteractionEvent>
      <Id>contact</Id>
      <TimeStamp>9015</TimeStamp>
    </InteractionEvent>
    <InteractionEvent>
      <Id>object-created</Id>
      <TimeStamp>12030</TimeStamp>
    </InteractionEvent>
```

Table 10: Final part of the full hand motion data with the list of runtime exercise events.

3.7 Main Results

This section presents and discusses the results concerning the patient's performance assessment and the overall system assessment from the perspective of the clinicians and patients in terms of system usability.

3.7.1 Patient's Performance Assessment

Since the RCT was not concluded due to the spread of COVID-19 pandemics, hereinafter several examples of the metrics used in the assessment of patients' performance are reported. In particular, the hand max reaching velocity for the reaching task (Figure 44) and the mean reach path during the goalkeeper task (Figure 45) are shown.

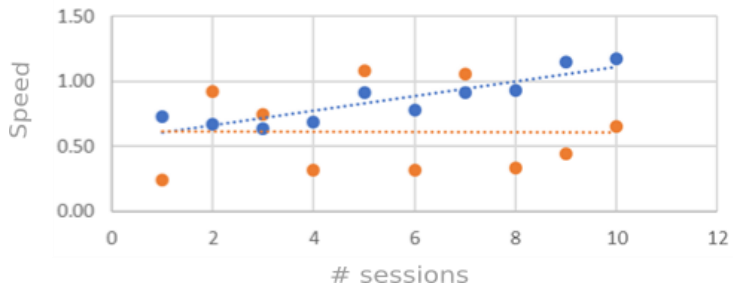

Figure 44: Hand max reaching velocity during the reaching task with respect to the session.

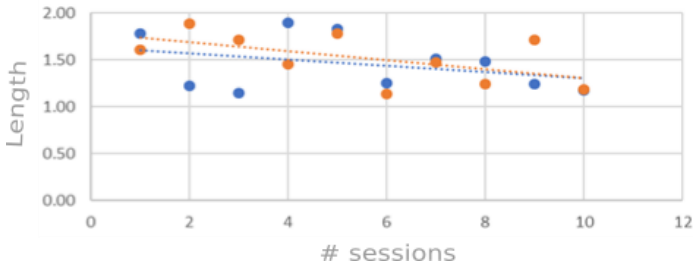

Figure 45: Mean reach path during the goalkeeper exercise with respect the sessions.

Patient 1 demonstrated an increasing performance in both the required tasks during the progress of the sessions. On the other hand, patient 2 (50 years old, male) reported an improvement in the goalkeeper as well, but a stable outcome in the reaching task. To also quantify the kinematic patterns and strategies used during the execution of the tasks, the joint kinematics was analyzed by exploiting the inertial measurement units; an example of the obtained decomposition is reported in Figure 46.

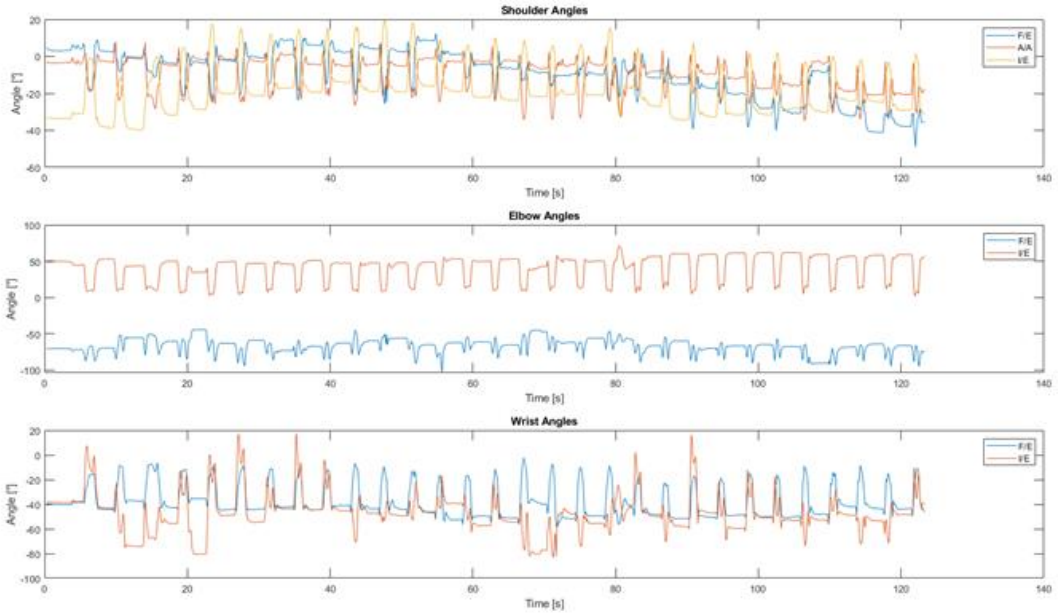

Figure 46: Example of upper limb kinematics for shoulder, elbow and wrist as acquired by the inertial measurement units, during the execution of the goalkeeper task.

3.7.2 System Assessment

3.7.2.1 Usability for the Clinical Staff

4 Only results about a 23-years old female subject has been collected for the SUS evaluation. Results must be interpreted as a first opinion about the clinical staff. The SUS score was 70, thus attested a good level of system usability. Detailed information about the answers given by the therapist is shown in Figure 47, meanwhile details about questionary's questions can be seen in Appendix A: SUS (System Usability Scale) and Reports.

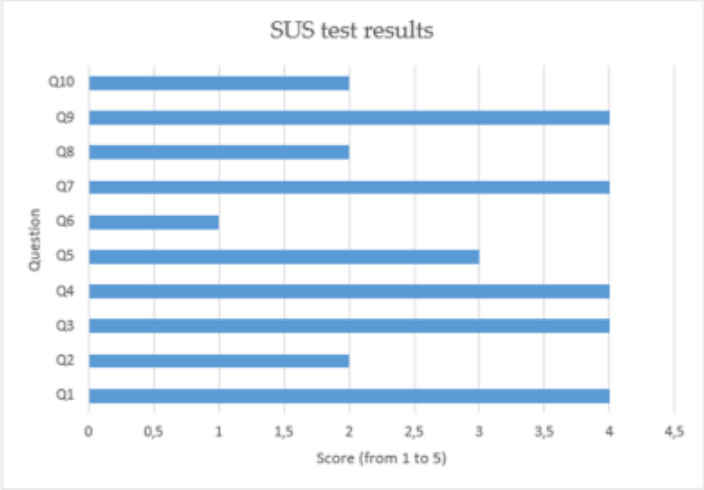

Figure 47: Details about SUS results.

In any question, a score higher than 4 has not been reached. In general, the clinician has a good opinion about the system. What results show is that the system is perceived easy to use (Questions 2,3,7,10), effective (Questions 1,9) but there is a need for a technician to support the clinical staff during clinical rehabilitation sessions (Question 4). Also, it is pointed out how improvements in some technical features of the system would be needed (Question 5).

The subject did not report any critical or non-critical errors in task completion. No evident fatigue insurgence was reported. For the first task (filling the Excel file) no issues were reported. The subject did not report any problem in the description of the system and in the description of the exercises to the patient (Task 2). In safety posture explanation to the patient (Task 3), no issue was reported but it was pointed out how, during the exercises, it was necessary to move the patient backward to re-align the patient in the correct position for the completion of the task. The sensors calibration procedure (Task 4) was perceived as an

easy and straightforward task. Sensor's placement (Task 5) was completed without any difficulty. Also, Task 6 (Pressure of Start Button for Each exercise) and Task 7 (Removing sensors and HMD) did not manifest any problems in their execution. From the external observation of the performed exercise, the clinician always reported some technical difficulties. In the Reaching task, she reported a problem in the correct detection of the reaching by the system. In Reach and Grasp task, the same problem reported for the Reaching task was noticed. The Goalkeeper task seemed to be the easiest one. No relevant issue was reported. In the Occupational task, often the hand of the subject made the virtual object disappeared so that the task could not be completed. Furthermore, during the execution of this exercise, the completion of the task was not detected by the system forcing the patient to repeat the exercise. During the AO phase, no technical issues were reported.

6.1.1.1 Usability for the Patient

The patient involved in the first session of the clinical trial was a 65-years old woman who had a stroke that impaired the right side of her body (right hemiparesis). Any motion sickness problems related to the use of the MR system were reported. Tasks were all completed without any critical errors. For exercise two (Reach and Grasp), three (Goalkeeper) and four (Occupational Task) some non-critical errors were encountered. For the exercise one, the patient noticed that sometimes the system was not able to correctly detect the task completion. In the second exercise, the subject was not able to complete the task in the first attempts. Only the introduction of feedback about the virtual hand solved this issue. The same problem was faced during the second exercise. The third exercise was perceived as the easiest one. Patient report that the Occupational Task was the hardest one. The cans appearing in the scene were not easily grabbed and the placement on the target was quite difficult because sometimes the target disappeared. The AO and video observation did not cause any problem to the patient although this part of the rehabilitation session was quite boring.

6.2 Discussion and Conclusions

The activities here reported presented the development of a hardware and software solution which provides an integrated approach – based on novel technologies – to use MR and AOT in post-stroke upper limb rehabilitation. The proposed solution provided a stand-alone approach to support and to extend standard rehabilitation protocols with AOT. Moreover, the same solution can also be used to validate new AOT approaches, allowing to

acquire performance metrics on the undergoing rehabilitation exercise such as: full upper limb motion dynamics and cinematic using inertial and magnetic sensors, hand, and fingers position, cinematic and dynamics using Leap Motion™ and, action events such as virtual object to hand interaction, virtual object destruction and, success versus failure exercise execution. A mechanism to monitor hand movements during AO has also been provided.

Preliminary results about the usability seem to suggest that the developed system was easy to use and effective in the realization of the rehabilitation sessions. Furthermore, questionnaires showed that the user tasks were well designed. This perspective is promising when considering the possibility of introducing this system within a clinical context. However, few technological issues were present (i.e., match between the position of the virtual hand and the real hand, shadowing of the objects, etc.). A clearer perspective of the overall system performance will be obtained by increasing the overall number of the involved users. From the patient's point of view, the system provided an optimal level of engagement, without critical issues. Furthermore, the system was able to monitor the advances reached by each patient during the training sessions, highlighting specific behavior due to both the increasing performance and the level of pathology. The proposed parameters represent optimal metrics to be used, not only in tracking the progresses of the patients, but also to automatically adapt the level of difficulty of the exercises.

This work showed an innovative and promising methodology for the rehabilitation of post-stroke patients. Scientific literature seems to support our novel approach and brings to hypothesize that the combination of AO and MR rehabilitation system could magnify the efficacy of rehabilitation treatment. Furthermore, the final system will be able to integrate different devices to give objective measures about the hand and upper limb functional improvement. Design, implementation and the first application of the system in the clinical environment have been described.

A lot of effort was put into the system design, testing and realization processes. Results obtained from the first pilot study are good although shows that further technical solution must be found to fix some issues related to the devices' integration. Nevertheless, this work can be intended as a first step in the realization of a new and effective system that can improve the functional recovery of post-stroke patients.

SHOULDER STABILITY ASSESSMENT

This chapter presents the work concerning the development of a portable solution to assess shoulder stability. As for the AOT based post-stroke rehabilitation solution, one of the main objectives is the realization of a solution which can be easily transferred to clinical environments, thus, eventually being easily employed in tele-care rehabilitation systems. As presented in this chapter the proposed solution for the shoulder can also be easily extended and generalized to easily acquired 3D motion data for other parts of the body providing pluggable and customizable mechanism for data analysis and patient status assessment.

The first part of the chapter concerns the shoulder complex and its biomechanics, the shoulder pathologies are briefly introduced and described. The section "Technologies and Methodologies" presents the protocol used to acquired motion data, and the acquired data themselves. The following section presents and explains the PKIs used to assess the shoulder status. The section "System Description" presents the details about the implemented solution whereas "Results" describes the methods and the results obtained applying the proposed solution in a real clinical context. "Subjects Classification and Neural Network Approach" show how a machine learning approach can be applied to the estimated SPKIs to realize an autonomous shoulder status assessment classifier. Finally, "Future development and applications" presents the possible future development of the proposed solution.

7.1 BACKGROUND AND MAIN OBJECTIVES

Science of human motion analysis involves a high number of disciplines and a wide range of applications from healthcare to wellness and sport. Motion analysis in term of biomechanics approach, started around 384 yeas BC with Aristotele [67]. During the years, many others scientist get involved in biomechanics studies: Leonardo Da Vinci, Galileo Galilei and later by Newton, Bernoulli, Euler, Poiseuille, Young and others [68]. It was Marey to take a scientific approach to motion analysis and biomechanics using pictures to correlate ground reaction forces with movements, pioneering modern motion analysis [67].

Historically, motion capture of human body dynamics was conducted using video acquisition devices. These solutions were expensive, complex to setup and require a precise positioning of well visible markers on the body. During the years, these solutions get improved, reduced in size, reduced in cost, and improved in quality of the acquired data. Unfortunately, video-based motion-capture still have a limit in the portability, flexibility, and outdoor applications. As opposed to optical methods, the main advantages of systems

based on inertial and magnetic devices are the determination of kinematical parameters without the limitation of a restricted capture volume, and with short-time costs for the measurement preparation and data analysis [69].

In the recent years, inertial devices is doing enormous improvements in term of precision, reportativity, and hardware quality, with a progressive size and cost reduction [70]. This new wearable technology is slowly replacing video-based motion capture solution due mainly to the following aspects: small size, lower costs, good quality, easy to setup, water-proof and free to be used indoor or outdoor. The main advantage of inertial and magnetic sensors is their possibility to be used almost anywhere so they get engaged also in the fields of sport motion analysis. Now-a-days inertial and magnetic devices (IMD) are widely used in field of rehabilitation, wellness and sports [71]–[73].

A wearable device is basically a tiny computer with sensing, processing, storage, and communication capabilities. Improvements in LiPo battery technology, reduced sensor consumption and thanks to the latest BLE (Bluetooth Low Energy) technologies even small devices can provide a long-lasting duration in between two consecutive charges. Wireless magneto-inertial devices are small computers with a set of MEMS (Micro-Electro-Mechanical-Systems) and magnetic sensors and a wireless communication channel. High performance micro-processors can collect data from sensors up to 1KHz data rate and to directly process on-board data applying data-fusion algorithm to estimate device rotation in space. Processed data and result can be stored locally or can be transmitted in real time over the wireless channel.

The clinical use of wearable technologies has gaining more and more impact in the recent decade. In particular, the need for quantitative evaluation of joint pathologies has been requiring innovative approaches able to provide reliable measurement of joint function, as to realize both accurate diagnosis and preventive treatment strategies. In this context, the main goal of this work is to design and develop a SSA (Shoulder Stability Assessment) mobile application running on commonly available smartphones or tablets which employing two inexpensive IMDs – placed on the acromion and on the humerus – allows to acquire dynamics motion data of underling associated bones while the subject executes upper limb abduction (ALU) on the scapular plane. Running on portable devices such as smartphones or tables in conjunction with a simple and fast application protocols, allows for a maximum portability providing an optimal solution in clinical environments. The overall shoulder assessment is immediately available to the clinicians which can take immediate actions. Acquired data are saved locally on the mobile device or can be optionally saved on cloud to

be further analyzed. A 3D real-time view shows the real-time bone's motion allowing to discover possible misconfiguration errors. Initial calibration is straightforward and take a maximum of 2 to 4 seconds to be completed. A flexible and extendible architecture allows for multiple IMD vendor support, whereas the current solution supports both Notch Pioneer Kit by Wearnotch and DOT by XSens.

To achieve the objective of the activities, i.e., to assess the status of the shoulder, a set of SPKIs indicator has been defined. These SPKIs are directly related with the 3D dynamics and kinesiology of the acromion and the humerus while executing a ULA on the scapular plane. With this work we would demonstrate how these SPKIs are good indicators of possible shoulder pathologies. As an extension, a third IMD can be used on the forearm to measure extra rotation of arm and forearm allowing to analyze the glenohumeral joint. Acquired data were used in a preliminary "proof of concept" study on volunteers as to identify specific motion patterns. Finally, a simple machine learning algorithm (i.e., multilayer artificial neural network) was applied on the analysis of the PKIs demonstrating the feasibility of an autonomous approach to classify and eventually predict shoulder status. The design of the system was realized with the support of Roberto Luongo, MD and his coworkers and the team at the Genetica Amica Association, Riva del Garda (TN), who suggested the need for a reliable but extremely easy-to-use solution.

7.2 State of the Art

With respect to scientific literature, in this research we specifically aimed at obtaining a system with the highest level of usability with respect to the specific application context, i.e. keeping into account both the clinical requirements, but also the constraints due to the environment itself (i.e., time and complexity). Shoulder functional analysis performed by using IMDs devices has been previously addressed in different studies, which reported different findings concerning applicability, intra- and inter-observer problem, reliability and precision, technical dynamic accuracy, automatic calibration, soft- and adipose-tissue problems, etc. [49], [74]–[77]. Within this work, we specifically aimed at obtaining a solution with a high technology readiness level (TRL), which in its simplicity resulted effective in identifying currently on-going dyskinesis for shoulder district even in case of asymptomatic subjects. In our study even the kinematic model and the calibration procedure, were optimized by reducing the number of the used sensors and considering a controlled setup. In the first analysis, we focused on the humerus abduction on the scapular plane and the scapula upward and downward rotation on the frontal plane as key element. Moreover,

always to keep thinks as simple as possible, we avoided to use an additional IMD on the chest, generally used to estimate scapula-thoracic complex [78], or to estimate subjects chest compensation movements, by working on a specific testing setup. Indeed, scapular kinematics are in general difficult to characterize due to the scapula's movement below muscle, fat, and skin but recent bone-pin measurements indicate that differences between symptomatic and asymptomatic individuals exist and that, although differences are small, they are significantly larger than measurement errors [78].

Another difference with respect to several studies on the shoulder complex, where the overall range of motion (ROM) is considered, or where further shoulder macro dynamics are taken into account [49], [78]–[81] and where – most of the time – all the dynamics range of shoulder complex are considered, in this analysis we defined a new set of shoulder primary key indicator (SPKI) – proposed for the first time – which aimed at characterizing the scapula-humeral dynamics in the very early stage of humerus abduction on the scapular plane in particular in the range from 0 to 15 degrees of humerus abduction. Furthermore, the dedicated mobile application followed the same "keep it simple, stupid" (KISS) approach. This approach was also consolidated by the introduction in the early stage of design of several clinicians, who participated in both the definition of the setup and commenting the main obtained findings. As reported in "Results and Discussion" the obtained results were very promising, demonstrating that the proposed approach used to functionally assess the shoulder status resulted simple and effective.

7.3 THE SHOULDER AND ITS PATHOLOGIES

The shoulder is a complex structure composed of synovial articulations and functional articulations. The shoulder is characterized by wide mobility to a detriment of an overall instability. The cooperative function, precisely regulated, among the various articulations guarantees the wide mobility of upper limbs on all its motion planes.

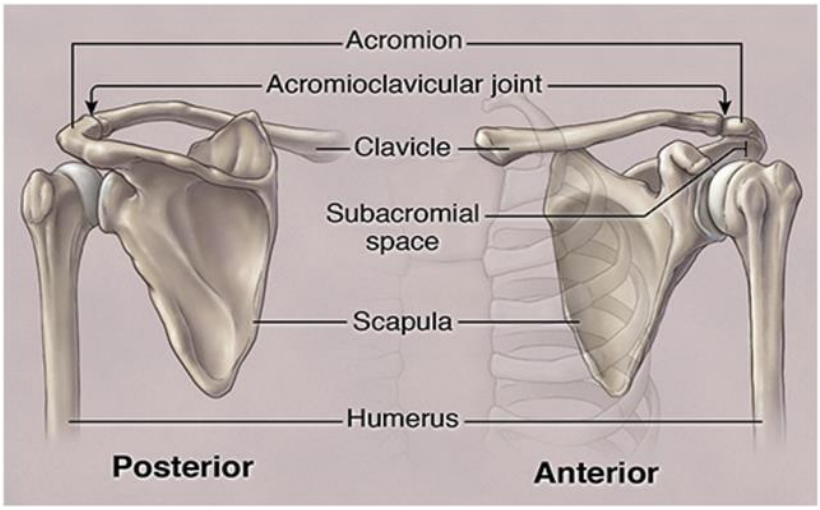

Figure 48: Shoulder bones, anterior and posteriori view.

Figure 48 (adapted from [82]) shows the shoulder bones from the posterior and anterior view. The shoulder complex is composed of the clavicula, the scapula and the humerus, each defining a specific joint controlled by correspondent muscles and tendons.

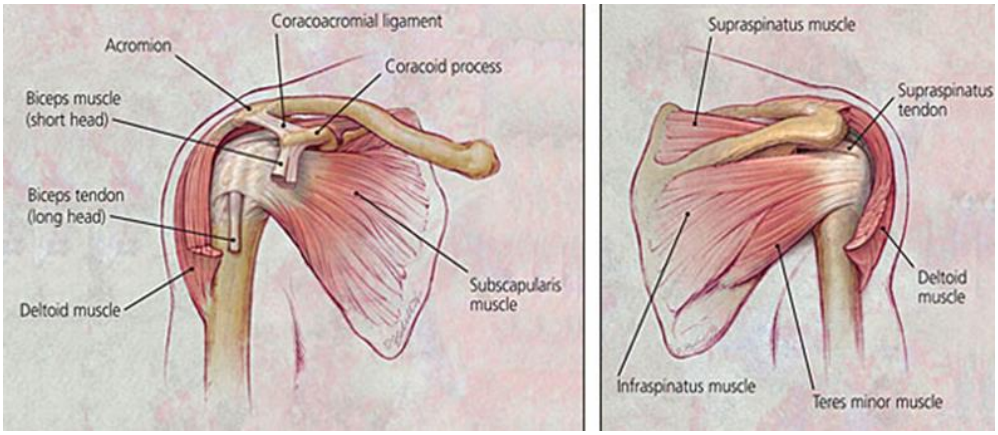

Figure 49: Anatomy of the shoulder and rotor cuff, anterior and posterior views.

Figure 49 (adapted from [83]) shows the anatomy of the shoulder with anterior and posterior view. The rotator cuff comprises four muscles — the subscapularis, the supraspinatus, the infraspinatus, and the teres minor — and their musculotendinous attachments. The subscapularis muscle is innervated by the subscapular nerve and originates on the scapula. It inserts on the lesser tuberosity of the humerus. The supraspinatus and infraspinatus are both innervated by the suprascapular nerve, originate in the scapula, and insert on the greater tuberosity. The teres minor is innervated by the axillary nerve, originates

on the scapula, and inserts on the greater tuberosity. The subacromial space lies underneath the acromion, the coracoid process, the acromioclavicular joint and the coracoacromial ligament. A bursa in the subacromial space provides lubrication for the rotator cuff [83]. The rotator cuff is the dynamic stabilizer of the glenohumeral joint so, understanding the functional anatomy of the rotator cuff assists in understanding its disorders and pathologies.

The deltoid abducts the shoulder. Without an intact rotator cuff, particularly during the first 60 degrees of humeral elevation, the unopposed deltoid would cause cephalad migration of the humeral head, with resulting subacromial impingement of the rotator cuff [84]. The space between the undersurface of the acromion and the superior aspect of the humeral head is called the impingement interval. This space is normally narrow and is maximally narrow when the arm is abducted. Any condition that further narrows this space can cause impingement. Impingement can result from extrinsic compression or from loss of competency of the rotator cuff [83]. Possible causes of this impingement are outlet impingement, subacromial spurs, type 2 and type 3 acromion, osteoarthritis spurs of acromioclavicular joint, thickened, or calcified coracoacromial ligament, nonoutlet impingement, loss of rotator cuff causing superior migration of humerus, secondary impingement from unstable shoulder, acromial defects, anterior or posterior capsular contractures, and thick subacromial bursa. In particular practical experience indicates that about 95% of the tears of the rotator cuff are initiated by impingement wear rather than circulatory impairment or trauma [85]. Management of such pathologies includes physical therapy, injections, and, for some patients, surgery [86]. Figure 50 (adapted from [85]) shows a detailed view of the area of impingement.

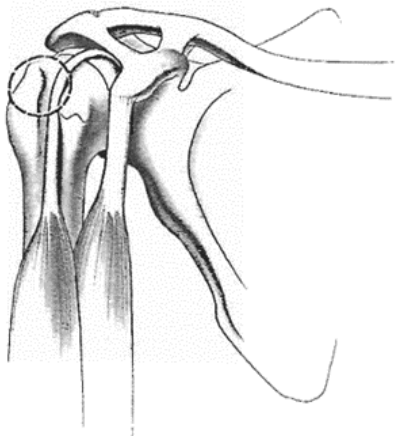

Figure 50: Ara of impingement.

According to population surveys, shoulder pain affects 18-26% of adults at any point in time, making it one of the most common regional pain syndromes. Symptoms can be persistent and disabling in terms of an individual's ability to carry out daily activities both at home and in the workplace. There are also substantial economic costs involved, with increased demands on healthcare, impaired work performance, substantial sickness absence, and early retirement or job loss [87]. Standardized classification systems based upon presumed patho-anatomical origins have proved poorly reproducible and hampered epidemiological research. Despite this, there is evidence that exposure to combinations of physical workplace strains such as overhead working, heavy lifting and forceful work as well as working in an awkward posture increase the risk of shoulder disorders. Psychosocial risk factors are also associated. There is currently little evidence ***to suggest that either primary prevention or treatment strategies*** in the workplace are very effective and more research is required, particularly around the cost-effectiveness of different strategies [87].

Shoulder pathologies could also be present in younger population for example due to an overwork/overload of the shoulder during training. In some cases, initial impingement manifest itself without significant pain, so the subject keeps load the shoulder instead of preventing the failure with work reduction or even with preventive treatments; having a practical tool to predict shoulder anomalies insurgency even when still there is no pain would indeed be a powerful tool in hand of clinicians in terms of shoulder treatment protocol to prevent shoulder disorders.

As reported in [85] a practical protocol to direct manipulation of the shoulder in order to identify impingement consist in the forced humerus abduction while blocking the scapula upward rotation as shown in Figure 51 (adapted from [85]). In this test the subject is seated on a stool and the clinician is positioned behind him facing the subject's backside. With one hand the clinician blocks the shoulder upward rotation meanwhile with the other hand rise the patient's arm in forced forward elevation (abduction); causing the greater tuberosity to impinge against the acromion. This maneuver causes pains in patients with impingement lesions of all stages. The maneuver causes also pain in patients with other shoulder conditions, including stiffness (partial frozen shoulder), instability (e.g., anterior subluxations), arthritis, calcium deposits, and bone lesions [85].

Figure 51: Forced humerus abduction blocking shoulder upward rotation

7.4 TECHNOLOGIES AND METHODOLOGIES

7.4.1 SYSTEM DESCRIPTION

Starting from a deep analysis of both the anatomy and function of the shoulder, and of the clinical requirements, the basic idea is to implement a solution which using a reduce number of IMDs (with a minimum number of two) positioned one on the acromion and the other on the external side of the humerus and using a smartphone allows to assess shoulder stability while the patient is executing a series of three to five ULAs. The shoulder assessment is based on a set of SPKIs which can characterize the shoulder complex dynamics in the first initial 10 to 15 degrees of abduction. The proposed solution addressed the previously described impingement test where the humerus vs. scapula 3D cinematics and dynamics is acquired during an against-gravity abduction on the scapular plane. Moreover, where required, also the external humerus rotation while executing an extra rotation of the humerus is acquired. During the test, the scapula is not forcibly blocked, but it is let free to rotate in all the three dimensions. Two IMD devices are placed on the acromion and on the external side of the humerus as shown in (a).

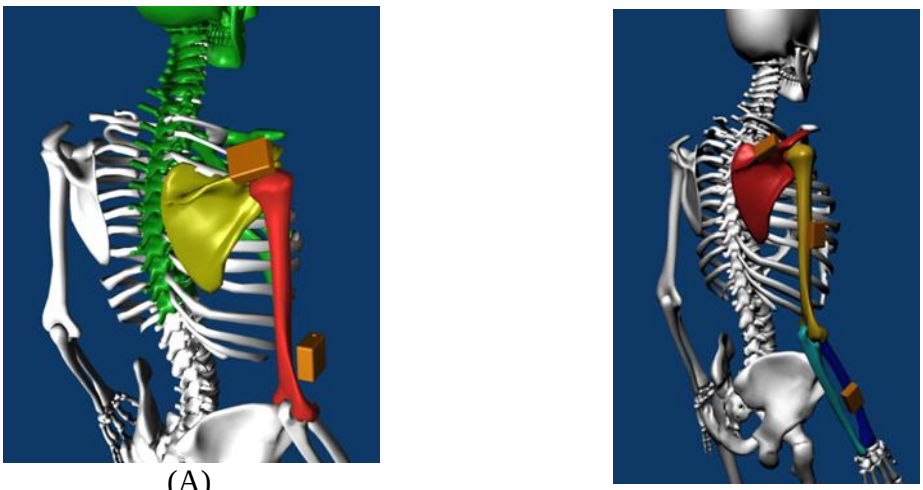

(A) (B)

Figure 52: MIDs device positioning on the subject body.

The data for upward and downward scapula rotation and upward and downward humerus abduction are fully acquired during a repetition of a series of ULA. Data are processed to identify each single ULA which is then processed to extract a set of SPKIs. In the overall analysis and given the typical impingement characteristic previously described, we are going to analyze data with particular attention to the initial phase of the movement for what concerns the relation in between the scapula rotation versus humerus abduction.

In this section we present the work behind the realization of the afore-described solution and the workflow, use-cases and user interface implemented.

7.4.1.1 Design requirements

This section presents the main design and functional requirements considered for the development phase. Particular attention has been dedicated to the portability, the usability – mainly from a clinician point of view – and the overall time required to complete the shoulder assessment which from a clinician point of view is of critical importance in daily work activity. Moreover, the design of the architecture has been enforced to the separation in between a **core** part – which would be of general value in any type of motion data analysis based on data acquired with inertial devices – and a **module** part where each module provides a specific data analysis such as the shoulder assessment which is one of these modules.

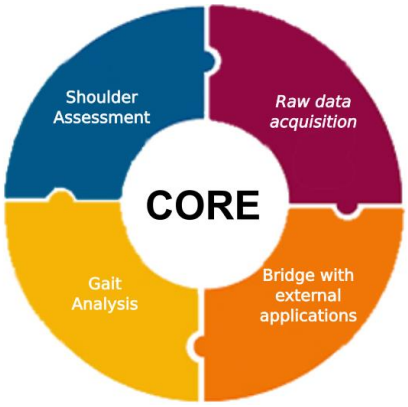

Figure 53: Core based architectural model

Figure 53 shows idea behind the architectural model of the shoulder assessment application, just showing few external modules, whereas many others can be foreseen and implemented. Clearly a CORE componente provides all the common services and API to all the other modules. CORE is now embedded inside the solution, but lately it would be separated and provided as a free SDK library for Android®. External developers can employee the CORE SDK and implement specific motion data analysis with a small effort. Moreover, a more sophisticated idea was to share the CORE SDK as an Android Application Service which can be invoked by external applications as it is currently possible with other Android services such as Agenda or the smartphone vide-camera. The following list reports the main functional requirements for the proposed mobile solution:

- **FR1**: Running on mobile devices or tables.
- **FR2**: Easy to use.
- **FR3**: Easy to acquire data (complete examination workflow).
- **FR4**: Easy to setup and configure.
- **FR5**: Allows for data storage.
- **FR6**: Multi-purpose.
- **FR7**: Providing 3D motion visualization.

In this work attention has been strongly dedicated to realizing a solution which would be extremely flexible and portable and that allows to complete the shoulder assessment or more in general the data acquisition process easily and rapidly. From our on-field experience the daily work of clinicians is critical in term of time to dedicate to each patient.

Modularity and general-purpose solution are other important aspects of the overall proposed solution. As already mentioned, a CORE component provides general and common services to allows the development of other motion analysis solutions. Moreover, the implemented solution can be used as a bridge in between an external generic application and the IMDs devices used to acquire the motion data. A wireless web-socket based communication channels is used to support a json-based protocol to exchange data.

Finally, effort has been dedicated to design a solution which results as much as possible transparent with respect the IMDs vendor. The current implementation already supports both the Notch Pioneer Kit by Wearnotch (https://wearnotch.com/) and the XSENS DOT by XSens (https://www.xsens.com/xsens-dot). Support many hardware device vendors allows the user to choose the preferred hardware solution on the market evaluating price and performances. In the next sections the various aspects of the implemented solution are presented and discussed and, the developed SAA mobile application is presented and discussed from the user's perspective.

7.4.1.2 The shoulder assessment application

Before presenting the technical details of the application, I would prefer to present the final solution from the user's perspective, to provide an overall idea of the application and of its usability. Later, in the subsequent sections, I would present the more technical aspects involved in the application development. The main workflow followed to complete the subject's status assessment is composed of the following steps:

- Patient selection.
- Select body part and device configuration.
- Setup steady position.
- Acquire data.
- Perform data analysis.

In the following of the section, we would present each of the main workflow step in detail starting from patient selection.

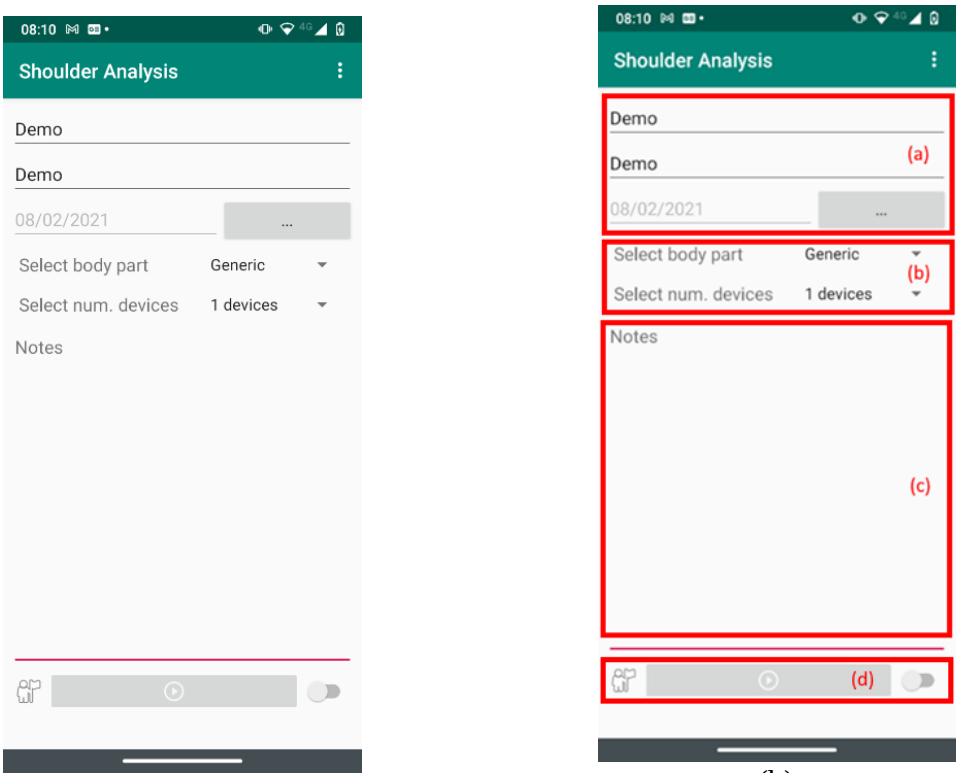

Figure 54: Initial page for the Android's SAA

Patient selection

Figure 54 (a) shows the initial page of the Android's shoulder assessment application. Figure 54 (b) highlight the main parts of the UI. On the top of the main page (in the area identified with letter a) are positioned the patient's data such as name, surname, and date of birth. A while-typing search is performed to lookup an already profiled patient while typing name or surname field. The bottom part, in the rectangle identified with letter c, is positioned a free-text filed where the clinician can write any note about the current patient. When application get started, the user's name and surname are initialized with the default values "Demo". Having an already initialized user's data, allows the clinician to directly start the analysis when interested only to a rapid evaluation of the patient.

Select body part and device configuration

The part of the subject's body to analyze and the associated device configuration to use are selected using the field "Select body part" and the field "Select num. devices" (shown in red rectangle b in Figure 54 (b)). The spinner "Select body part" allows the clinician to select the part of the body to evaluate, meanwhile spinner "Select num. devices" allows the

clinician to select the number of devices to be used on that body part to perform the data acquisition, as shown in Figure 55 (a) and (b).

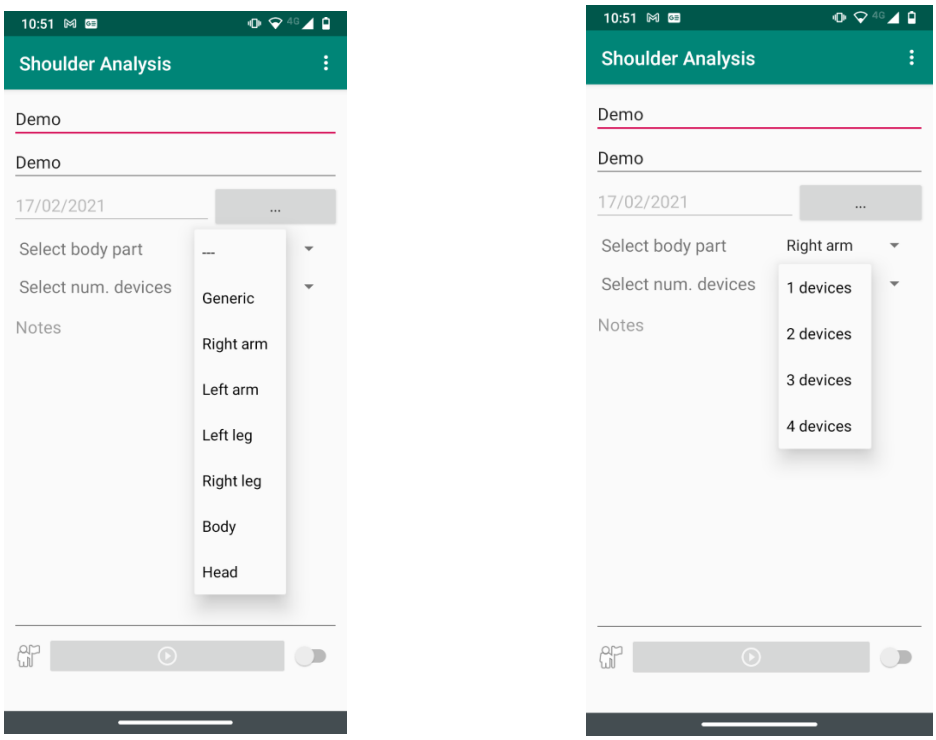

Figure 55: Body parts and num. devices options.

Currently the application allows to select the following parts of the body and the following number of devices:

- Generic.
- Right arm.
- Left arm.
- Left leg.
- Body.
- Head.

- 1 device.
- 2 devices.
- 3 devices.
- 4 devices.

The selected devices are applied to the subject's body follows a top-down sequence; to be clear, in case of upper arm (left or right is not important) the first device is on the scapula, the second on the external side of humerus, the third on the forearm (right before the wrist), and finally the fourth on the external side of the hand's palm. In case of the lower limb, it would be the first device on the hip, the second on the external side of the upper leg,

the third on the external side of the lower limb and the fourth on the upper side of the foot. In the current version the option Body is not yet supported.

A particular case is Generic. In this case the application is not aware neither of the part of the body to analyze nor where the devices are positioned; so, the raw device data are acquired and recorded without performing any type of data analysis. In this case raw data acquired are stored in the persistence layer to be later analyzed. The values of "Select body part" and "Select num. devices" are saved in the application's cache, so the same configuration would be reloaded at next time the application get started.

Setup steady position

Selected the type of body part to analyze and selected the number of devices to use, the workflow proceeds to setup steady position pressing the menu item "Set steady position" shown in Figure 55.

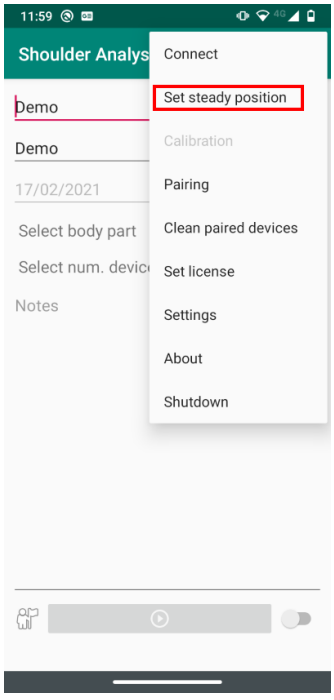

Figure 56: Start set steady position

The steady position setup performs the association between the device and the bones under analysis based on the selected body part and the selected number of devices. Given the part of the body and the number of devices, a single workout definition file is identified. The workout definition contains the mapping information of the device with respect the bone where the device is attached to. The steady position is the zero position of the parts under

analysis, in case of the shoulder assessment the zero position is with the arm under analysis relaxed laying down the lateral side of the body. In the steady position all the quaternion expressing the bone's position should return the quaternion identity, this means that, in steady position, any computed rotation is zero.

The association between the device and the bone is driven by the Bluetooth device association process. This process is by nature random because not always the first identified device is the same of previous association process. As we will see later the workout description file does not contains the information of the bone to device mapping based on the Bluetooth id of the device but contains only the subset of bones that would be considered by the workout itself. So, the association in between the device and the bone is random and could change depending on the device vendor. The current version of the SSA application supports both the Notch and the Xdot device types which both provide a different bone to device association process.

Wearnotch bone to device association

In case of Notch devices, a colored led is used to identify the bone to device association. The bone to color mapping is defined in the workout definition file where for each included bone is specified the color of the led. Meanwhile the Bluetooth process proceeds identifying the devices, the device's led color is set based on the content of the workout definition. The application allows to view the bone to color mapping pressing the button positioned in the bottom left part of the main page, as shown in Figure 57 (a).

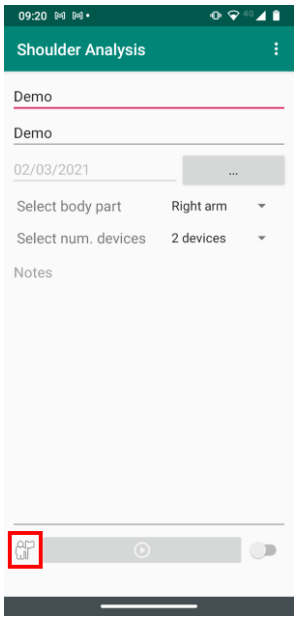

(a)

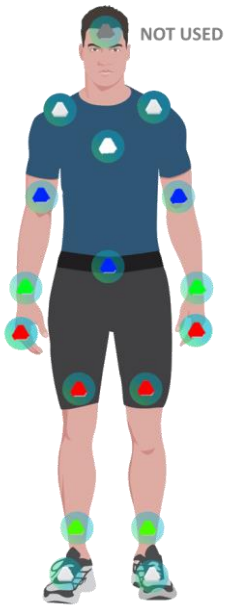

(b)

Figure 57: Button to open bone to device association (a) and the bone to color mapping (b).

Figure 57 (b) shows the model with the mapping of the colors with respect the subject's bones. After setup steady position process has been completed, it is possible to proceed positioning the IMD devices on the subject following the color mapping. Currently it is not possible to change device to bone association for the Notch devices once the setup steady position process gets completed.

XDot bone to device association

In case of DOT by XSens, things are different since XDot devices have a single monochrome led. Xdot devices can be identified only by a specific flashing sequence of the installed led (shown in Figure 57 (a)). In this case, to better support clinicians in doing their work, a bone-to-device remapping mechanism has been implemented. As for Notch devices, the bone-to-device mapping is activated pressing the button shown in Figure 58 (a).

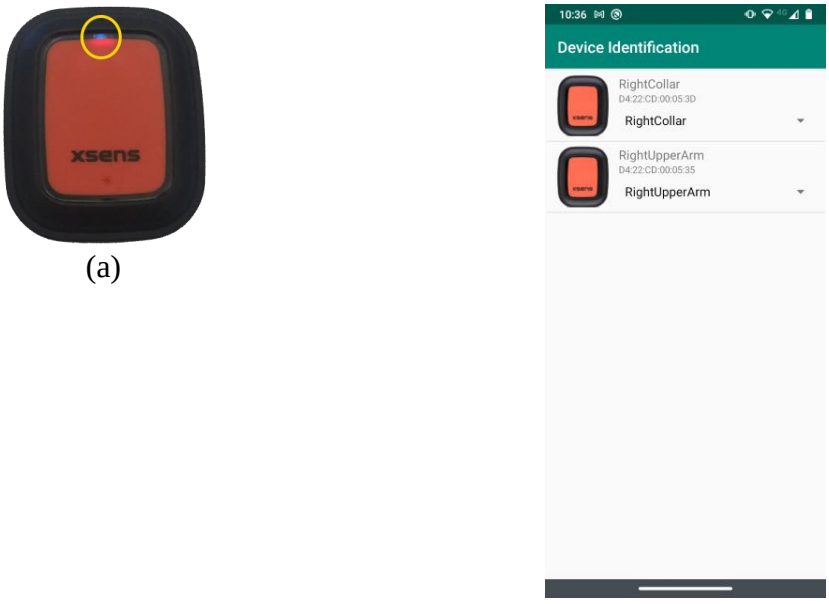

(a) (b)

Figure 58: The XDot led position (a) and the XDot bone-to-device mapping page (b)

Figure 59 (b) shows the bone-to-device association page. The associated devices are listed in order one by one. Clicking on the device's icon force the XDot device's led start flashing allows the clinician to identify the correspondent physical device. Furthermore,

using the provided spinner the clinicians can change the bone associated to each single device.

Data acquisition

Completed the steady position setup, the workflow proceeds with the data acquisition phase. The data acquisition starts pressing the button “play” positioned at the bottom of the main page, as shown in Figure 59 (a).

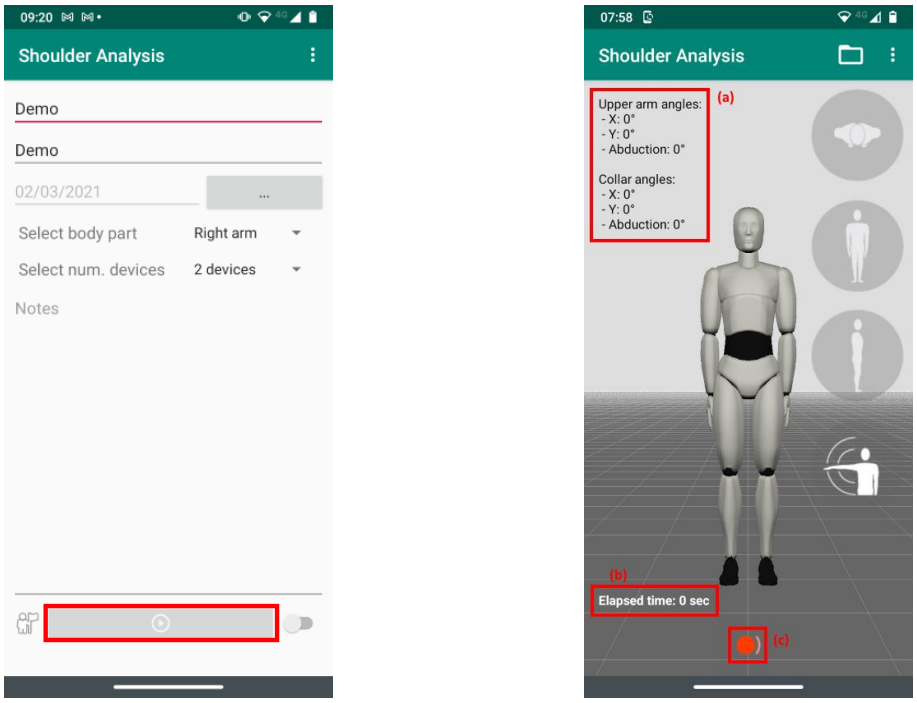

(a) (b)

Figure 59: The button to start data recording (a) and the 3D model page during data recording (b).

Starting data acquisition open the “data acquisition” page, where the 3D human model is used to show the patient’s real-time movements. At this time, the data are not yet recorded but data acquisition has already started.

In the upper left corner of the page is reported the real-time value of the computed abduction for both upper arm and the collar (see Figure 59 (b)). At the bottom left is reported the elapsed time since recording has started, and finally, at the bottom center of the page is placed the button used to start/stop the recoding. Once recording has started, the start button switches to the stop button which can be used to stop data recording when the subject completed the required movements.

When the stop recording button is pressed, the application asks to save data. If the operation is cancelled, the application remains on the “data recording” page. At the contrary, the recorded data get saved and the main humerus abduction and scapula upward/downward rotation are plotted, as shown in Figure 60 (a).

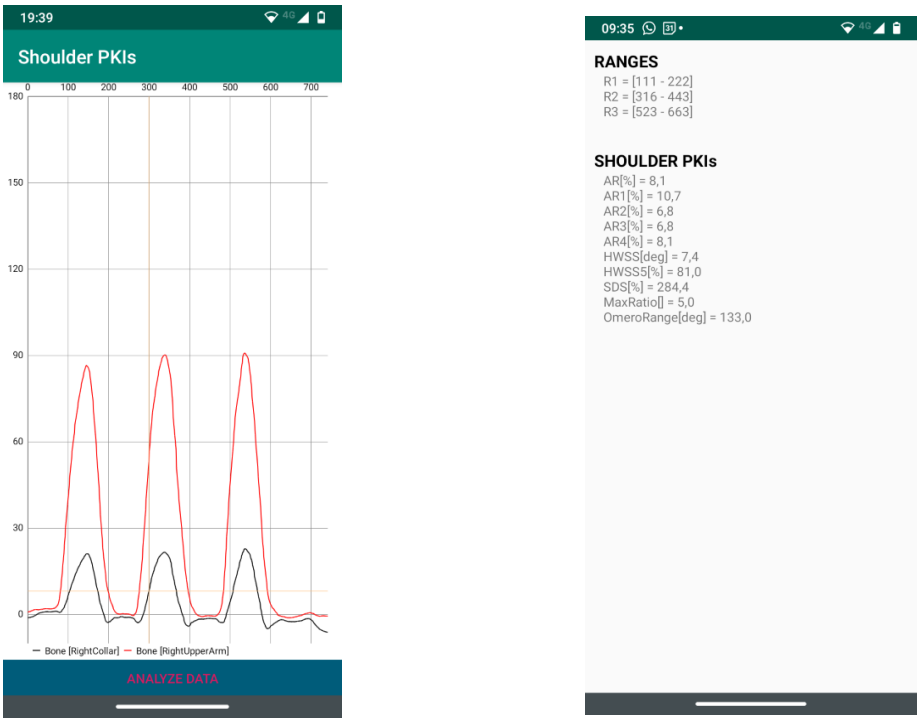

(a) (b)

Figure 60: The main data graph for humerus and scapula (a) and the final page with the estimated SPKIs values (b)

This plot allows the clinician to evaluate the acquired data that would then be used to estimate SPKIs. If the graph is clean, it is possible to proceed to the data analysis pressing the button “analyze data” at the bottom of the page.

Data analysis

The final step of the application’s workflow consists in the analysis of the acquired data to estimate the SPKIs. If the acquired data for humerus abduction and scapular upward/downward rotation are considered acceptable, the button “Analyze data” allows to start the analysis of the acquired data to estimate the SPKIs. The values of the SPKIs are then presented to the user. Currently, there is not a clear idea of how to present such data to the user. For the moment, the final estimation SPKIs values are saved along the data on the persistence storage and raguly plotted to the user one by one, as shown in Figure 60 (b).

7.4.1.3 Application options

Previous section presented the main application's workflow starting from the patient identification up to the final estimation of the SPKIs values. In this section we present the set of application's options that can be controlled by the user to configure the behavior of the application.

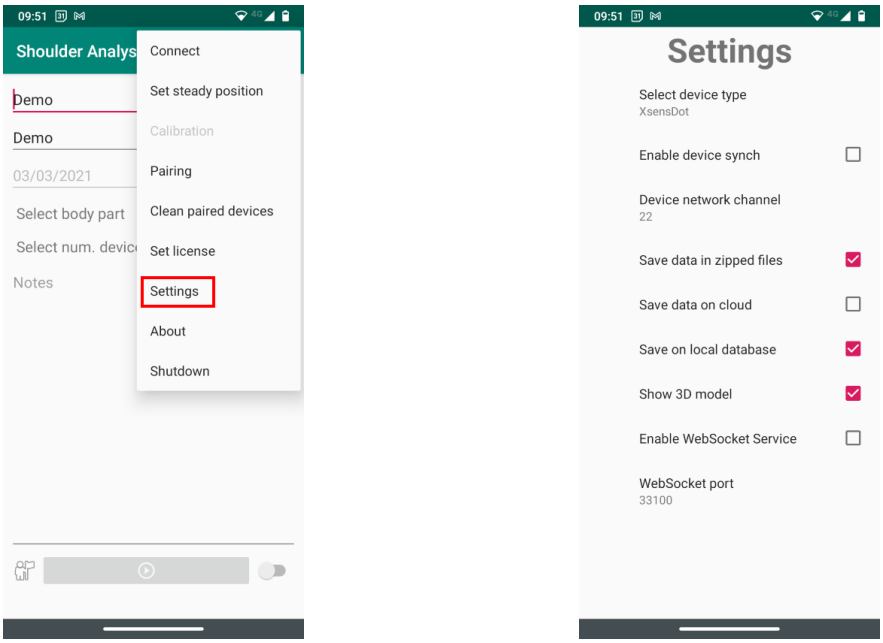

(a) (b)

Figure 61: Application's main menu (a) and application settings page (b)

The application settings page can be activated using the menu item "Settings" from the application's main menu, as show in Figure 61 (a). In Figure 61 (b) is shown the application options page. From this page the user can configure the following options:

- Select device vendor.
- Enable or disable device synchronization.
- Set the device communication channel.
- Enable or disable save zipped file.
- Enable or disable save data on cloud.
- Show or hide 3D human model during data acquisition.
- Enable or disable web socket service and set the web-socket port.

Device synchronization is a feature supported bay both XDot and Notch. Device synchronizations force all the devices to synchronize to a common clock to provide a more precise timing on the acquired data.

Save data in zipped format does not avoid saving data on local storage, but if enabled allows to save data in zipped format to reduce disk space usage.

Showing or hiding 3D model makes sense if the "general" mode has been selected to acquire data. In this case there could be no match in between the device and the subject's bones. For example, if we are interested to acquired motion data of a tennis racket using a single device attached to the bottom of the rachet handle, we are not interested to the real time visualization of the racket motion.

Finally, web-socket configuration is used when the application works as a bridge in between a second client application and the Bluetooth devices. In this case the service IP is the one associated to the mobile device, meanwhile the port can be manually configured. If enabled, when the service starts, the full web-socket URL is printed to the user to be used to configure the client application. Moreover, in this case, we strongly suggest providing a static IP address to the mobile device to avoid changing client configuration each time the application is started, and a new IP get assigned by the DHCP service.

7.4.1.4 Multi-vendor support

As already reported in previous section, one of the key requirements for the implemented mobile solution is to be able to support multiple IMDs vendors. This characteristic has been one of the major efforts of the overall application development because each vendor provides a specific SDK to interact with their proprietary hardware solution. Moreover, each SDK supports specific concepts and different levels of functionalities which must be "normalized" among all the supported vendors. Figure 62 shows the implemented architecture. The application interacts with a singleton Device Manager providing common high-level API which in turn matches the basic functional use-cases. The device manager relay on a standard API for device access creating a specific Device API Implementation based on the user configuration. Both Device Manager and Device API are provided by the CORE SDK. Specific Device API implementations would rely on other external libraries.

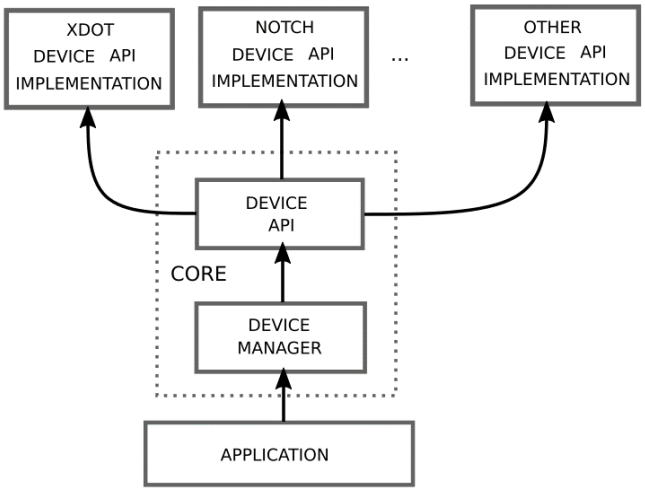

Figure 62: Device manager architecture.

As first step in developing this application layer, we started looking at both SDK the NOTCH and the XDOT trying to extrapolate the common feature. NOTCH SDK with respect the DOT one's supports more interesting features which are reported in the following list:

- Global skeleton definition file.
- Specific workout definition file.
- 3D model to visualize acquired data in real time.
- A well-defined asynchronous callback framework.

The NOTCH SDK features get implemented also in XDOT device implementation interface. A device service factory provides the code for generic interface instantiation. The Device Manager uses the device instance service factory to get a reference to the device API implementation. The device service factory returns the reference if the device implementation has been already created, otherwise checks the user configuration, and decide which implementation to instantiate.

7.4.1.5 Skeleton and workout description files

A key aspect of the application is the solution adopted to describe the whole human skeleton and the single workout used in the data acquisition phase.

The full human body is described by a skeleton description file (SDF). The skeleton description file is a json file which describes the whole human body starting from a virtual root node. In the description, each node has a name, a mass ratio, and a bone vector. A parent-

child relation is defined for each node. Each node is the equivalent of a bone in the real human model. There could be various skeleton models such as for male and female subjects for example. The skeleton model is composed of 26 bones reported in the following list:

- Hip
- Tummy
- ChestBone
- ChestTopo
- LeftCollar
- LeftUpperArm
- LeftForeArm
- LeftHand
- RightCollar
- RightUpperArm
- RightForeArm
- RightHand
- Neck
- Head
- LeftHip
- LeftLowerLeg
- LeftFootTop
- LeftFootFront
- LeftHeel
- RightHip
- RightThigh
- RightLowerLeg
- RightFootTop
- RightFootFront
- RightHeel

Left side of Table 11 shows the initial part of the skeleton description file. The json starts with a version field followed by the skeleton element. The skeleton contains all the nodes representing the bones. The Root node is not associated to any bone but is only used

as the starting skeleton element. The root node is also used to specify the point in 3D space where to place the skeleton model. The right side of Table 11 shows – as an example – the node description for the hip bone, in this case the parent node is the root node.

Table 11: Skeleton representation file. The first node (left), a generic node (right)

```
{
    "version": 2,
    "skeleton": [
        {
            "name": "Root",
            "mass_ratio": 0,
            "bone_vector": [
                0,
                0,
                0
            ],
            "parent_name": "Root"
        },
…
```

```
…
{
      "name": "Hip",
      "mass_ratio": 0,
      "bone_vector": [
                  0,
                  0.04,
                  0
      ],
      "parent_name": "Root"
},
…
```

Each node has a “parent_node” element used to define the joints between nodes. In this version of the application, the skeleton description file is embedded inside the application, but it could also be loaded externally allowing the users to provide their custom skeleton model.

The skeleton description file describes the whole human skeleton in terms of bone names, bone position, bone size and the joints between nodes. To describe the single analysis, we introduced the workout description file (WDF). If the SDF describes the single physical bone and joints of the whole body, the WDF is a json file used to identify the subset of bones involved in the analysis, the color for each bone, the data acquisition frequency, and the master bone of the analysis.

Table 12: An example of workout description file

```
{
    "bones": [
        {
            "name": "RightCollar",
            "color1": "White",
            "color2": "White",
            "frequency": 40
         },
        {
            "name": "RightUpperArm",
            "color1": "Blue",
            "color2": "Blue",
            "frequency": 40
        }
    ],
    "master_bone": "RightUpperArm",
    "special": {
        "bone": "RightUpperArm",
        "orientation": "Right"
    }
}
```

Table 12 shows the WDF file for the SSA application in case of the assessment of the right shoulder. The WDF contains the main element “bones” which is an array of bone nodes where each node contains the following attributes:

- Name
- Color1
- Color2
- Frequency

The attribute Name identifies one of the bones in the SDF file. The fields color1 and color2 provide the color of the device’s led (where applicable) and finally the field frequency provides the desired device data sampling frequency. The data at the end of the file concerns special information such as the master bone name and the reference orientation. A pre-configured set of WDF files is provided with the application, but other WDF files could be provided externally to support custom workout analysis. In the SSA application, the spinners “Select body part” and “Select num. devices” are combined to automatically identify one of the provided WDF files which would then be used to setup the analysis.

7.4.1.6 Persistence architecture

In this section we present and discuss the persistence architecture implemented by the SSA application. One of the most valuable features is the possibility to use the application in any possible context without losing functionalities. In this concern, the persistence layer – the part of the application dedicated to persisting acquire data – would support the very same feature, providing persistence functionalities in any working condition. Android devices do not provide local support for high quality DBMS, usually such devices support light DBMS such as SQLite and similar products. In the SSA application many repeated data acquisitions can lead to a huge number of stored data. Unfortunately, local light DBMS are not adequate to handle all those data; moreover, local databases are not shareable among other devices. To support multiple DBMS vendors and to provide a quite flexible architecture based on a shred database, we envisage the use of a central repository implemented with high-quality DBMS. Each single device does not directly access the CR (Central Repository) but the access to the central repository is mediated by a DPS (Data Provisioning Service), as shown in Figure 63. DPS takes care of bidirectional data synchronization in between the local SQLite database on the mobile device and the CR.

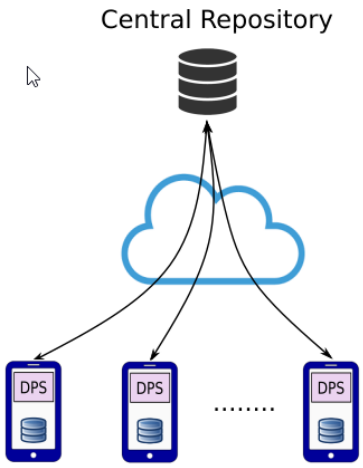

Figure 63: Persistence model.

The DPS service is implemented as an Android service installed separately from the main SSA application. If the DPS is not present data would be saved locally and never synchronized with the external database. In case DPS is present, local data would be periodically synchronized with the CR. Synchronization would also clean local DB removing old data (as configurable option) to keep local DB light and performant. This makes sense if we consider the mobile device to be ultimately a recording device and a real-

time patient status assessment. In this case historical data about examination do not have sense in the local database. If in future, the android application would also provide historical data analysis, a custom application would be developed which in turn would directly access the CR. Central repository can be a Microsoft SQL Server Express or any other DBMS such as Postgress or MySql to cite some, installed in the cloud (as a service) or installed locally on the customer LAN. Whenever a network connection is available in between the DPS and the CR and the synchronization timeout has expired, data get synchronized in between the local DB and the CR.

7.4.1.7 Database architecture

In this section we present and discuss the DB architecture employed by the SSA application. The minimal requirements for the local database are expressed below:

- Store patient identities.
- Store acquired data.
- Store overall shoulder assessment.
- Track historical data.

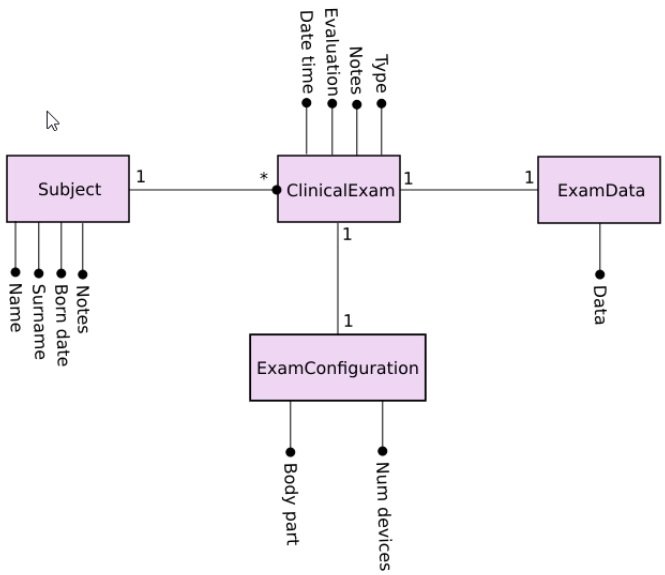

Figure 64: Database model.

Figure 64 shows the initial database model implemented. The model contains four entities (or DB tables): **Subject**, **ClinicalExam**, **ExamData** and **ExamConfiguration**. The entity Subject represents the patient. The ClinicalExam represents a clinical evaluation of

the subject. The ExamData is used to store raw data acquired by the sensors, whereas the data are saved as zipped XML file. Finally, the entity ExamConfiguration keeps the details about the exam configuration. Among various obvious considerations we want to better detail ExamData and ClinicalExam.

ExamData contains the raw data acquired during the single examination. The data are stored as zipped file which contains the XML data acquired during subject examination. These data can easily export and used to improve the analysis if required. This table is the heavier in the whole database, but compression helps considerably to reduce table size and synchronization speed. **ClinicalExam** contains the field named Evaluation which is a string field which contains the JSON representation of the final evaluation result estimated by the application. The DPS provides the synchronization in between the local DB and the remote CR based on its configuration. Each entity has an additional field, not represented in Figure 64, called *TimeStamp*. This field contains the timestamp of each operation on the entity such as insert or update. The TimeStamp field is used by DPS to determine how to execute the entity synchronization. If the timestamp value is more recent on the CR the entity is updated locally, at the contrary, if the timestamp is more recent locally the entity is update on the CR. In normal use a major part of the synchronizations would be from local storage to the central repository to update (upload) the new executed exams. More rarely, synchronization would be performed from CR to local storage, mainly to synchronize subject's data if needed.

To access local database on the mobile device, we decided to employ the use of the Android Room Persistence Library (ARPL) which provides an abstraction layer over SQLite to allow for more robust database access while harnessing the full power of SQLite. The description of how to use ARPL is out of the scope of this document, more on this topic can be found in Internet. In any case raw data are always stored locally as zipped file or – if the option is enabled – the raw data are also saved on a google cloud storage. These zipped files are mainly used as backup copies of the data stored in the database.

7.4.2 SYSTEM CALIBRATION

As already discussed, the IMDs positioning on the body can be different depending by the person that position the IMD devices for data acquisition. To reduce the changes in measurements due to different device positioning, an initial calibration phase is foreseen as key step in the proposed data acquisition protocol.

Device positioning error can be introduced in mainly two different ways: differences in the device's orientation and differences on the specific spot where the devices are

positioned on the subject's body. Differences in device orientation can be mitigated by a calibration phase which takes no more than 2 seconds to be completed. The errors due to a different device positioning with respect reference points (acromion on the shoulder and the external side of the humerus) cannot be mitigated with a calibration process. In this latest case it is the experience of the clinicians and the associated practice which drive the process. In this work we have not performed a deep analysis of the impact of the positioning error on the overall result of the stability shoulder assessment. But the positioning error get mitigated if the same clinicians is used to apply the devices to the subject's body. Intraclass correlation coefficients problematic is described later in section "Intra-class and Inter-class Correlation Coefficients". Is our opinion that the used reference points (one on the acromion and the other on the external side of the humerus) are quite easy to be identified by a clinician and eventually a practical identification process, mainly for the device on the acromion, can even help to reduce device positioning errors.

The calibration process is obtained acquiring two seconds of IMDs samples with a frequency of 60Hz producing around 120 orientation samples for each device. Rotation samples are used to compute the mean rotation value. All the rotations are expressed using a quaternion-based representation. Quaternion were first introduced and formalized by Sir. William Rowan Hamilton around the 1843 as extension to complex numbers [88]. A quaternion is represented as in the following equation:

$$a + b\boldsymbol{i} + c\boldsymbol{j} + d\boldsymbol{k} \qquad \textit{Eq 8}$$

Where a, b, c, and d are real numbers and i, j and k are symbols that represents imaginary unity as for complex numbers. Quaternions are widely used in the representation of rotations in 3D space. In the quaternion representation, a is the "scalar" part and the remaining are the "vector" part. Another way to express Eq 8 is as follows:

$$i^2 + j^2 + k^2 = i\,j\,k = -1 \qquad \textit{Eq 9}$$

Quaternions enjoy various mathematical properties which we do not present herein, for whom more interested on this topic we suggest reading specific bibliography. The real advantage of using quaternion representation with respect Euler Angles is that Euler Angles suffer of the well-known phenomenon of "gimbal lock" which prevents them from

measuring orientation when the pitch angle approaches +/- 90 degrees. Quaternions are less intuitive with respect Euler Angles but at least do no suffer of "gimbal lock" problem.

All the quaternion expressed by the IMDs are represented with respect the absolute world frame also known as inertial frame, where the zero position – the one where all the imaginary parts are zero and the real part of the quaternion is 1 – depends on hardware characteristics of the device. Each rotation of the device produces a new quaternion which in turn represents the rotation of the device in the inertial frame. By the multiplication of a point P in the global frame with the quaternion, we get the point P' which is the position of point P after the rotation represented by the quaternion q, as reported in the following equation:

$$\overline{P_b} = \overline{q_i^b} \left(\frac{0}{\overline{P_i}}\right) \left(\overline{q_i^b}\right)^{-1} \qquad \textit{Eq 10}$$

When a device is positioned on the subject's body, let us suppose on the acromion, the device is clearly rotated with respect the inertial frame as shown in . But in that position, we want that the bone quaternion – the quaternion which represents the rotation of the bone in the world's frame – is the identity quaternion (the zero position). Moreover, we want that the bone rotation being represented in the bone's reference system, shown in Figure 71. To obtain such a result we compute the mean of the quaternions obtained during calibration phase in the world's reference frame. Given the mean quaternion we can compute the bone quaternion in the world's frame with the following equation:

$$q_b = R\left(\bar{q}_i^b \left(\overline{q_{m_i}}^b\right)^{-1}\right) \qquad \textit{Eq 11}$$

In the equation the term $\overline{q_{m_i}}^b$, is the mean quaternion obtained during calibration process, and R is the rotation process applied to the imagery part of the final quaternion to report rotation in the bone reference frame. The $\overline{q_{m_i}}^b$ for each bone are the result of the calibration process and are archived and reused during data acquisition. The calibration process is usually done once each time the devices are repositioned on the body's subject for any reason.

7.4.3 Shoulder Assessment Procedure

This section presents the movement execution and the data acquired during the standardized data acquisition protocol used for the shoulder status assessment. Based on the

consideration discussed with the clinicians, the main idea is to acquire scapula rotation and humerus abduction while ULA execution on the scapular plane. Acquired data are analyzed with particular attention of what happen in the humerus-scapula dynamics in the first degrees of humerus abduction. During the ULA execution, the subject is seated on a stool which is regulated for the patient to have a 90 degrees angle at the knee, as shown in Figure 65.

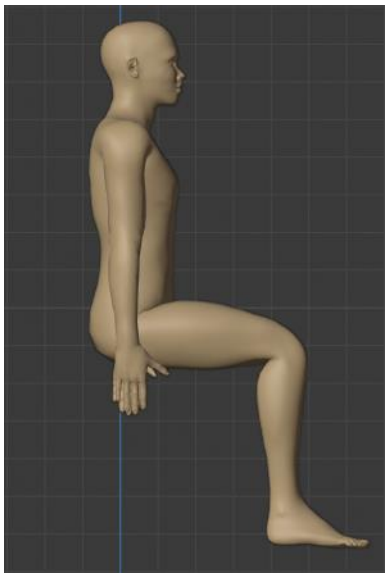

Figure 65: Subject position while executing ULA.

The ULA is executed on the scapular plane, which is positioned at around 30 to 40 degrees anterior with respect frontal plane, as shown in Figure 66. The scapular plane is the more natural position for the scapula in normal relaxed state. As reported in [89] understanding scapular kinematics during scapular plane elevation is important for clinicians, since the kinematic data helps determine appropriate physical therapy after shoulder injury or surgery. In the same position there is a more natural and reduced interaction in between the humerus and the scapula itself while humerus abduction.

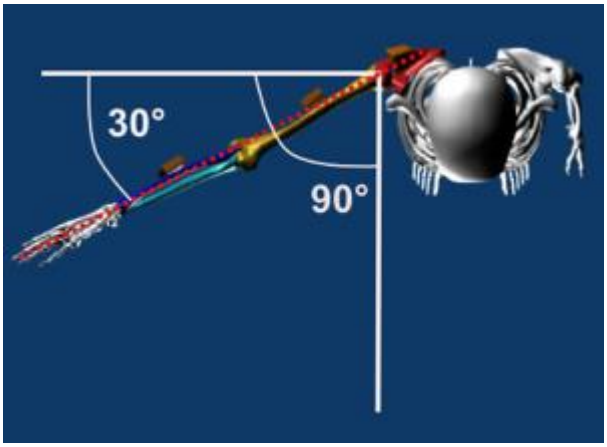

Figure 66: Scapular plane

During abduction, the scapula normally rotates on the three main axes executing a rotation on the frontal (upward rotation), sagittal (anterior/posterior tilt) and transversal plane (internal/external rotation) as shown in Figure 67 (adapted from [89]). In our work we consider only the main rotation which happen on the frontal plane. A justification for this approach is related with the fact that we are interested in the humerus-scapular interaction in early stages of humerus abduction – from 0 to 10/15 – degrees where the overall scapula tilt is almost neglected and not significative [89]. Moreover, the overall humerus abduction is considered in the overall shoulder stability assessment but not the humerus-scapula interaction when humerus abduction is over 20 degrees.

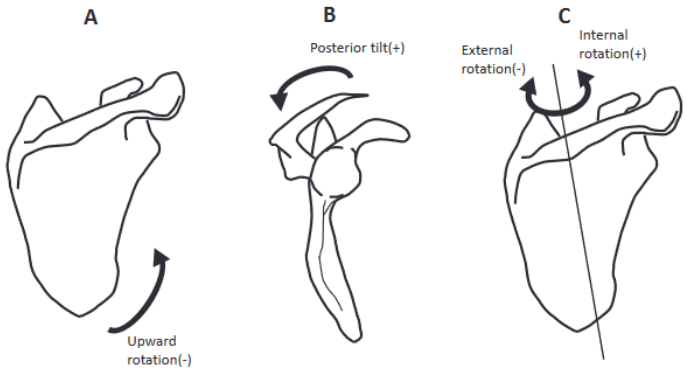

Figure 67: Definitions of scapular motion. (a) Upward rotation, (b) Anterior/posterior tilt and (c) Internal/external rotation

The abduction movement, other than being executed on the scapular plane, is required to get executed at a constant speed of about 60 degrees per seconds. The abduction is executed against gravity, so it means the subject must win gravity to execute the abduction

movement. In this situation the shoulder muscles complex gets activated producing an overall effect of stabilization on the mechanic shoulder complex. The humerus abduction is requested to reach the maximum value possible without feeling any pain, and without creating a non-natural abduction movement. Basically, the idea is to allow the subject to execute the ULA in the most natura possible manner with a fluid movement execution. Future work – as would be explained later - and future experimentation have been already planned to investigate effect of passive or loaded ULA execution on the overall shoulder stability assessment. Passive ULA (PULA) means that the abduction movement is controlled by the clinician which would rise the humerus of the patient while the patient maintains a relaxed muscles condition. Loaded ULA (LULA) instead, requires the subject to autonomously execute the ULA while an elastic stripe is used to apply a resistive force to the abduction movement. Elastic strips with various elasticity would be used to analyze their effects on the overall shoulder mechanics and dynamics.

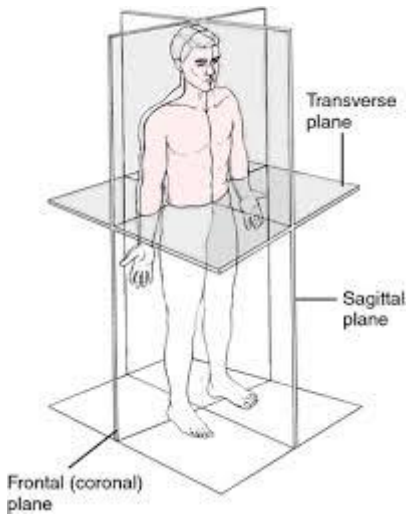

Figure 68: Reference planes: frontal plane, sagittal plane, and transverse plane.

To have multiple measures, a series of tree ULA is requested to the subject; each ULA is executed after a pause period of 5 seconds giving the time to the shoulder muscles to relax back to their initial position. The clinician drives the patient during the ULA series execution, providing the overall rhythms of UAL execution, the position of the humerus during abduction to be on scapular plane and the speed of abduction movement execution.

The use of a real-time visual feedback to drive the ULA movement execution and rhythms was initially introduced in the protocol, with the idea to provide an autonomous solution. Unfortunately, as detailed in section "Visual Feedback considerations ", the obtained effect on the fluidity of the overall ULA execution were completely messed up. In particular, the use of the real time video feedback was pushing the subject to correct time by time one of the three controlled parameters introducing an error on the others most of the time producing a non-natural and non-fluid ULA movement. Working on field we have seen that the best solution – which has been also introduced in the protocol – is to preventively show the movement to the subject by the clinician, mimic the full ULA execution movement, and then allows the subject to try the movement 2/3 times before proceeding to data acquisition. At this point the clinician has only to schedule the single ULA execution over the series of three ULA repetitions. As reported in [90], good effect has been reported in unilateral neglect patients in the execution of a natural task, just showing a video of the overall movement to be executed before the real execution of the task.

The humerus anteposition of 30 degrees to keep during ULA execution is indicated manually by the clinicians considering the characteristics of each single subject, eventually it is possible to indicate a reference in the environment to point with the hand during ULA execution; this can be even a line on a wall reproduced with colored thin strips of tape or anything else available. In the following table we summarize the final acquisition protocol sequence.

Table 13: Data acquisition protocol.

1	Set the patient on a stool and set the stool's height to have a 90 degrees angle at the subject's knees.
2	Place the IMDs on the reference points on the subject's body.
3	Explain the exercise and show the ULA movement to the subject.
4	Perform calibration
5	Allows the subject to repeat the movement and correct if needed.
6	Wait for 10 seconds to allow the patient to recover from previous step.
7	Start the data acquisition asking the subject to execute the movement. After each ULA, wait 5 seconds before to start the second ULA execution. Repeat for 3 to 5 ULA execution.
8	Stop data acquisition and perform analysis.

Orientation data for the scapula, and humerus from each sensor were collected at a sampling rate of 60 Hz[1], usually the maximum sampling rate allowed for the used devices when data get streamed real-time over a Bluetooth channel. The scapular rotation angle relative to thorax was defined as follows: in accordance with International Shoulder Group (ISG) recommendations [91], the rotation of the scapula around the X-s axis was defined as downward rotation being positive and upward rotation negative; rotation around the Y-s axis was defined as internal rotation being positive and external rotation negative; and rotation around the Z-s axis was defined as posterior tilt being positive and anterior tilt negative.

In this work we decided not consider the possible oscillations of the chest while executing the ULA movement. The reasons for this approach can be synthetized in the following points:

1. Keep the overall protocol as simple as possible.
2. On field experimentation showed that chest compensatory movement is almost neglectable.
3. We are interested in relative dynamics of humerus vs. scapula which is not directly affected by chest movements.
4. Compensation can be reduced with a bilateral ULA (ULA executed at the same time with left and right arm) or manually blocking chest compensation.

Beside all the possible justification, we decide not to use thorax IMD device to keep the overall approach, protocol, and application as simple as possible. Only in a second time if practical data would show that the overall performance are worst and a thorax compensation would be needed, then we would start to infer how to include thorax compensation in the proposed solution.

There is deep reason to try to keep solution as simple as possible, and this came from my experience. In past years I participated to the developed of an IMDs based solution to quantify postural recovery for post keen ligament surgery at 3, 6, and 12 months far from the intervention. The protocol was requiring 4 IMDs to be placed on the lateral side of the right and left leg on the femur and tibia. Data were acquired while walking on a Tapis-Roulant at a constant speed of 5 Km/h. Where possible, other speeds were acquired such as 6 Km/h, 7 Km/h and 8 Km/h. Tapis-Rulant was used to have a common standard reference for walking

[1] The reported sampling rate of 60Hz is the one supported by the Xsens DOT IMU devices and Wearnotch devices.

speed. Data were processed and some indicators were extracted. The experiment was ruled out in a private clinic where post-surgical knee ligament intervention subjects were going for post-hospitalization rehabilitation. Each IMD was painted with an arrow to indicate the correct device direction when mounted on the subject and a number on the device was indicating the device-bone association. Beside the data and results, what emerged from this experience was that one of the main drawbacks and clinicians complain was the positioning of the 4 IMDs on the body. Clinician was most of the time placing the devices without too much attention and they discover the positioning problem only after the first data series was acquired. This was leading a too much time consuming process and in a real world where time is a critical resource, this was creating problems to the overall process during normal daily activity. It is from this experience that we decide to try to assess shoulder stability using the minimum number of IMD to avoid hitting against the same problem again.

For the shoulder stability assessment two IMDs device were used, one placed on the scapula's acromion and the second on the external side of the humerus. The two devices were first covered by a paper tape and then placed on the reference points using a medical rounded double-sided adhesive patch as shown in Figure 69. Body surface at the contact points was previously cleaned with disinfectant. Rounded double-sided medical adhesive and paper tape were replaced for each subject to avoid transmission of possible skin infections.

Figure 69: Medical double-sided round tape patches used to position IMDs on subject body

As already reported, the two IMDs used for the shoulder stability assessment must be placed one on the scapula's acromion and the other on the external side of the humerus as shown in Figure 70.

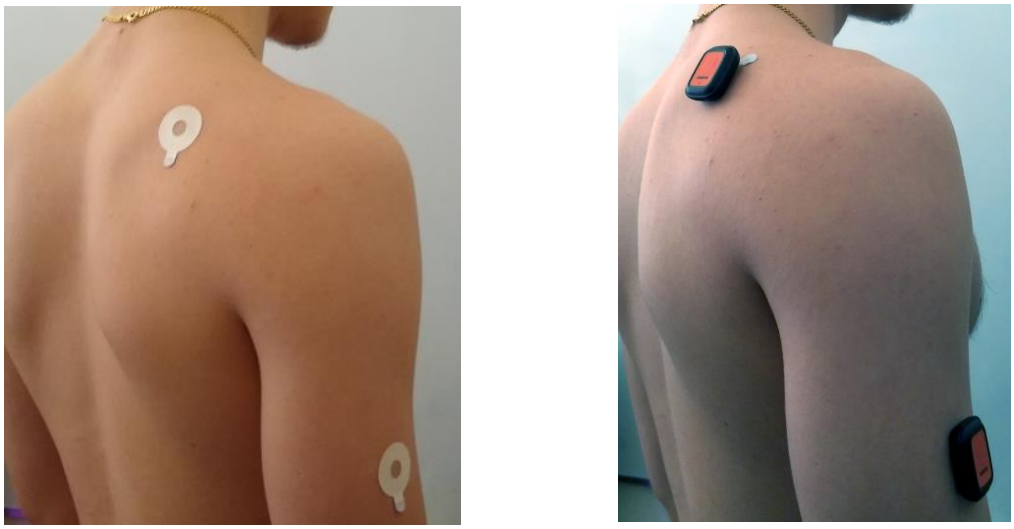

(A) (B)

Figure 70: Patch and device positioning on the shoulder.

The device must be placed with a specific direction. Calibration phase in the protocol (see Table 13) takes 2 seconds of IMDs steady position data to compute the correction matrix to be applied to transform IMD rotations in inertial frame to bone rotation. Bones frame references are shown in Figure 71 (adapted from [89]). As shown in the figure, the frame reference for scapula and humerus are chosen to be orthogonal to the reference planes frontal, sagittal and transversal, shown in Figure 68.

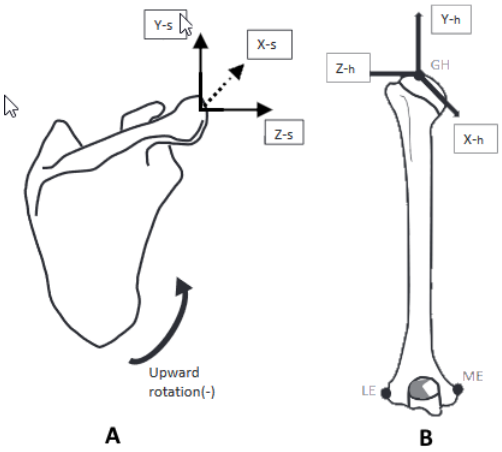

Figure 71: Reference frames for scapula (A) and for humerus (B).

The calibration mechanism aims to correct device positioning with respect the associated bone, so rotation on a generic direction is remapped to one of the orthogonal bone

frame axes. Figure 72 shows a possible device positioning on the shoulder bones. As shown, the device orientation does not perfectly match the reference frame on the bone.

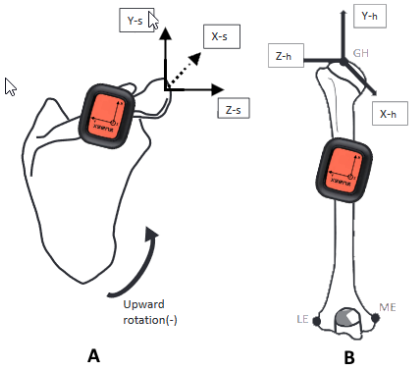

Figure 72: Device positioning on shoulder's bones.

Device positioning most of the time result to be different clinicians by clinicians, so the calibration process aims to fix this positioning error, reducing intra-operation correlation coefficients for the overall shoulder stability assessment; more on this topic can be found in "Intra-class and Inter-class Correlation Coefficients" later in this document.

7.4.4 DATA ACQUISITION AND PROCESSING

Once the calibration phase has been completed, it is possible to proceed to the data acquisition during the execution of ULA movements. The scapula and humerus 3D rotations – expressed as quaternions and computed as reported in "System calibration" – are saved on the persistent storage, and finally processed to compute the scapula rotation on the frontal plane (upward and downward rotation) and the humerus abduction on the scapular plane, as shown in Figure 73.

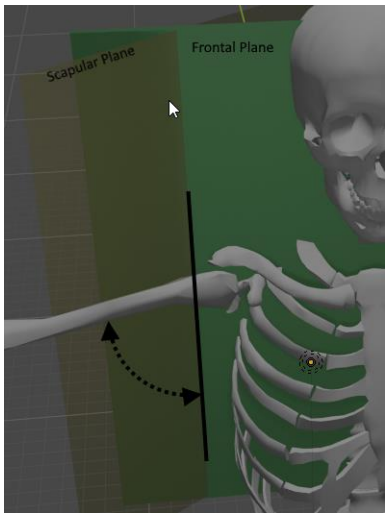

Figure 73: Abduction plane and measured angle.

Abduction degrees are considered zero when the arm is laying down along the lateral side of the body. Figure 74 shows the humerus as a vector V in 3D space. Humerus device rotations – represented as quaternions – are used to compute the angle shown in the figure. The humerus abduction angle remains constant even if the humerus rotates on his main axis or if it changes the overall abduction angle.

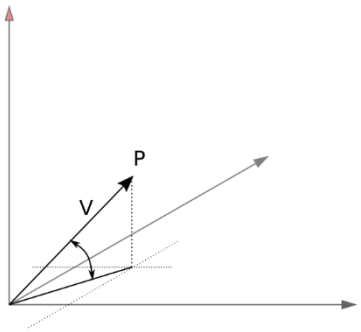

Figure 74: Humerus as 3D vector representation.

The scapula rotations and the humerus abduction expressed in degrees for three consecutive ULA repetitions are shown in Figure 75. Scapula rotation is represented by the line (a) meanwhile humerus abduction with line (b). The plot represents a typical pattern for scapula vs. humerus abduction for a sane and athletic subject. The pattern shows a direct correlation in between the two curves. It is possible to note that the first action of the scapula in the initial phase of the abduction is a small downward rotation, which acts to compensate the humerus load while rising the arm. The scapula downward rotation stands for a while

and then changes from downward rotation to upward rotation up to reaching its maximum value almost in correspondence of the humerus maximal abduction.

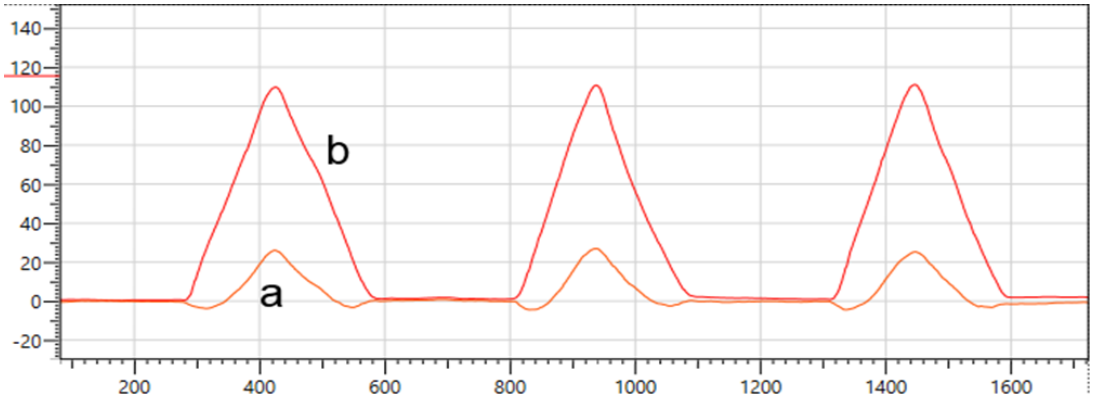

Figure 75: Scapula rotation (a) Vs. humerus abduction (b).

In this work we are interested in the scapula vs. humerus behavior and motion patterns in the initial interaction in between the two elements, and this happen in the first 10 to 15 degrees of humerus abduction (remember that zero degrees abduction is when the humerus lying down along the body). In our opination anomalies in the initial interaction pattern in between scapula and humerus are important information not only to assess the present shoulder pathologies, but also to predict future pathologies in subject which still not feel shoulder pains. This point is crucial in the development of the overall shoulder assessment solution. At the beginning of the project Dr. Luongo, and I were not sure if such hypothesis could have been demonstrated to be valid or not. Our work was initially opened to any possible result, even a failure, demonstrating that our initial hypothesis was completing wrong. Fortunately, as presented in this thesis, the results we obtained are promising and they fully support out initial hypothesis.

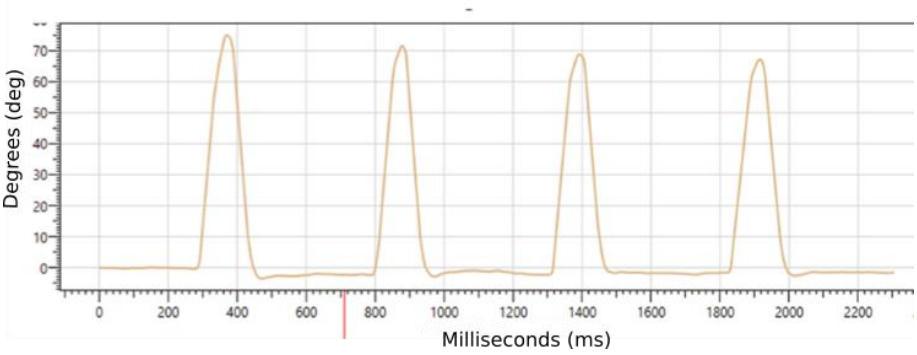

Figure 76: Humerus extra-rotation graph.

Other data, not directly correlated with the humerus vs. scapula interaction in the initial phase of the abduction, are acquired, and processed. In the experimentation we also acquire and investigate the maximum scapula upward rotation, the maximum of humerus abduction and the degrees or humerus extra rotation. Figure 76 shows the graph associated to the measure of the humerus extra-rotation, meanwhile Figure 77 shows how the humerus extra rotation movement is executed by the subject. All these data participate to the overall shoulder assessment.

At this point we needed to find out a mechanism to describe the scapula vs. humerus interaction in the initial phase of the ULA. To describe and characterize the dynamics of the bone's interaction in the initial phase of the ULA, we introduced a set of so called SPKIs: Shoulder Primary Key Indicators. In the overall algorithm, the series of ULAs executed by the subject are separated one each other and the SPKIs are mediated along all the executed ULAs. The presentation and discussion of the SPKIs and the explanation on how those SPKIs are computed is fully described in section "Shoulder Primary Key Indicators", but before explaining SPKIs, we would present and discuss our experience with the use of visual feedback to drive the subject's abduction movement.

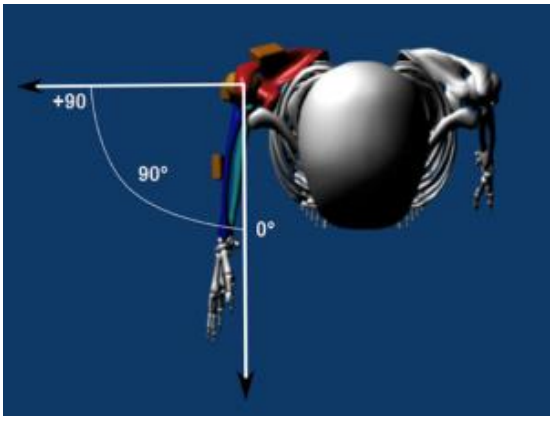

Figure 77: References for the humerus extra rotation movement.

7.4.5 VISUAL FEEDBACK CONSIDERATIONS

As previously reported, the adopted protocol to assess overall shoulder stability, foreseen the execution of the ULA on the scapular plane at a constant speed of around 60 degrees per second (DPS) with multiple repetition (normally tree) and with a pause in between each ULA execution. The main objective behind this approach, is to allow the subject to execute the ULA in the most natura possible manner. As already mentioned, the scapular plane position is roughly indicated to the patient by the clinician, analogously is for the speed of movement execution and the overall rhythm of single ULA execution over the ULA series repetition.

To better drive the subject to correctly execute ULA movement, we initially decided to introduce a real time visual feedback to allow the subject to better control the humerus abduction angle, the abduction speed, and the UAL execution rhythms. The visual feedback was represented as a sphere (called reference sphere) moving up and down in the middle of two vertical bars. An acoustic signal was notifying the start of the ULA and the sphere were moving up and down with the configured speed as requested by the protocol. A second sphere (called controlled sphere) were representing the real subject humerus abduction and speed. The correctness of the movement execution was obtained when the two spheres (the reference sphere and the controlled sphere) were perfectly matching one each other. Figure 78 shows the visual feedback used.

Figure 78: Visual feedback for ULA execution.

Unfortunately, the proposed visual feedback mechanism produced completely unnatural ULA movement execution. All the patients were trying to match the controlled sphere with the reference sphere position as if they were playing in arcade game. The major drawbacks we noticed were:

1. A non-fluid start-up of the humerus abduction.
2. A non-constant speed execution.
3. A non-uniform and constant humerus abduction direction (scapular plane).
4. Lack of attention on the fluidity of the ULA movement.

When the initial beep was signaling the start of the ULA, the subject was starting the abduction too fast, thinking to be late with respect the reference sphere on the visual feedback. During the abduction movement, if the controlled sphere was above the reference one, the subject immediately was reducing the abduction speed, going too slow. At this point the reference sphere was going above the controlled one and the subject immediately increase abduction speed to correct the position, overwhelming the reference sphere again and generating a critical oscillation behavior which in turn was producing a non-constant abduction speed during the ULA execution. As for the abduction speed, the same happened to be true also for the humerus abduction direction which should have been the natural scapular plane. In this case the subject was moving the humerus too anterior or too posterior with respect transversal plane each time the controlled sphere was not matching the reference one. Moreover, in some cases, the subject to correct the humerus position, was moving the humerus in the wrong direction, backward when the real correction was forward direction, generating a still worst ULA movement. Even explaining to the subjects that the perfect matching in between the two spheres was not required, and that they shall concentrate on the

execution of the movement the effect was always the same. The failure experienced with the use of visual feedback does not mean that visual feedback is not a valid tool, but only that the visual feedback approach must be well studied, tailored, and tested before being adopted in each real context. The use of visual feedback to drive subject's movements is out of the scope of this work, so we did not investigate this topic.

7.4.6 SHOULDER PRIMARY KEY INDICATORS

As previously reported in this document, we suppose that the shoulder stability assessment, and the possibility to foreseen shoulder pathologies for non-pathologic subjects, can be obtained analyzing the scapula vs. humerus interaction in the first 10 to 15 degrees of humerus abduction while executing an ULA on the scapular plane and against gravity.

The overall protocol requires the subject to execute a series of ULA movements with a pause of 5 seconds in between each executed ULA. The IMDs positioned on the acromion and on the external side of the humerus are used to acquire 3D motion data for scapula and humerus, respectively. Figure 75 shows the scapula upward rotation on the frontal plane with respect the humerus abduction during the execution of three consecutive ULA.

To describe the dynamics of scapula vs. humerus interaction in the first 10 to 15 degrees of abduction we introduced for the first time a new set of SPKIs. With respect many other studies on the shoulder complex, where the overall range of motion (ROM) is considered, or where other shoulder's macro dynamics are taken into account [49], [78]–[81] and where in general all the dynamics range of shoulder bones' are taken under analysis, in this study we define a new set of shoulder primary key indicator – proposed for the first time in literature – which aims to characterize the humerus vs. scapula dynamics in the very early stage of humerus abduction on the scapular plane in particular in the range from 0 to 15 degrees of humerus abduction. This section presents such SPKIs and describes their meaning and how those SPKIs are computed.

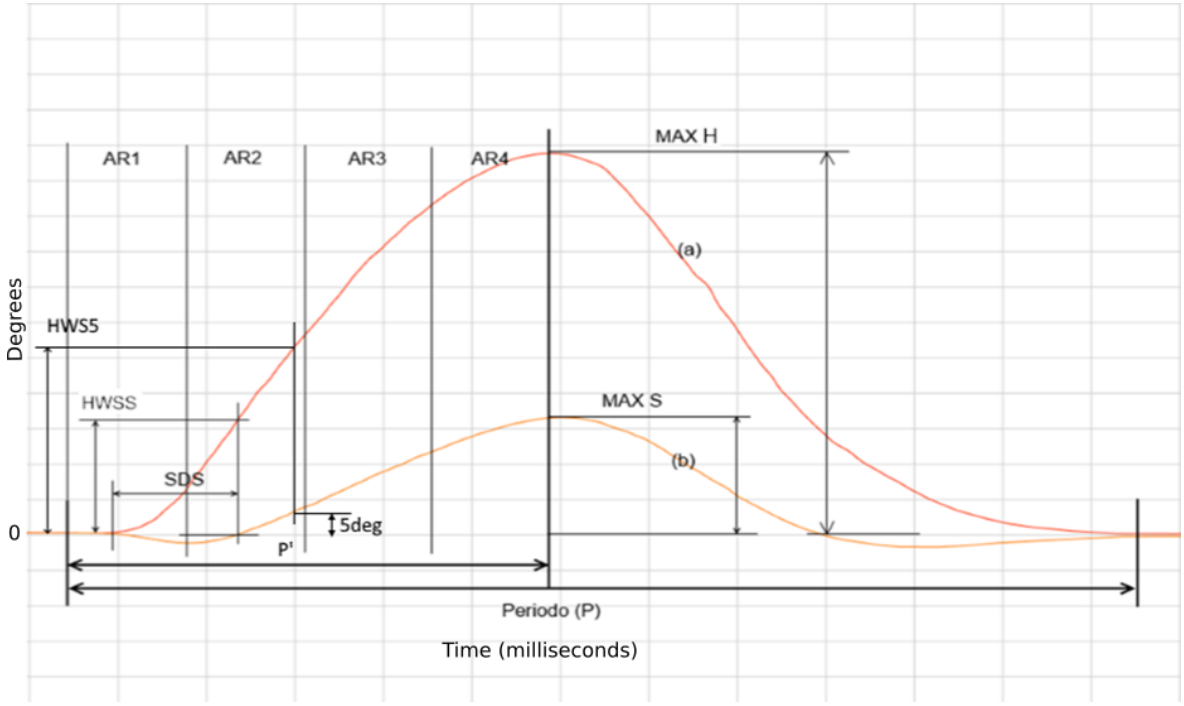

Figure 79: Details of scapula (b) vs. humerus (a) during a single ULA.

Figure 79 shows the details of the scapula vs. humerus acquired data while executing a single ULA. Line (b) represents the scapula upward/downward rotation on the frontal plane, meanwhile line (a) represents the humerus abduction; all data are expressed in degrees.

The overall stability assessment protocols require to execute a minimum of 3 ULAs to compute the SPKI values as a mean value over the executed ULAs. Given the series of *n* ULAs, the algorithm initiate identifying the start-time and end-time of each single ULA. This allows to identify the period P and the semi-period P' of each single ULA. The semi-period P' is considered from the beginning of the period P up to the point in which the humerus abduction reaches it maximum value, it is not always the half of a period P.

Inside the period P we compute two basic value: the maximum of the humerus abduction and the maximum of the scapula upward rotation, MAXH and MAXS, respectively. From MAXH and MAXS we also compute the MAXR named max-ratio and computed as the ration in between MAXS divide by MAXR, as in the following equation:

$$MAXS = \max(s(t))|_P \qquad \text{Eq 12}$$

$$MAXH = \max\left(h(t)\right)|_{P} \quad \text{Eq 13}$$

$$MAXR = \frac{MAXS}{MAXH} \quad \text{Eq 14}$$

Where:

- s(t) is the curve of the scapula upward rotation in the period P.
- h(t) is the curve of the humerus abduction in the period P.
- P is the overall ULA period.

MAXR is a pure number, MAXS and MAXH are expressed in degrees. Another parameter which is directly related with the curves in a static manner is the overall area ratio, defined as the ratio in between the overall area of the curve of the scapula with respect the sum of the area of the curve of the scapula added with the area of the curve of the humerus expressed in %, as described by the following equation:

$$AR = 100 * \left(\frac{|A_s|}{|A_s| + |A_h|}\right) \quad \text{Eq 15}$$

Where:

- A_s is the area of the scapula and
- A_h is the area of the humerus.

As previously stated, we are interested in the behavior of the humerus vs. scapula in the first 10 to 15 degrees of abduction, so we introduced other SPKIs which are more related with the shoulder behavior in the initial phase of the abduction. Such parameters are listed below:

- Partial Area Ratio.
- Scapula delta-start.
- Humerus abduction when scapula starts.
- Humerus abduction when scapula is 5 deg.

Partial Area Ratio

The PAR (Partial Area Ratio) parameter is really a set of 4 area ratios computed in the first 4 parts of the semi-period P' of a single ULA, as shown in Figure 79. The semi-period P' is divided in four equals parts: PAR^1, PAR^2, PAR^3 and PAR^4. On each part the area ratio is computed as for the parameter AR expressed in Eq 15.

$$PAR^i = 100 * \left(\frac{|A_s^i|}{|A_s^i| + |A_h^i|} \right) \qquad \textit{Eq 16}$$

The more interesting PAR are the first two values: PAR^1 and PAR^2, which are more related with the initial behavior of the humerus-scapula joint. PAR^3 and PAR^4 are computed for completeness but are less important in our analysis.

In our hypothesis we suppose that shoulder pathologies would impact the dynamics of the humerus vs. shoulder interaction, so we expect that any changes in the interaction in between humerus and scapula would produce a correspondent change in PAR^1 and PAR^2 values.

Scapula Delta Start

The SDS parameter measure the time required by the scapula upward rotation to reach the zero position after the initial negative value due to the load of the humerus on the scapula itself, as previously explained presenting the overall shoulder mechanics. The time in which scapula upward rotation pass through zero is then normalized with respect the overall period of the ULA and expressed in %, as in the following equation:

$$SDS = 100 * \frac{\left(t|_{s(t)>0 \;\&\; t>0}\right)}{P} \qquad \textit{Eq 17}$$

Where:

- t is the time.
- s(t) is the scapula upward rotation at time t.
- t is set to zero at the beginning of the period P of each ULA.
- P is the overall ULA period in seconds.

With respect of our idea of initial humerus vs. shoulder interaction for non-pathological vs. pathological shoulders, we can foresee that SDS values would be higher in

healthy shoulder with respect pathological ones. This means that the scapula would get activated later for non-pathological shoulders with respect pathological shoulders. SDS is a pure number.

Humerus Abduction When Scapula Starts

The HWSS is the degrees of abduction of the humerus when first scapula reaches the zero degrees value after being reaching its lover value, as shown in Figure 79. We define HWSS as reported in the following equation:

$$HWSS = 100 * \frac{\left(h(t)|_{s(t)<0 \,\&\, s(t+1)>0}\right)}{P} \qquad \textit{Eq 18}$$

Where:

- h(t) is the humerus abduction degrees at time t.
- s(t) is the scapula upward rotation at time t.
- P is the overall period P of the ULA.

The idea behind this parameter is that higher values of HWSS are present in non-pathological shoulders. Meanwhile pathological shoulders should present lower values of HWSS due to the earlier interaction in between the humerus and the scapula. The value of HWSS is a pure number.

Humerus When Scapula is 5 Degrees

Other that HWSS parameter we introduced a more relaxed parameter which is the same of HWSS but instead to measure the humerus abduction when scapula first rise above zero, the HWS5 parameter measure the humerus abduction when scapula reaches 5 degrees of upward rotation, as shown in Figure 79. The HWS5 is expressed by the following equation:

$$HWSS = 100 * \frac{\left(h(t)|_{s(t)<5 \,\&\, s(t+1)>5}\right)}{P} \qquad \textit{Eq 19}$$

Where:

- h(t) is the humerus abduction degrees at time t.
- s(t) is the scapula upward rotation at time t.

- P is the overall period P of the ULA.

As for the HWSS the HWS5 we expect to have higher values for non-pathological shoulders and lower values for pathological ones. HWS5 is a pure number.

In general, for what concerns expectation on the values of the SPKIs – the doctors and the team of expertise participating on the on-field test – expect that SPKIs values would manifest low or very low variance among non-pathological subjects, indicating a stable shoulder complex. At the contrary, in the case of pathological subjects, the expertise would expect high variability on the computed SPKIs values do to a non-stable shoulder complex.

7.4.7 Intra-class and Inter-class Correlation Coefficients

In previous section the SPKIs have been introduced and motivated from a clinical point of view presenting what are the expected SPKIs behavior for non-pathological and pathological shoulders. This section discusses the intraclass correlation coefficients (ICC). The point is to understand and eventually quantify how SPKIs and the overall shoulder stability assessment would change when the protocol is administered by different operators (clinicians) executing the same shoulder status assessment. It is evident that various operators would place the IMDs devices with different "precision" on the reference points. These minimal differences would somehow have direct or indirect impact on the acquired data and consequently on the overall shoulder assessment results. Moreover, not only there are differences in IMDs positioning among different operators but even when the same operator place IMDs on the body of different subjects. In this case we refer to inter-rater ICC, meanwhile in the previous case we refer to intra-rater ICC.

Intraclass correlation coefficient (ICC) is a widely used reliability index in test-retest, intra-rater, and inter-rater reliability analyses [50]. In particular, Correlation Coefficients are measures of agreement between paired variables (xi, yi), where there is one independent pair of observations for each subject [51]. In a simple form the ICC is an index that express the fact that results are independent by the subject that prepared the environment and the patient for data acquisition.

In our case "preparing the environment" correspond to the positioning of the IMDs on the reference points on the shoulder of the subject. There are two possible positioning errors that operators can fall-in: error on the spatial point where the single IMD is placed and the orientation of the IMD with respect the reference orientation as shown in Figure 72.

In our opinion, the reference points used in this work are relatively easy to be identified. For the scapula, the protocol requires to position the IMD on the acromion which is quite easy to be identified by trained clinicians using hand palpation; meanwhile, for the humerus, the protocol requires to position the IMD on the external side of the bone in the middle in between the elbow and the end of the humerus bone. Moreover, device orientation errors would have been reduced by the device calibration phase execute before each data acquisition session on a different subject. In conclusion, to reduce the influence of ICC on the results, in our on-field experimentation, we decided to train a single clinician and to allow only that clinician to perform the shoulder assessment.

In this initial work on shoulder status assessment, we were not sure of what could have been the results, so we preferred to post-pone the ICC investigation for a second phase in case the on-field experimentation of the proposed solution would have produced valid results (as it fortunately was).

7.4.8 Subjects Classification and Neural Network Approach

Previous sections presented and discussed the SPKIs distribution over classification ranges and SPKIs distribution over the subjects' age. In this section we investigate, with a preliminary study, the possibility to identify classification threshold and eventually the possibility to use Neural Networks (NN) to automatically solve the classification problem for shoulder status assessment.

For this specific purpose, we adopted an AI approach based on NN (Neural Networks) to properly classify the shoulder status in between non-pathological and pathological using the following SPKIs: HWSS, SDS, AR1, HWSS5 and AR2. The NN input vector is composed of 5 elements this because to the primary SPKIs (HWSS, SDS and AR1) we added two others SPKIs which are HWSS5 and AR2. HWSS5 is the abduction degrees of the humerus when the scapula reaches 5 degrees of upward rotation. AR2 is the area-ratio computed in sector 2. To keep things simple, we decided to investigate the possibility to find an autonomous classifier able to classify among two main classes: non-pathological and pathological. To design the NN we used FANN Tool[2] (FANT). FANT provides backpropagation training functionalities which can be used to automatically design and define the NN. After the target classes have been defined, an ANN is trained to

[2] FANN Tool is an open-source fast artificial neural network library with GUI which implements multilayer artificial neural networks which supports for both fully connected and sparsely connected networks. http://leenissen.dk/fann/wp/

automatically classify input vectors – never seen before – telling which is the container the given input vector belongs to. FANT is a powerful tool to define, process and test NN; moreover, its libraries can also be used to integrate NN functionalities in general-purpose applications.

In the design of the NN we kept separated female group from male group, designing two separated NNs. In the design of the NN we considered an input vector of dimension 5 and a single output of dimension 1 (a scalar value). The output value 0 means a pathologic shoulder, meanwhile a value of 1 means a non-pathologic shoulder. The input vector result defined by the following values: HWSS, SDS, HWSS5, AR1 and AR2.

The training file for female group, has been manually written and is composed of 14 input vectors associated to non-pathological female subjects and 9 input vectors associated to pathological female subjects. Which means, for non-pathological subjects, a total of 14 training data over a population of 27 female subjects; meanwhile, for the pathological subject, 9 training data over a population of 18 female subjects which result to be around to 50% of the entire female population. In the very same way, a test file has been created using the data of the female group not used for the training file. The training file and the test file are enough for FANT to define, finalize and test the ANN. FANT requires the following steps to generate an artificial NN:

- Detect optimum training algorithm.
- Detect optimum activation function.
- Train ANN.

FANT allows to set the following configuration parameters before start processing data file to compute the final NN:

- Stop function type.
- Epoch between reports.
- Max number of epochs.
- Number of layers.
- Number of nodes in hidden layer 1.
- Number of nodes in hidden layers 2.

In our case we used the following basic configuration:

Stop function type: **FANN_STOPFUNC_MSE**

Epoch between reports: **1000**

Max number of epochs: **500000**

Number of layers: **4**

Number of nodes in hidden layer 1: **4**

Number of nodes in hidden layers 2: **3**

After the training phase, FANT identifies the optimal training method and the optimal activation function for both hidden and output nodes. Preliminary results concerning the identified population are reported in the "Subjects Classification" section.

7.4.9 Experimental Evaluation

For the on-field evaluation, 72 voluntary subjects have been selected with an age in between 19 and 80 years. In the subject set there were 45 females and 27 males. Of the 45 females, 27 did not present pathologies at the shoulder whereas the remaining 18 reported specific pathologies or previous trauma. Of the 37 males, 22 did not present any pathology at the shoulder and 15 reported previous traumas or lesions.

To properly select the subjects to admit to the on-field experimentation, a precise and schematic specialistic medical examination has been performed by the team of expertise. All the subjects undergo to the Visual Analogue Scale (VAS) for overall subjective shoulder pain assessment. The subjects were classified based on the subjective quantification of the omalgia by considering the pain scale. From all the possible subjects to include in the experimentation, all the subjects with following characteristics were excluded:

1. Subjects with cervico-dorsal backache.
2. Subjects with previous trauma at the shoulder or spine.
3. Subjects employed on repetitive work with humerus abducted more than 45 degrees for more than 12 months a year.
4. Subjects suffering of ligament laxity and collagenopathies.
5. Subjects in ongoing anti-inflammatory drug therapy.

In conclusion the following groups have been identified:

Group A

The group A (GA) contains all the female subjects without reported shoulder pathologies and normal shoulder functionalities. In this group there were 27 subjects asymptomatic for omalgia with a VAS scale in between 0 to 1.

Group B

The group B (GB) contains all the female subjects with reported shoulder pathologies. This group contains 18 pathological subjects with VAS scale above 4 and with limited passive articulation for humerus abduction and extra rotation in range 0 to 50% of normal physiological range.

Group C

The group C (GC) contains all the male subjects with no reported shoulder pathologies and with normal shoulder mobility. In this group there were 22 subjects asymptomatic for omalgia with a VAS scale in between 0 and 1.

Group D

The group D (GD) contains all the male subjects with reported shoulder pathologies. This group contains 15 patients with VAS scale above 4 and with limited passive articular mobility in humerus abduction and extra rotation in the range 0 to 50% of the normal physiological range.

Table 14 reports the overall subdivision in between pathological and non-pathological subjects. All subjects included in the on-field experimentation have been previously informed on the study and, at the same time of the visit, they were asked to sign an informed consent.

N. subjects	Pathological	Non-Pathological
45 females	18	27
37 males	15	22

Table 14: Subjects overview subdivision by pathological and non-pathological

In various moment during the period of the on-field experimentation, selected subjects were analyzed using the SSA mobile application. The same clinician expert previously trained on the use of the solution and trained on the overall application's protocol was using the SSA to acquire subject's data. 3D motion data ant the overall SPKIs estimated by the proposed solution were save on the local device and on the database for further investigation and analysis.

The overall procedure was conducted as reported below:

1. The subject was first asked to remove the clothes were covering the shoulder to have scapula and humerus fully uncovered. Eventually, where bra cords were impacting the scapula, the subject was asked to partially remove the bra to avoid scapula interferences.
2. The subject was seated on the stool and the stool regulated to have a 90 degrees angle at the subject's knee.
3. The subject's zones were IMDs were placed were cleaned with an alcoholic solution to remove impurity and to disinfect the area.
4. A medical bi-adhesive tape patches were applied to the reference point for acromion and humerus, as already explained.
5. IMDs device were positioned on the bi-adhesive patches with the right orientation, well painted on the device itself.
6. The clinicians explain the movements to the subject and ask him/her to mimic the very same movement up to when the subject seems being confident with the movement itself.
7. After a steady period of 10 seconds to recover, the clinicians start IMD calibration, which takes no more than 2 to 3 seconds.

8. After calibration, the clinician starts data recording on the SSA solution and drive the patient during the execution of the movement timing the start of the ULA and the overall natural speed. The clinician drives the subject to the execution of at least 3 ULA with a maximum of 5 ULA a steady period of 5 seconds is required in between each single ULA.
9. If clinicians discover abnormal movement, it stops the recording and after a steady period of 10 seconds starts a new recording as explained in previous point 8.
10. If the movement get executed correctly the clinician save acquired data and estimated SPKIs.
11. The session gets concluded, and the subject allowed to get dressed.

The overall process takes no more than 10 minutes to get completed. Usually after the data acquisition the clinicians execute an overall medical evaluation of the subject's shoulder.

7.5 Results and Discussion

In this section we present and discuss the preliminary results obtained from the data analysis on the 72 analyzed subjects. Data analysis has been separated in between male and female subjects. The data analysis identified that most significative SPKIs to assess shoulder stability are the following: HWSS, SDS and AR1.

7.5.1 Pathology Effect on SPKIs

To better highlight the obtained results, the SPKIs values have been divided in categories where the threshold has been empirically identified based on the SPKI range. The following ranges have been defined:

- S1 [0 – 6)
- S2 [6 – 11)
- S3 [11 – 16)
- S4 ≥ 16

The ranges have been kept the same for all the SPKIs, we think this is not an optimal choice but adequate as first approach to the overall classification problem.

Table 15 summarizes the SPKIs classification based on the previously identified ranges for non-pathological and pathological female subjects. Table 16 reports same data for male subjects.

Table 15: Characteristic SPKIs for female divided by non-pathological and pathological subjects.

Data	NON pathologic	Pathologic
Quantity	27	18
Age		
MIN	30	25
MAX	86	80
MEAN	56	59
HWSS		
From [0 – 6)	0	1
From [6 – 11)	0	11
From [11 – 16)	5	6
Above 16	22	0
SDS		
From [0 – 6)	0	7
From [6 – 11)	10	11
From [11 – 16)	14	0
Above 16	3	0
AR1		
From [0 – 6)	13	0
From [6 – 11)	6	2
From [11 – 16)	5	5
Above 16	3	11

Table 16:Characteristic SPKIs for male divided in non-pathological and pathological subjects.

Data	NON pathologic	Pathologic
Quantity	22	15
Age		
MIN	19	44
MAX	72	77
MEAN	46	62
HWSS		
From [0 – 6)	0	0
From [6 – 11)	0	9
From [11 – 16)	2	2
Above 16	20	4
SDS		
From [0 – 6)	0	5
From [6 – 11)	2	8
From [11 – 16)	8	2
Above 16	12	0
AR1		
From [0 – 6)	12	1
From [6 – 11)	7	1
From [11 – 16)	1	5
Above 16	2	8

Just looking at the tables above, it is possible to see how the SPKIs can classify and clearly separate the pathological subject from non-pathological subjects. The SPKIs behavior is still more evident if we plot the classes on a bar graphs, as reported in the following set of figures.

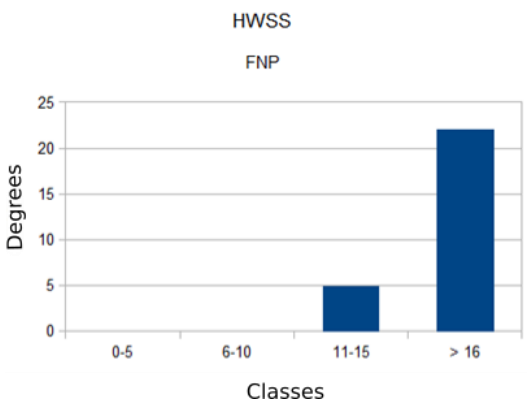

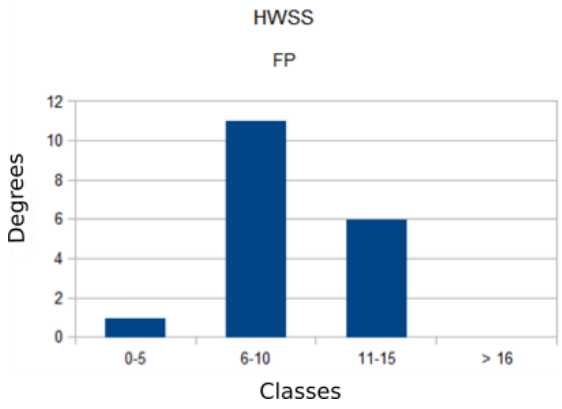

Figure 80: HWSS bar graph for NPFG (left) and PFG (right) groups.

Figure 80 shows the HWSS classes for non-pathologic and pathologic female subjects. From the figure it is evident how the HWSS discriminates clearly between pathologic and non-pathologic subjects. More than 81% of non-pathologic female subjects (NPFG) shows an HWSS value above 16. Meanwhile, in pathologic female subjects (PFG) 100% of the subjects has an HWSS lower than 16.

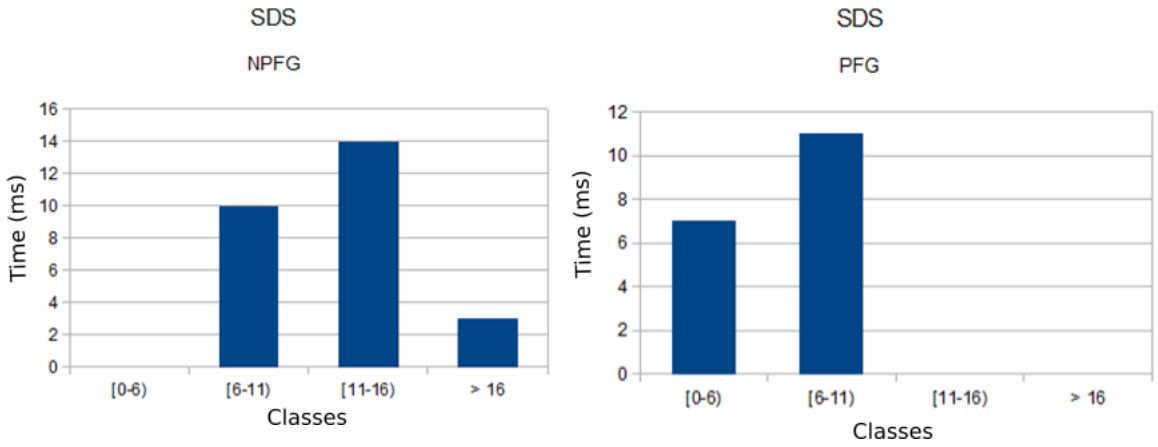

Figure 81: SDS bar graph for NPFG (left) and PFG (right) groups.

The SDS SPKIs distribution is shown in Figure 81. As for HWSS, even SDS well discriminates pathological vs. non-pathological subjects. In PFG 100% of the subject has a value lower than 11. In NPFG, around 63% of the subjects are above 11 and 37% of the subjects remain in the range S2. From the data it is evident that also this SPKIs works well to discriminate between the two groups (NPFG and PFG) but the threshold we used to define the classes is not the optimal selection. We discuss this point later in this thesis.

Figure 82 shows the AR1 classes for NPFG and PFG. AR1 is quite a good indicator for the identification of the presence of a dyskinesis in the humerus-scapular joint. With this SPKI, 100% of subjects in PFG have a value above 6 and only the 11% is below 11 with an 89% of the subjects with value above 11. Meanwhile, in the NPFG the 70% of the subjects have a value of AR1 below 11.

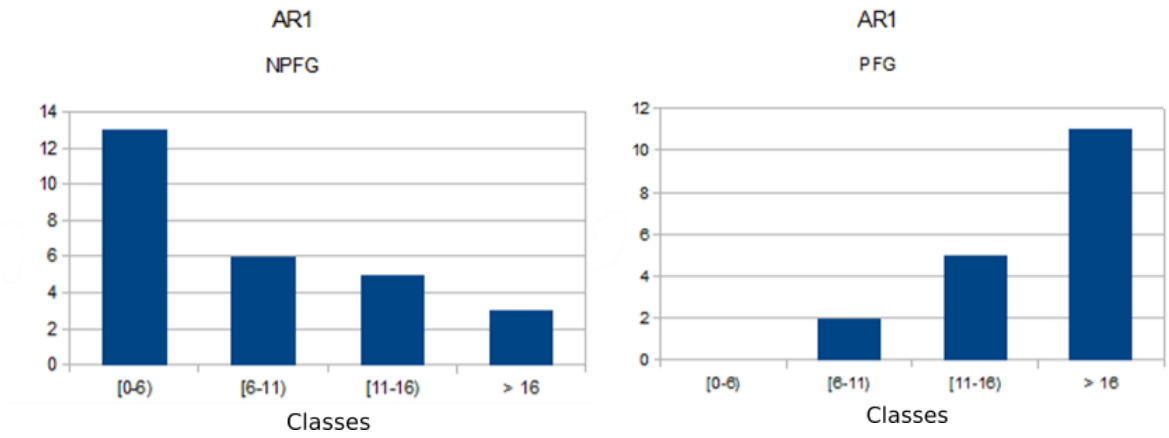

Figure 82: AR1 bar graph for NPFG (left) and PFG (right) groups.

The very same consideration remains valid even for the male groups, as shown in the following summarizing set of graphs reported in Figure 83. From the graphs relative to the female groups and from the graphs relative to the male groups, it is possibile to see how the SPKIs value distribution for the selected SPKIs have very symmetric characteristics passing from non-pathological to pathological groups, both for male and female groups.

In Figure 83 (a) and (b) is reported the HWSS index for the non-pathological (a) and pathological (b) male group. In the non-pathological male group, 90.91% of the subjects present HWSS values above 16, meanwhile, in pathological subjects' group, only the 26.67% present HWSS values above 16 and a major part of them (around the 60%) present HWSS values between 6 and 10.

The distribution values for SDS from pathological and non-pathological males is shown in Figure 83 (c) and (d) respectively. In this case 20 non-pathological subjects have a SDS value above 11 (90.91%), meanwhile, only 2 pathological subjects (13.33%) have SDS values above 11.

AR1 distribution for male group is shown in Figure 83 (e) and (f) respectively for non-pathological and pathological subjects. In case of non-pathological group, 19 subjects – the 86.36% - present AR1 values above 10. In case on pathological subjects there are only 2 subjects – corresponding to the 6.67% - with AR1 values below 10 and 13 subjects – the 86.67% - with values above 10.

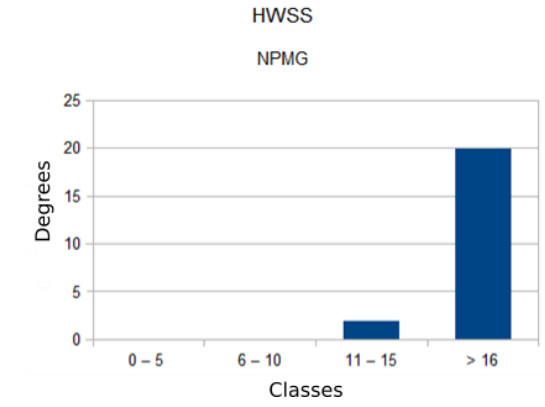

(a)

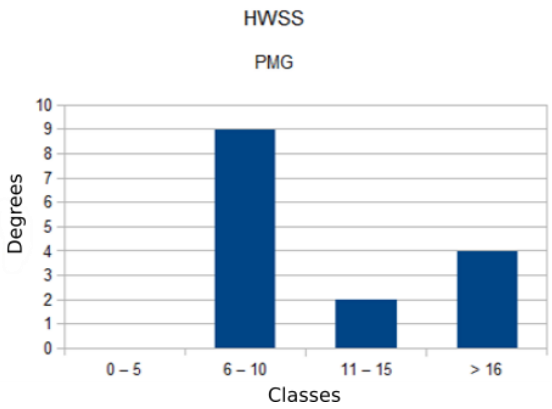

(b)

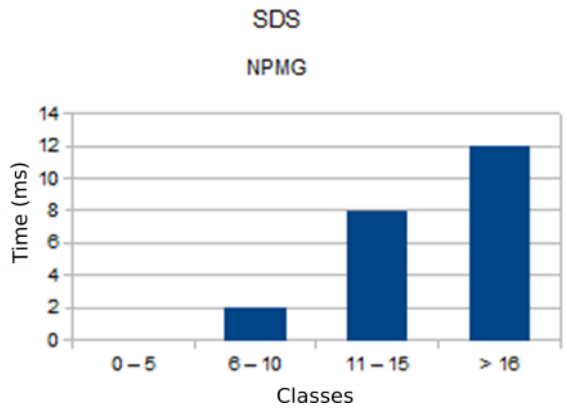

(c)

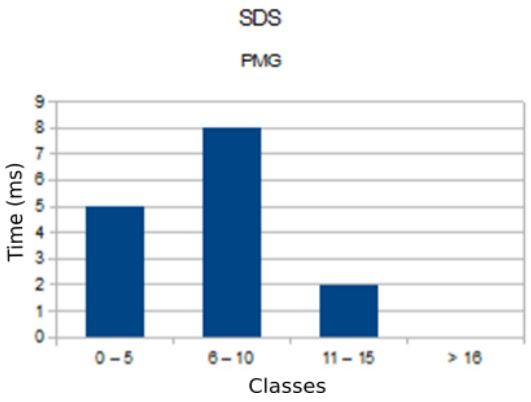

(d)

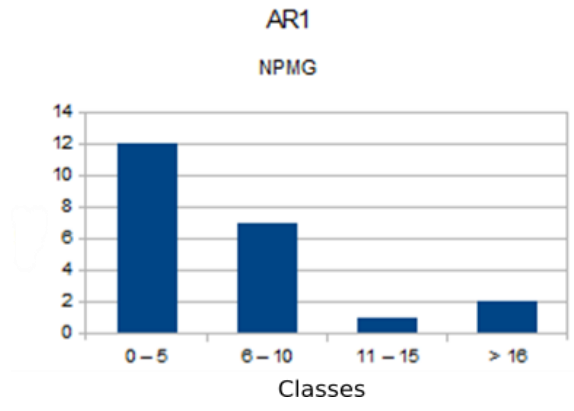

(e)

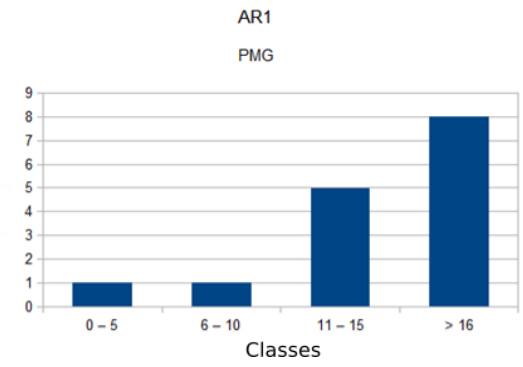

(f)

Figure 83: HWSS, SDS and AR1 for NPMG (left) and PMG (right).

In previous section, when presenting the SPKIs used to assess shoulder stability, we made suppositions about what would have been the possible expectation on the variance of the selected SPKIs in between pathological and non-pathological subjects. We argue that non-pathological subjects would have SPKIs with less variance with respect pathological ones and this both for male and female groups.

Table 17: Variance comparison in between SPKIs for NPFG and PFG groups.

	NPFG	**PFG**
HWSS	6.62	3.07
SDS	3.56	1.85
AR1	7.09	8.72

Table 17 show the variance of the selected SPKIs for the NPFG and the PFG groups. Contrary to what we expected before the on-field test, we can see that from a general point of view, the variance for the HWSS and SDS SPKIs – but not the one of AR1 – is lower in pathological female group with respect non-pathological groups. This behavior for the SDS and HWSS SPKIs, can be explained – from our point of view – with the fact that the humerus vs. scapula behavior in the initial phase of the humerus abduction on the scapular plane result to be different subject to subject due to a different well-performing shoulder complex where each subject performs with his/her specific but functional initial dynamics which is characterized by the specific shoulder muscles activation dynamic. At the contrary, in case of pathological subject, the effect of shoulder pathology acts on almost all the subjects the same way, reducing the variability of the shoulder dynamics. In pathological subjects, the dynamics tent to unifying and flattening manifesting a common behavior to all pathological subjects.

The AR1 index works instead as previously expected and contrary to SDS and HWSS indexes. In case of AR1 index, we still do not have a clear answer, and we think that more investigation is required to assess the real meaning of this SPKIs index even if it works great to separate among pathological and non-pathological subjects.

Table 18: Variance comparison in between SPKIs for NPFG and PFG groups.

	NPMG	**PMG**
HWSS	13.01	4.45
SDS	5.04	2.83
AR1	7.76	14.94

Table 18 show the variance for the selected SPKIs indexes in case of pathological and non-pathological male groups. As for female groups, the selected SPKIs have the same variance characteristics. SDS and HWSS are more variable in NPMG with respect PMG, whereas the AR1 index works at the contrary as for female group.

The general concordance behavior of SPKIs in between female and male groups for both pathological and non-pathological subjects means that the selected indexes are somehow correct and that can be effectively used to identify shoulder pathologies and to identify anomalous dynamic shoulder patterns.

7.5.2 Age Effect on SPKIs

In previous section the primary SPKIs used to assess the shoulder stability have been presented among the values obtained with on-field experimentation. Presented data were quite interesting because very symmetric wither respect pathological and non-pathological subjects sustaining their ability the characterize the dynamics of shoulder behavior in the initial phase of abduction.

In this section we present the distribution of the HWSS, SDS and AR1 SPKIs indexes with respect the age of the subjects, always divided by non-pathological and pathological ones.

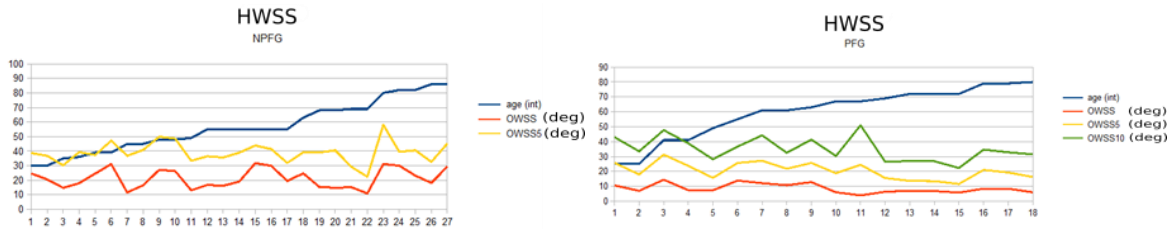

(a) (b)

Figure 84: HWSS vs. subject's age for non-pathological (a) and pathological (b) female subjects.

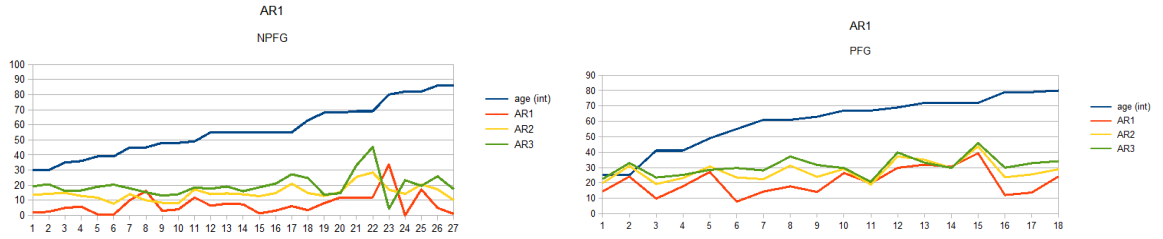

(a) (b)

Figure 85: AR1 vs. subject's age for non-pathological (a) and pathological (b) female subjects.

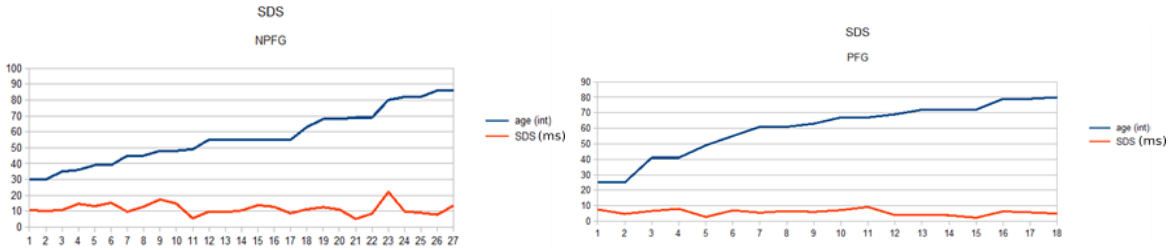

(a) (b)

Figure 86: SDS vs. subject's age for non-pathological (a) and pathological (b) female subjects.

Figure 84, Figure 85, and Figure 86 shows the HWSS, AR1 and SDS SPKIs indexes for both non-pathological (column a) and pathological (column b) female subjects. From this graphical representation we can argue two considerations for SPKIs HWSS, SDS and AR1 indexes:

- SPK Indexes are quite smoother in pathological with respect non-pathological subjects.
- SPK Indexes are stable varying the age of the subjects, presenting same/common characteristics among all the ages considered in our on-field experimentation.

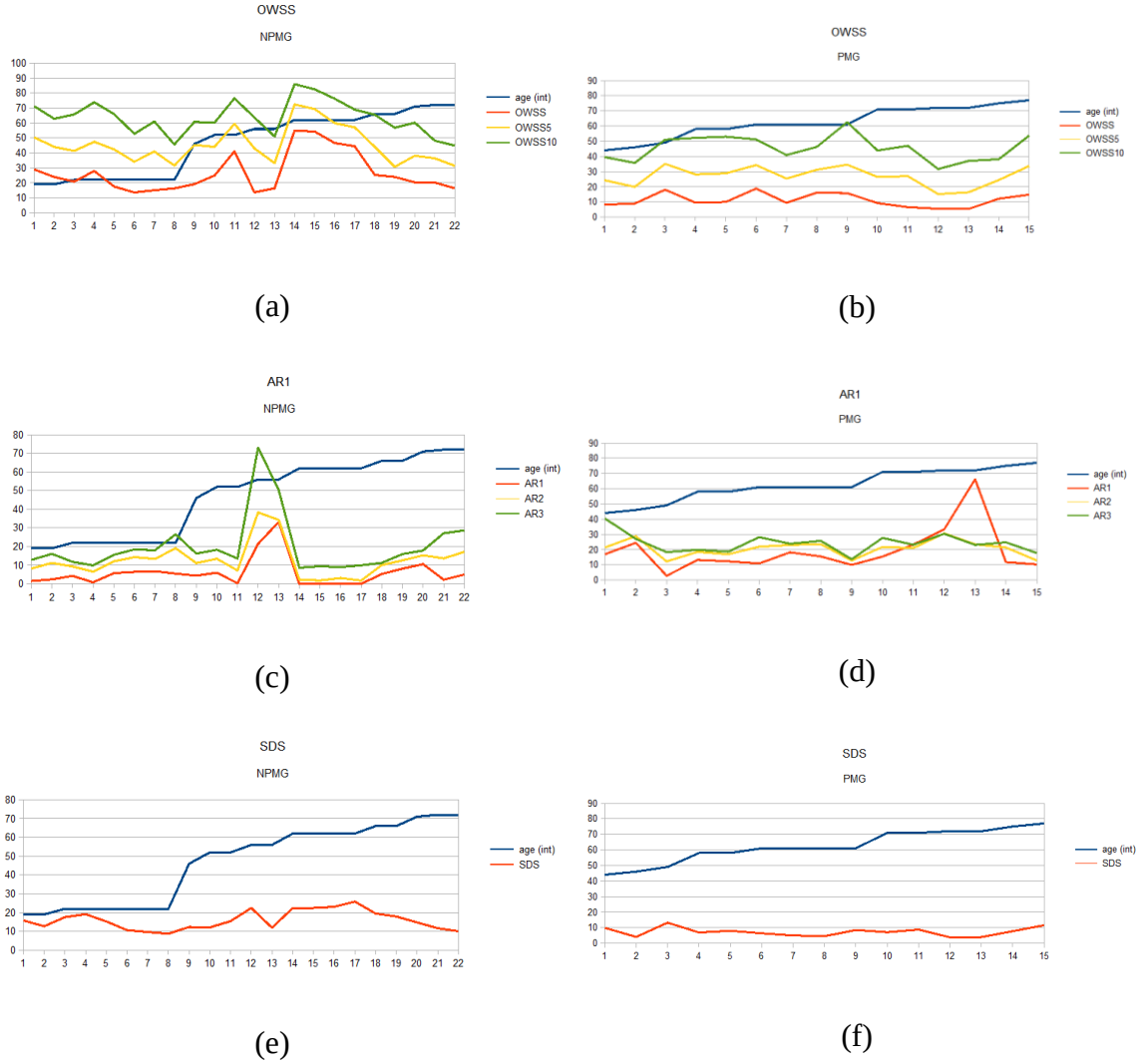

Figure 87: HWSS, AR1 and SDS vs. subject's age for non-pathological (a) and pathological (b) male subjects. HWSS is measured in degrees (deg), ARx are pure numbers and SDS are measured in milliseconds (ms).

Observations valid for SPKIs vs. subjects' age for female group are still valid for male group as shown in Figure 87.

7.5.3 SUBJECTS CLASSIFICATION

Based on the data obtained by on-field experimentation and presented in previous sections, we would investigate the possibility to identify reference threshold values for HWSS, SDS and AR1 able to distinguish with a good approximation a pathological shoulder

from a non-pathological one. Moreover, we introduce a *band* of uncertainty in which the provided values are not enough to express any judgement about the status of the shoulder.

The discriminant threshold values (DTV) have been selected to have 80% of the subjects belonging to the primary selected class. For each of the selected SPKIs we identified the threshold values with the same approach identifying for each SPKI a minimum and maximum threshold value. Threshold values are kept separated from the female and the male groups. Applying previous logic on the female group we have been able to identify the following classification thresholds:

Table 19: SPKIs threshold values for pathological and non-pathological subjects in female group.

HWSS			
	MIN	**MAX**	**%**
NPFG		15	81.48
PFG	13		88.89
SDS			
	MIN	**MAX**	**%**
NPFG		8	88.89
PFG	8		88.89
AR1			
	MIN	**MAX**	**%**
NPFG	12		88.89
PFG		13	83.33

Table 19 reports the maximum and minimum threshold values for the selected SPKIs for female subjects. In this case we can asserts that a female subject with HWSS value above or equal to 15 would not present shoulder pathologies. At the contrary, a female subject with HWSS value below or equal 13 would present shoulder pathologies. In this case a deeper clinical investigation is required to precisely assess the shoulder pathology if any. The very same consideration can be done for the other two SPKIs: SDS and AR1.

Table 20: SPKIs threshold values for pathological and non-pathological subjects in male group.

HWSS			
	MIN	**MAX**	**%**
NPMG		16	86.36
PMG	16		80.00
SDS			
	MIN	**MAX**	**%**
NPMG		11	81.82
PMG	9		80.00
AR1			
	MIN	**MAX**	**%**
NPMG	8		81.82
PMG		10	86.67

Table 20 reports the threshold values for male group for the selected SPKIs: HWSS, SDS and AR1. All considerations emerged for the female group are applicable to the male group. Eventually it is possible to force a more restrictive threshold augmenting the value chosen for the DTV, passing for example from 80% to 90% having more restrictive bands.

The SPKIs are correlated one each other and to identify the correlation for a human being is not immediate, it would be of value to have an autonomous solution able to identify the correlation and automatically classify the measured date considering the multidimensionality of the classification problem. In this context, ANN are very promising. In the following section, we would investigate the possibility to introduce ANN to infer shoulder stability and pathology considering all the SPKIs. As reported, this has been a preliminary study with the aim to investigate the main feasibility of the proposed approach. In this initial study we used only the main three SPKIs, but we already have in mind the possibility – in future investigation – to extend the SPKIs set including other and more complex indicators.

Given the NN, is it now possible to proceed to test the NN on a test set. To test our NN we used the test file previously created. The result obtained with the test function of FANT on the NN result to be **95.45%** of accuracy in the shoulder classification. We think this is a very good result which really support our research and initial hypothesis. In this context there is still margin for improvements for example considering to extends the NN

output including second dimension to capture undetermined situation. Other improvements could be the extension of the input vector adding other parameters extracted from the overall humerus-scapular dynamics in the first degrees of humerus abduction. As for example the dynamics of scapula tilt and humerus axial rotation while executing the ULA movement.

7.6 FUTURE DEVELOPMENT AND APPLICATIONS

This section discusses the possible future development and implementations for the proposed shoulder status assessment mobile application. The discussed improvements concern both the technical implementation from one side and the shoulder analysis approach from the other side. In the following we would start with the future development concerning the shoulder analysis approach and then moving to discuss and present new development for the application itself.

7.6.1 DATA ANALYSIS IMPROVEMENT

As presented in the previous sections, in the shoulder stability assessment we considered only three main SPKIs: HWSS, SDS and AR1. These parameters were those better indicating shoulder pathologies considering the first 10/15 degrees of humerus abduction. These parameters were extracted considering the projection of the scapula upward and downward rotation on the frontal plane and considering only the humerus abduction on the scapular plane. Considering the good results obtained with only those three parameters, future development would take in consideration a more extended set of SPKIs, considering not only the projections of scapula upward rotation and humerus abduction, but considering the full 3D motion of the scapula and humerus.

As reported in [89] during the humerus abduction, the scapula execute a 3D rotation composed of an upward rotation on the scapular plane, an posterior/anterior tilt and an internal/external rotation, as shown in Figure 88.

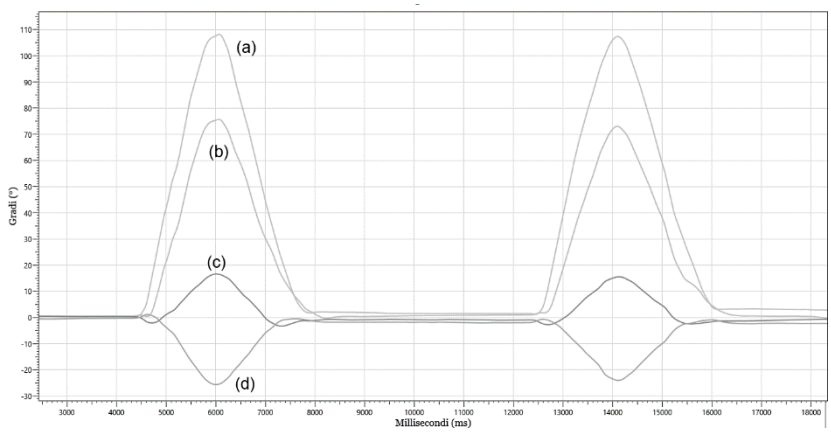

Figure 88: Full scapula and humerus 3D motion during abduction. (a) humerus abduction, (b) humerus axial rotation, (c) scapula upward rotation and (d) scapula tilt degrees.

In Figure 88 the curve (b) represents the humerus axial rotation while humerus abduction, meanwhile curve (d) represents the scapula tilt rotations during full humerus abduction on the scapular plane. As visible in the figure, all the 3D curves are somehow related one each other with specific patterns in the first degrees of humerus abduction. Future development would include all these data in the overall shoulder model to improve shoulder pathologies classification with autonomous ANN. Including more data and dynamic we would improve the classification performances of the system without impacting on the already defined application protocols, which would remain easy and rapid as already explained. Moreover, we would better investigate the ranges to be considered for each single SPKIs for the classification problem and perform analysis while applying a resistive force to the humerus abduction while executing ULAs; starting from zero – where the movement is fully driven by the clinician – to various weight to analyze and study how such SPKIs would change their behavior among pathological and non-pathological subjects. From this extended approach we expect to improve pathological vs. non pathological classification, to better foreseen future shoulder pathologies and finally being able to investigate the possibility to identify the shoulder pathology itself. Finally, we would also proceed to the validation of the proposed solution with respect canonical optical reference systems also with the aim to measure the effect of inter- and intra-operator effects on the proposed protocol.

In the next section we present and discuss future improvement concerning the application itself extending to a general-purpose application for motion data acquisition and analysis.

7.6.2 IMPROVEMENTS OF TECHNOLOGY

Mobile applications and small IMDs are perfect combination for fast and everywhere analysis of motion data. In the presented work we developed a mobile application which uses IMDs devices to acquire 3D motion data of scapula and humerus to assess shoulder status. Future development would move forward generalize the architecture to develop a common mobile "core" to provides general-purpose function for data acquisition on which specific data-analysis modules can be "plugged-in" to perform various real-time patient's mobility assessment solutions. These considerations are valid in general, not only for patient assessment, but also for sport performance evaluation. The idea is to proceed to develop a common platform and infrastructure which then can support even at-home rehabilitation and monitoring solutions differentiating various cases with a minimal implementation effort having mobile solution as central hub for the development of general-purpose applications, as shown in Figure 89.

Figure 89: Mobile device as central hub for various applications

As first step in this direction the "core" of the SSA application has been used in the previous post-stroke rehabilitation solution as a more practical alternative to the acquisition of 3D upper arm motion while executing rehabilitation exercise. The mobile application was working as a bridge in between the main controller and the peripheral IMDs devices using web-socket protocol over a wireless communication channel. In this context – thanks to the flexible architecture based on web-socket protocol – even the main controller desktop

application can be easily replaced with a mobile application where the clinicians can operate to setup and control patient's rehabilitation sessions.

Initially, the post-stroke rehabilitation solution based on exergaming and mixed reality – presented at the beginning of this thesis – was implemented acquiring upper-arm motion data using the Cometa WaveTrack Inertial System. This solution is quite cumbersome because requires a wireless received to be attached to the PC and the full set of IMDs is composed of 12 devices racked into a quite large carrying on case, reducing mobility and complexify handling. To bypass this drawback, the developed mobile solution for shoulder assessment has been used as a "bridge" in between the main application and the IMDs device, as shown in Figure 90.

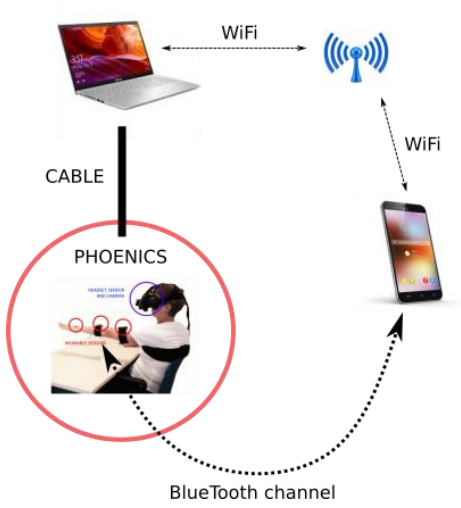

Figure 90: PHOENICS with Bluetooth IMDs

With this solution the main application controller (desktop application) connects to the mobile "bridge" solution using web-socket protocol over a WiFi connection and communicate using a well-defined json based protocol. The mobile "bridge" control IMDs device connected over a Bluetooth channel. When the subject starts the exercise, the controller sends a message to the "bridge" to start data acquisition. During the exercise execution the "bridge" store data locally. When exercise get completed, the controller sends a message to the "bridge" to return all the acquired data. The "bridge" package all the data in zip file format and sent it back to the controller. For the controller application, the possibility to use the "bridge" or to use the default solution based on Cometa WaveTracker is completely transparent and easily configurable.

GENERAL CONCLUSIONS

The main goal of the present thesis was to investigate the possibility to develop solutions, based on use of the latest off-the-shelf technologies, able to support clinicians in their daily activities, from the post-stroke rehabilitation up to the shoulder functional assessment. The main findings obtained from this work, underlined how solutions which are designed with the engagement of interested subjects in a co-design approach, and which in turn provide a good overall stability and a flexible architecture, result to be well accepted and used.

This level of overall usability was particularly good for the solution developed for the post-stroke rehabilitation by integrating AOT, exergames in mixed-reality and kinematic-based metrics for performance. Despite the complexity and the high integration-level of various off-the-shelf technologies, the solution demonstrated to be well accepted both from the patient and from the clinicians, even though further improvements are still needed. From the realized activities, it is worth noting how off-the-shelf technologies can successfully be integrated to support AOT approach in rehabilitation context. From this work emerged how virtual-reality and mixed-reality well fitted together to support AOT approach, but at the same time the videos realization for the AO phase resulted to be quite complex to be realized. In general, we experimented how important is the joint definition of both the rehabilitation exercises and the correspondent AO videos, which need to be used during the AO phase within the overall protocol. The proposed solution other than support post-stroke rehabilitation following the paradigm of AOT, it also provides innovative technologies and original kinematic-based metrics to measure and to monitor patient's performances during the rehabilitation exercise execution. Particular attention was dedicated to the software development. Indeed, the developed solution contains interesting approaches to the overall architectural design which are of value if you want easily support change request and bug fixing, keeping an eye on the application scalability. The functional separation between the user console and rehabilitation application provided the possibility to make "remote" (also in terms of adopted software technologies) the application, highlighting the capacity of the system to be exploited within a telemedicine solution. The adoption of a light web-socket based communication protocol allowed for scalability and extensibility of the solution, as underlined in the development of the Android-based inertial measurement systems or for a possible implementation of an Android-based console application. The development of the rehabilitation application itself was realized using Unity. Also, in this context a scalable

approach was implemented to provide standard high-level components and basic utilities components which in turn allows for a rapid development and extension of the set of exercises controlled by the solution. The data acquired during the preliminary "proof of concept" study, well supported he solution from a usability point of view; clearly, in order to better understand the efficacy of the solution to support post-stroke rehabilitation, further complete clinical studies are required. Nevertheless, the solution is still under test at the IRCCS Fondazione Don Carlo Gnocchi ONLUS in Rovato (BS). All the experimenters are confident that right after this COVID-19 pandemic, further on-field tests will start involving a higher number of patients in a proper randomized clinical trial.

The second study on the SSA solution demonstrated how practical application for rapid status assessment – the shoulder in our case, but we are not limited to – would be of value in clinical context. With this work, we underlined how with two IMDs and a fast protocol was possible to acquire shoulder kinematics in an outpatient setting, as to rapidly assess shoulder function and stability by identifying the presence of humerus vs. scapular dyskinesis. A wide on-field test on several voluntary subjects reported good results in term of usability and possibility of analysis. At current state of development, the application is still limited to a research environment, despite the fact we are all aiming at obtaining a solution with a high TRL. To reach this objective, further on-field tests and application development should mainly be performed, above all for what concerns final data visualization and synthesis.

Nevertheless, the main findings of this thesis showed that the proposed designs and solutions present a great translational potential and impact. This work can be used as a milestone reference for the development of further similar technologies addressing both the clinical context and the possibility of industrial transfer.

ACKNOWLEDGES

For the collaboration, for the support during the design phase and for the on-field test of the AOT based post-stroke virtual-reality and mixed-reality based solution, I want to thank the group of clinicians and the all the healthcare personnel at the IRCCS Fondazione Don Carlo Gnocchi ONLUS, Rovato (BS) with particular thanks to Dr. Stefano Lazzarini, Doctor of Physical Therapy at the same institute.

A special mention goes to Dr. Roberto Luongo for the clear explanation of the characteristic of the shoulder complex and for the support in design and development of the final solution of the shoulder stability assessment mobile application; I would also thank all the team of expertise at Genetica Amica Association, Riva del Garda (TN).

The last but not the least, I must thank Prof. Nicola Francesco Lopomo, PhD for the support and dedication expressed and for supporting me and sustaining me during all the three long years of this work.

Thanks also to all my friends and family to friendly acknowledge me when I was telling them about my thesis's work and research.

APPENDIXES

10.1 APPENDIX A: SUS (SYSTEM USABILITY SCALE) AND REPORTS

1. I think that I would like to use this system frequently

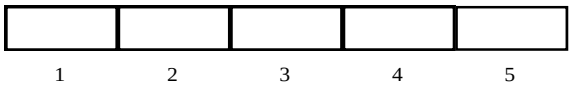

3. I thought the system was easy to use

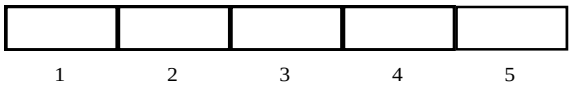

4. I think that I would need the support of a technical person to be able to use this system

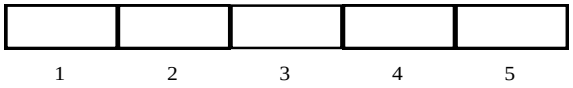

5. I found the various functions in this system were well integrated

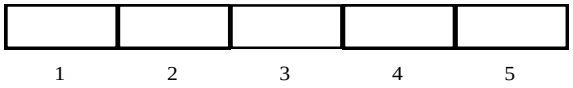

6. I thought there was too much inconsistency in this system

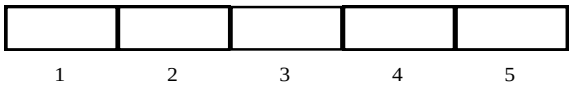

7. I would imagine that most people would learn to use this system very quickly

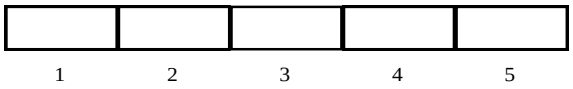

8. I found the system very cumbersome to use

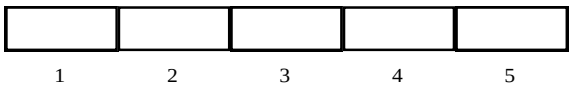

9. I felt very confident using the system

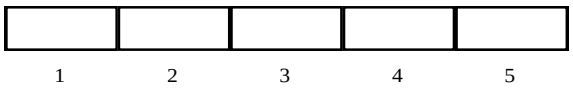

10. I needed to learn a lot of things before I could get going with this system

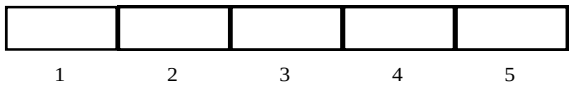

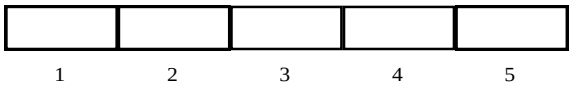

10.2 QUATERNIONS

This appendix reports some information about quaternion representation.

10.2.1 QUATERNION TO EULER ANGLES

It is always possibile to convert quaternion representation to Euler Angles using the following equations:

$$\emptyset = arctan\left(\frac{2\,(ab + cd)}{a^2 - b^2 - c^2 + d^2}\right) \qquad \textit{Eq 20}$$

$$\theta = -arcsin\big(2\,(bd - ac)\big) \qquad \textit{Eq 21}$$

$$\varphi = arctan\left(\frac{2\,(ad + bc)}{a^2 + b^2 - c^2 - d^2}\right) \qquad \textit{Eq 22}$$

10.2.2 ROTATION OF A POINT BY A QUATERNION

This equation shows how to apply a rotation expressed by a quaternion q to a point P in the reference frame:

$$\overline{P_b} = \overline{q_i^b}\left(\frac{0}{P_i}\right)\left(\overline{q_i^b}\right)^{-1} \qquad \textit{Eq 23}$$

In the equation, $\overline{q_i^b}$ is the quaternion which represents the rotation from the inertial frame (i) to the body frame (b).

REFERENCES

[1] A. Adomavičienė, K. Daunoravičienė, R. Kubilius, L. Varžaitytė, and J. Raistenskis, "Influence of New Technologies on Post-Stroke Rehabilitation: A Comparison of Armeo Spring to the Kinect System," *Med. Kaunas Lith.*, vol. 55, no. 4, Apr. 2019, doi: 10.3390/medicina55040098.

[2] Global Burden of Disease Study 2013 Collaborators, "Global, regional, and national incidence, prevalence, and years lived with disability for 301 acute and chronic diseases and injuries in 188 countries, 1990-2013: a systematic analysis for the Global Burden of Disease Study 2013," *Lancet Lond. Engl.*, vol. 386, no. 9995, pp. 743–800, Aug. 2015, doi: 10.1016/S0140-6736(15)60692-4.

[3] E.-J. Kuk, J.-M. Kim, D.-W. Oh, and H.-J. Hwang, "Effects of action observation therapy on hand dexterity and EEG-based cortical activation patterns in patients with post-stroke hemiparesis," *Top. Stroke Rehabil.*, vol. 23, no. 5, pp. 318–325, Jul. 2016, doi: 10.1080/10749357.2016.1157972.

[4] Z. Chen *et al.*, "Action observation treatment-based exoskeleton (AOT-EXO) for upper extremity after stroke: study protocol for a randomized controlled trial," *Trials*, vol. 22, no. 1, p. 222, Mar. 2021, doi: 10.1186/s13063-021-05176-x.

[5] C. D. Wolfe, "The impact of stroke," *Br. Med. Bull.*, vol. 56, no. 2, pp. 275–286, 2000, doi: 10.1258/0007142001903120.

[6] World Health Organization, Ed., *International classification of impairments, disabilities, and handicaps: a manual of classification relating to the consequences of disease*. Geneva : [Albany, N.Y: World Health Organization ; sold by WHO Publications Centre USA], 1980.

[7] E. S. Lawrence *et al.*, "Estimates of the prevalence of acute stroke impairments and disability in a multiethnic population," *Stroke*, vol. 32, no. 6, pp. 1279–1284, Jun. 2001, doi: 10.1161/01.str.32.6.1279.

[8] W. J. Harmsen, J. B. J. Bussmann, R. W. Selles, H. L. P. Hurkmans, and G. M. Ribbers, "A Mirror Therapy-Based Action Observation Protocol to Improve Motor Learning After Stroke," *Neurorehabil. Neural Repair*, vol. 29, no. 6, pp. 509–516, Jul. 2015, doi: 10.1177/1545968314558598.

[9] G. Kwakkel, B. J. Kollen, J. van der Grond, and A. J. H. Prevo, "Probability of regaining dexterity in the flaccid upper limb: impact of severity of paresis and time since onset in acute stroke," *Stroke*, vol. 34, no. 9, pp. 2181–2186, Sep. 2003, doi: 10.1161/01.STR.0000087172.16305.CD.

[10] P. Langhorne and L. Legg, "Evidence behind stroke rehabilitation," *J. Neurol. Neurosurg. Psychiatry*, vol. 74 Suppl 4, pp. iv18–iv21, Dec. 2003, doi: 10.1136/jnnp.74.suppl_4.iv18.

[11] P. Langhorne, F. Coupar, and A. Pollock, "Motor recovery after stroke: a systematic review," *Lancet Neurol.*, vol. 8, no. 8, pp. 741–754, Aug. 2009, doi: 10.1016/S1474-4422(09)70150-4.

[12] A. Pollock *et al.*, "Interventions for improving upper limb function after stroke," *Cochrane Database Syst. Rev.*, no. 11, p. CD010820, Nov. 2014, doi: 10.1002/14651858.CD010820.pub2.

[13] G. Buccino, "Action observation treatment: a novel tool in neurorehabilitation," *Philos. Trans. R. Soc. Lond. B. Biol. Sci.*, vol. 369, no. 1644, p. 20130185, 2014, doi: 10.1098/rstb.2013.0185.

[14] S. Sütbeyaz, G. Yavuzer, N. Sezer, and B. F. Koseoglu, "Mirror therapy enhances lower-extremity motor recovery and motor functioning after stroke: a randomized

controlled trial," *Arch. Phys. Med. Rehabil.*, vol. 88, no. 5, pp. 555–559, May 2007, doi: 10.1016/j.apmr.2007.02.034.
[15] M. Angelini, M. Fabbri-Destro, N. F. Lopomo, M. Gobbo, G. Rizzolatti, and P. Avanzini, "Perspective-dependent reactivity of sensorimotor mu rhythm in alpha and beta ranges during action observation: an EEG study," *Sci. Rep.*, vol. 8, no. 1, p. 12429, Dec. 2018, doi: 10.1038/s41598-018-30912-w.
[16] G. di Pellegrino, L. Fadiga, L. Fogassi, V. Gallese, and G. Rizzolatti, "Understanding motor events: a neurophysiological study," *Exp. Brain Res.*, vol. 91, no. 1, pp. 176–180, 1992, doi: 10.1007/BF00230027.
[17] G. Rizzolatti and V. Gallese, "Mirror Neurons," in *Encyclopedia of Cognitive Science*, L. Nadel, Ed. Chichester: John Wiley & Sons, Ltd, 2006, p. s00360. doi: 10.1002/0470018860.s00360.
[18] M. Fabbri-Destro and G. Rizzolatti, "Mirror neurons and mirror systems in monkeys and humans," *Physiol. Bethesda Md*, vol. 23, pp. 171–179, Jun. 2008, doi: 10.1152/physiol.00004.2008.
[19] M. Diers, C. Christmann, C. Koeppe, M. Ruf, and H. Flor, "Mirrored, imagined and executed movements differentially activate sensorimotor cortex in amputees with and without phantom limb pain:," *Pain*, vol. 149, no. 2, pp. 296–304, May 2010, doi: 10.1016/j.pain.2010.02.020.
[20] Z. Yongxiang *et al.*, "Mirror therapy versus action observation therapy: effects on excitability of the cerebral cortex in patients after strokes," *Int. J. Clin. Exp. Med.*, vol. 13, 2019.
[21] V. S. Ramachandran, "Phantom limbs, neglect syndromes, repressed memories, and Freudian psychology," *Int. Rev. Neurobiol.*, vol. 37, pp. 291–333; discussion 369-372, 1994, doi: 10.1016/s0074-7742(08)60254-8.
[22] D. Ezendam, R. M. Bongers, and M. J. A. Jannink, "Systematic review of the effectiveness of mirror therapy in upper extremity function," *Disabil. Rehabil.*, vol. 31, no. 26, pp. 2135–2149, 2009, doi: 10.3109/09638280902887768.
[23] G. Rizzolatti *et al.*, "Neurons related to reaching-grasping arm movements in the rostral part of area 6 (area 6a beta)," *Exp. Brain Res.*, vol. 82, no. 2, pp. 337–350, 1990, doi: 10.1007/BF00231253.
[24] A. Bisio, M. Bassolino, T. Pozzo, and N. Wenderoth, "Boosting Action Observation and Motor Imagery to Promote Plasticity and Learning," *Neural Plast.*, vol. 2018, pp. 1–3, Nov. 2018, doi: 10.1155/2018/8625861.
[25] K. A. Garrison, L. Aziz-Zadeh, S. W. Wong, S.-L. Liew, and C. J. Winstein, "Modulating the motor system by action observation after stroke," *Stroke*, vol. 44, no. 8, pp. 2247–2253, Aug. 2013, doi: 10.1161/STROKEAHA.113.001105.
[26] S. L. Small, G. Buccino, and A. Solodkin, "The mirror neuron system and treatment of stroke," *Dev. Psychobiol.*, vol. 54, no. 3, pp. 293–310, Apr. 2012, doi: 10.1002/dev.20504.
[27] N. Brihmat *et al.*, "Action, observation or imitation of virtual hand movement affect differently regions of the mirror neuron system and the default mode network," *Brain Imaging Behav.*, vol. 12, no. 5, pp. 1363–1378, Oct. 2018, doi: 10.1007/s11682-017-9804-x.
[28] J. Fu *et al.*, "Effects of action observation therapy on upper extremity function, daily activities and motion evoked potential in cerebral infarction patients:," *Medicine (Baltimore)*, vol. 96, no. 42, p. e8080, Oct. 2017, doi: 10.1097/MD.0000000000008080.
[29] M. Franceschini *et al.*, "Clinical relevance of action observation in upper-limb stroke rehabilitation: a possible role in recovery of functional dexterity. A randomized clinical

trial," *Neurorehabil. Neural Repair*, vol. 26, no. 5, pp. 456–462, Jun. 2012, doi: 10.1177/1545968311427406.
[30] C.-H. Kim and D.-H. Bang, "Action observation training enhances upper extremity function in subacute stroke survivor with moderate impairment: a double-blind, randomized controlled pilot trial," *J. Korean Soc. Phys. Med.*, vol. 11, no. 1, pp. 133–140, Feb. 2016, doi: 10.13066/kspm.2016.11.1.133.
[31] D. Ertelt *et al.*, "Action observation has a positive impact on rehabilitation of motor deficits after stroke," *NeuroImage*, vol. 36 Suppl 2, pp. T164-173, 2007, doi: 10.1016/j.neuroimage.2007.03.043.
[32] D.-H. Bang, W.-S. Shin, S.-Y. Kim, and J.-D. Choi, "The effects of action observational training on walking ability in chronic stroke patients: a double-blind randomized controlled trial," *Clin. Rehabil.*, vol. 27, no. 12, pp. 1118–1125, Dec. 2013, doi: 10.1177/0269215513501528.
[33] L. R. Borges, A. B. Fernandes, L. P. Melo, R. O. Guerra, and T. F. Campos, "Action observation for upper limb rehabilitation after stroke," *Cochrane Database Syst. Rev.*, vol. 10, p. CD011887, Oct. 2018, doi: 10.1002/14651858.CD011887.pub2.
[34] T. J. Brigham, "Reality Check: Basics of Augmented, Virtual, and Mixed Reality," *Med. Ref. Serv. Q.*, vol. 36, no. 2, pp. 171–178, Jun. 2017, doi: 10.1080/02763869.2017.1293987.
[35] K. Stanney and G. Salvendy, "Aftereffects and Sense of Presence in Virtual Environments: Formulation of a Research and Development Agenda," *Int. J. Hum.-Comput. Interact.*, vol. 10, no. 2, pp. 135–187, Jun. 1998, doi: 10.1207/s15327590ijhc1002_3.
[36] J. M. Loomis, J. J. Blascovich, and A. C. Beall, "Immersive virtual environment technology as a basic research tool in psychology," *Behav. Res. Methods Instrum. Comput.*, vol. 31, no. 4, pp. 557–564, Dec. 1999, doi: 10.3758/BF03200735.
[37] G. Rizzolatti and L. Fogassi, "The mirror mechanism: recent findings and perspectives," *Philos. Trans. R. Soc. Lond. B. Biol. Sci.*, vol. 369, no. 1644, p. 20130420, 2014, doi: 10.1098/rstb.2013.0420.
[38] V. Caggiano *et al.*, "View-based encoding of actions in mirror neurons of area f5 in macaque premotor cortex," *Curr. Biol. CB*, vol. 21, no. 2, pp. 144–148, Jan. 2011, doi: 10.1016/j.cub.2010.12.022.
[39] K. E. Laver, B. Lange, S. George, J. E. Deutsch, G. Saposnik, and M. Crotty, "Virtual reality for stroke rehabilitation," *Cochrane Database Syst. Rev.*, vol. 11, p. CD008349, Nov. 2017, doi: 10.1002/14651858.CD008349.pub4.
[40] P. H. McCrea, J. J. Eng, and A. J. Hodgson, "Biomechanics of reaching: clinical implications for individuals with acquired brain injury," *Disabil. Rehabil.*, vol. 24, no. 10, pp. 534–541, Jul. 2002, doi: 10.1080/09638280110115393.
[41] K. Stanley, "Design of randomized controlled trials," *Circulation*, vol. 115, no. 9, pp. 1164–1169, Mar. 2007, doi: 10.1161/CIRCULATIONAHA.105.594945.
[42] M. A. Murphy, C. Willén, and K. S. Sunnerhagen, "Kinematic Variables Quantifying Upper-Extremity Performance After Stroke During Reaching and Drinking From a Glass," *Neurorehabil. Neural Repair*, vol. 25, no. 1, pp. 71–80, Jan. 2011, doi: 10.1177/1545968310370748.
[43] K. C. Collins, N. C. Kennedy, A. Clark, and V. M. Pomeroy, "Getting a kinematic handle on reach-to-grasp: a meta-analysis," *Physiotherapy*, vol. 104, no. 2, pp. 153–166, Jun. 2018, doi: 10.1016/j.physio.2017.10.002.
[44] StellaM. Michaelsen, S. Jacobs, A. Roby-Brami, and MindyF. Levin, "Compensation for distal impairments of grasping in adults with hemiparesis," *Exp. Brain Res.*, vol. 157, no. 2, Jul. 2004, doi: 10.1007/s00221-004-1829-x.

[45] S. Balasubramanian, A. Melendez-Calderon, A. Roby-Brami, and E. Burdet, "On the analysis of movement smoothness," *J. NeuroEngineering Rehabil.*, vol. 12, no. 1, p. 112, Dec. 2015, doi: 10.1186/s12984-015-0090-9.
[46] S. L. DeJong, S. Y. Schaefer, and C. E. Lang, "Need for Speed: Better Movement Quality During Faster Task Performance After Stroke," *Neurorehabil. Neural Repair*, vol. 26, no. 4, pp. 362–373, May 2012, doi: 10.1177/1545968311425926.
[47] N. Lehrer, S. Attygalle, S. L. Wolf, and T. Rikakis, "Exploring the bases for a mixed reality stroke rehabilitation system, Part I: A unified approach for representing action, quantitative evaluation, and interactive feedback," *J. NeuroEngineering Rehabil.*, vol. 8, no. 1, p. 51, 2011, doi: 10.1186/1743-0003-8-51.
[48] P. Picerno *et al.*, "Upper limb joint kinematics using wearable magnetic and inertial measurement units: an anatomical calibration procedure based on bony landmark identification," *Sci. Rep.*, vol. 9, no. 1, p. 14449, Dec. 2019, doi: 10.1038/s41598-019-50759-z.
[49] A. G. Cutti, A. Giovanardi, L. Rocchi, A. Davalli, and R. Sacchetti, "Ambulatory measurement of shoulder and elbow kinematics through inertial and magnetic sensors," *Med. Biol. Eng. Comput.*, vol. 46, no. 2, pp. 169–178, Feb. 2008, doi: 10.1007/s11517-007-0296-5.
[50] T. K. Koo and M. Y. Li, "A Guideline of Selecting and Reporting Intraclass Correlation Coefficients for Reliability Research," *J. Chiropr. Med.*, vol. 15, no. 2, pp. 155–163, Jun. 2016, doi: 10.1016/j.jcm.2016.02.012.
[51] J. I. Gallin, F. P. Ognibene, and L. L. Johnson, Eds., *Principles and practice of clinical research*, Fourth edition. London, United Kingdom: Academic Press, 2018.
[52] M. E. Wiklund, J. Kendler, and A. Y. Strochlic, *Usability testing of medical devices*, Second edition. Boca Raton, FL: CRC Press, Taylor & Francis Group, 2016.
[53] J. Brook, "SUS: A quick and dirty usability scale," *Novemb. 1995*.
[54] A. Pfister, A. M. West, S. Bronner, and J. A. Noah, "Comparative abilities of Microsoft Kinect and Vicon 3D motion capture for gait analysis," *J. Med. Eng. Technol.*, vol. 38, no. 5, pp. 274–280, Jul. 2014, doi: 10.3109/03091902.2014.909540.
[55] S. Ikbali Afsar, I. Mirzayev, O. Umit Yemisci, and S. N. Cosar Saracgil, "Virtual Reality in Upper Extremity Rehabilitation of Stroke Patients: A Randomized Controlled Trial," *J. Stroke Cerebrovasc. Dis. Off. J. Natl. Stroke Assoc.*, vol. 27, no. 12, pp. 3473–3478, Dec. 2018, doi: 10.1016/j.jstrokecerebrovasdis.2018.08.007.
[56] J. Han, L. Shao, D. Xu, and J. Shotton, "Enhanced computer vision with Microsoft Kinect sensor: a review," *IEEE Trans. Cybern.*, vol. 43, no. 5, pp. 1318–1334, Oct. 2013, doi: 10.1109/TCYB.2013.2265378.
[57] X. Xu, M. Robertson, K. B. Chen, J.-H. Lin, and R. W. McGorry, "Using the Microsoft Kinect™ to assess 3-D shoulder kinematics during computer use," *Appl. Ergon.*, vol. 65, pp. 418–423, Nov. 2017, doi: 10.1016/j.apergo.2017.04.004.
[58] J. Adolf, J. Dolezal, and L. Lhotska, "Affordable Personalized, Immersive VR Motor Rehabilitation System with Full Body Tracking," *Stud. Health Technol. Inform.*, vol. 261, pp. 75–81, 2019.
[59] S. H. Lee, H.-Y. Jung, S. J. Yun, B.-M. Oh, and H. G. Seo, "Upper Extremity Rehabilitation Using Fully Immersive Virtual Reality Games With a Head Mount Display: A Feasibility Study," *PM R*, vol. 12, no. 3, pp. 257–262, Mar. 2020, doi: 10.1002/pmrj.12206.
[60] M. Erhardsson, M. Alt Murphy, and K. S. Sunnerhagen, "Commercial head-mounted display virtual reality for upper extremity rehabilitation in chronic stroke: a single-case design study," *J. Neuroengineering Rehabil.*, vol. 17, no. 1, p. 154, Nov. 2020, doi: 10.1186/s12984-020-00788-x.

[61] A. Borrego, J. Latorre, M. Alcañiz, and R. Llorens, “Comparison of Oculus Rift and HTC Vive: Feasibility for Virtual Reality-Based Exploration, Navigation, Exergaming, and Rehabilitation,” *Games Health J.*, vol. 7, no. 3, pp. 151–156, Jun. 2018, doi: 10.1089/g4h.2017.0114.

[62] Y. Feng, U. A. Uchidiuno, H. R. Zahiri, I. George, A. E. Park, and H. Mentis, “Comparison of Kinect and Leap Motion for Intraoperative Image Interaction,” *Surg. Innov.*, vol. 28, no. 1, pp. 33–40, Feb. 2021, doi: 10.1177/1553350620947206.

[63] M. N. Ögün, R. Kurul, M. F. Yaşar, S. A. Turkoglu, Ş. Avci, and N. Yildiz, “Effect of Leap Motion-based 3D Immersive Virtual Reality Usage on Upper Extremity Function in Ischemic Stroke Patients,” *Arq. Neuropsiquiatr.*, vol. 77, no. 10, pp. 681–688, 2019, doi: 10.1590/0004-282X20190129.

[64] P. Fernández-González *et al.*, “Leap motion controlled video game-based therapy for upper limb rehabilitation in patients with Parkinson’s disease: a feasibility study,” *J. Neuroengineering Rehabil.*, vol. 16, no. 1, p. 133, Nov. 2019, doi: 10.1186/s12984-019-0593-x.

[65] F. Weichert, D. Bachmann, B. Rudak, and D. Fisseler, “Analysis of the Accuracy and Robustness of the Leap Motion Controller,” *Sensors*, vol. 13, no. 5, pp. 6380–6393, May 2013, doi: 10.3390/s130506380.

[66] A. H. Smeragliuolo, N. J. Hill, L. Disla, and D. Putrino, “Validation of the Leap Motion Controller using markered motion capture technology,” *J. Biomech.*, vol. 49, no. 9, pp. 1742–1750, Jun. 2016, doi: 10.1016/j.jbiomech.2016.04.006.

[67] D. Roetenberg, “Inertial and magnetic sensing of human motion,” s.n.], S.l., 2006.

[68] J. D. Bronzino, Ed., *The biomedical engineering handbook*, 3rd ed. Boca Raton: CRC/Taylor & Francis, 2006.

[69] A. Krüger and J. Edelmann-Nusser, “Application of a Full Body Inertial Measurement System in Alpine Skiing: A Comparison with an Optical Video Based System,” *J. Appl. Biomech.*, vol. 26, no. 4, pp. 516–521, Nov. 2010, doi: 10.1123/jab.26.4.516.

[70] O. Deppe, G. Dorner, S. König, T. Martin, S. Voigt, and S. Zimmermann, “MEMS and FOG Technologies for Tactical and Navigation Grade Inertial Sensors-Recent Improvements and Comparison,” *Sensors*, vol. 17, no. 3, Mar. 2017, doi: 10.3390/s17030567.

[71] Avci, A., Bosch, S., Marin Perianu M., Marin Perianu, R., and Havinga, P. J. M, “Activity Recognition Using Inertial Sensing for Healthcare, Wellbeing and Sports Applications: A Survey,” Feb. 2010, pp. 167–176.

[72] S. Patel, H. Park, P. Bonato, L. Chan, and M. Rodgers, “A review of wearable sensors and systems withapplication in rehabilitation,” *BioMed Cent.*, 2012, doi: 10.1186/1743-0003-9-21.

[73] E. Sazonov and M. R. Neuman, Eds., *Wearable sensors: fundamentals, implementation and applications*. Amsterdam: AP, Academic Press is an imprint of Elsevier, 2014.

[74] E. Turgut, Ø. Pedersen, I. Duzgun, and G. Baltaci, “Three-dimensional scapular kinematics during open and closed kinetic chain movements in asymptomatic and symptomatic subjects,” *J. Biomech.*, vol. 49, no. 13, pp. 2770–2777, Sep. 2016, doi: 10.1016/j.jbiomech.2016.06.015.

[75] W. H. K. de Vries, H. E. J. Veeger, A. G. Cutti, C. Baten, and F. C. T. van der Helm, “Functionally interpretable local coordinate systems for the upper extremity using inertial & magnetic measurement systems,” *J. Biomech.*, vol. 43, no. 10, pp. 1983–1988, Jul. 2010, doi: 10.1016/j.jbiomech.2010.03.007.

[76] J. C. van den Noort, S. H. Wiertsema, K. M. C. Hekman, C. P. Schönhuth, J. Dekker, and J. Harlaar, "Measurement of scapular dyskinesis using wireless inertial and magnetic sensors: Importance of scapula calibration," *J. Biomech.*, vol. 48, no. 12, pp. 3460–3468, Sep. 2015, doi: 10.1016/j.jbiomech.2015.05.036.
[77] K. Matsuki *et al.*, "In vivo 3-dimensional analysis of scapular kinematics: comparison of dominant and nondominant shoulders," *J. Shoulder Elbow Surg.*, vol. 20, no. 4, pp. 659–665, Jun. 2011, doi: 10.1016/j.jse.2010.09.012.
[78] A. Seth, R. Matias, A. P. Veloso, and S. L. Delp, "A Biomechanical Model of the Scapulothoracic Joint to Accurately Capture Scapular Kinematics during Shoulder Movements," *PLOS ONE*, vol. 11, no. 1, p. e0141028, Jan. 2016, doi: 10.1371/journal.pone.0141028.
[79] I. Parel, E. Jaspers, L. DE Baets, A. Amoresano, and A. G. Cutti, "Motion analysis of the shoulder in adults: kinematics and electromyography for the clinical practice," *Eur. J. Phys. Rehabil. Med.*, vol. 52, no. 4, pp. 575–582, Aug. 2016.
[80] F. Lorussi, N. Carbonaro, D. D. Rossi, and A. Tognetti, "A bi-articular model for scapular-humeral rhythm reconstruction through data from wearable sensors," *J. NeuroEngineering Rehabil.*, vol. 13, no. 1, p. 40, Dec. 2016, doi: 10.1186/s12984-016-0149-2.
[81] N. Aslani, S. Noroozi, P. Davenport, R. Hartley, M. Dupac, and P. Sewell, "Development of a 3D workspace shoulder assessment tool incorporating electromyography and an inertial measurement unit-a preliminary study," *Med. Biol. Eng. Comput.*, vol. 56, no. 6, pp. 1003–1011, Jun. 2018, doi: 10.1007/s11517-017-1745-4.
[82] H. Beach and P. Gordon, "Clinical Examination of the Shoulder," *N. Engl. J. Med.*, vol. 375, no. 11, p. e24, Sep. 2016, doi: 10.1056/NEJMvcm1212941.
[83] A. E. Fongemie, D. D. Buss, and S. J. Rolnick, "Management of shoulder impingement syndrome and rotator cuff tears," *Am. Fam. Physician*, vol. 57, no. 4, pp. 667–674, 680–682, Feb. 1998.
[84] N. K. Poppen and P. S. Walker, "Normal and abnormal motion of the shoulder," *J. Bone Joint Surg. Am.*, vol. 58, no. 2, pp. 195–201, Mar. 1976.
[85] C. S. Neer, "Impingement lesions," *Clin. Orthop.*, no. 173, pp. 70–77, Mar. 1983.
[86] A. K. Harrison and E. L. Flatow, "Subacromial impingement syndrome," *J. Am. Acad. Orthop. Surg.*, vol. 19, no. 11, pp. 701–708, Nov. 2011, doi: 10.5435/00124635-201111000-00006.
[87] C. H. Linaker and K. Walker-Bone, "Shoulder disorders and occupation," *Best Pract. Res. Clin. Rheumatol.*, vol. 29, no. 3, pp. 405–423, Jun. 2015, doi: 10.1016/j.berh.2015.04.001.
[88] S. G. Brush, "Thomas L. Hankins. Sir William Rowan Hamilton. Baltimore: John Hopkins University Press. 1980. Pp. 474. $32.50.," *Albion*, vol. 13, no. 3, pp. 315–316, 1981, doi: 10.2307/4048861.
[89] H. Nakayama, H. Onishi, M. Nojima, K. Ishizu, and M. Kubo, "Analysis of scapular kinematics in three planes of shoulder elevation: A comparison between men and women," *J. Phys. Fit. Sports Med.*, vol. 7, no. 1, pp. 65–74, 2018, doi: 10.7600/jpfsm.7.65.
[90] K. Tham and R. Tegnér, "Video feedback in the rehabilitation of patients with unilateral neglect," *Arch. Phys. Med. Rehabil.*, vol. 78, no. 4, pp. 410–413, Apr. 1997, doi: 10.1016/s0003-9993(97)90234-3.
[91] G. Wu *et al.*, "ISB recommendation on definitions of joint coordinate systems of various joints for the reporting of human joint motion--Part II: shoulder, elbow, wrist

and hand," *J. Biomech.*, vol. 38, no. 5, pp. 981–992, May 2005, doi: 10.1016/j.jbiomech.2004.05.042.

(Page intentionally left black)